# Nonradiative Electronic Relaxation under Collision-Free Conditions

PHAEDON AVOURIS, WILLIAM M. GELBART, and M. A. EL-SAYED*

*Contribution No. 3781 from the Department of Chemistry, University of California, Los Angeles, California 90024*

*Received February 22, 1977*

## Contents



## I. Introduction

During the past several years, there has been a great deal of research in the field of radiationless transitions between electronic states or organic molecules. Theoretical studies of these processes examined their description in terms of, for example, the best wave functions to use, the part of the molecular Hamiltonian responsible for inducing the transition, the dependence of the relaxation rate on the manner in which the initial state is prepared, and on the excess vibrational energy in the excited electronic state. At the same time, new experimental techniques made it possible to determine a detailed wealth of information about these radiationless transitions. For example, fast decay rates can now be measured accurately using pulsed excitation sources (nanosecond flash lamps and lasers and picosecond lasers) and time-resolved spectroscopy detection techniques (time-correlated single photon counting, boxcar integration, streak cameras, etc.). Much of this recent work has been conducted in the low-pressure gas phase, although most earlier work had been carried out in the condensed phase. The mechanism of the electronic relaxation between the lowest excited singlet and triplet states in solids has also been studied, most successfully through the techniques of phosphorescence–microwave double resonance spectroscopy.

The study of radiationless transitions continues to be a very active research area and undoubtedly will expand in the future because of the fundamental and applied interest on the problem. The necessary instrumentation (tunable lasers, lifetime apparatuses, etc.) is being introduced widely in spectroscopic and photochemical laboratories. It is thus felt that the time is ripe to review the results, language, and understanding that have thus far been accumulated. There are many other review articles in this field that have appeared during the past several years; a list is given in Table IV. The present review is written with three important points in mind.

First, we have attempted to address workers primarily outside the field of theoretical chemistry and chemical physics, who may not already be familiar with the background formalisms and techniques. The theory presented is accordingly more heuristic than it is rigorous. Our purpose is to rationalize the key features of the experimental effects which have been observed to date, rather than to present a general, "first-principles" theory. Thus, for example, we do not treat detailed questions concerning the effects of light source and molecular line-shape characteristics on the preparation and decay of initial states. Instead, we attempt to explain qualitatively why the initial state of "large" molecules can be thought of as a pure singlet and why it (almost always) decays exponentially at low pressures with less-than-unity fluorescence quantum yields. Similarly we gloss over many subtleties and special limits of the "intermediate" case, choosing instead to emphasize how *bi*exponential, pressure-dependent decays are most natural for these systems. The mathematical level is kept low throughout our discussion; wherever we believe that theoretical rigor has been breached, reference is made to original papers for more careful (and more sophisticated) analyses.

Secondly, we have tried to allot a comparable amount of space for discussing theory and experimental results. Unlike many of the previous reviews, we have not allowed the theoretical part to overshadow the discussion of experimental methods and data. This is appropriate insofar as theoretical productivity in the field has slowed down during the past few years, while experimental work has accelerated.

Thirdly, we have confined our review to studies in the low-pressure gas phase, concentrating on the (essentially collision-free) electronic relaxations in organic species which do not involve dissociation or significant molecular rearrangement. Most of the earlier studies of radiationless transitions have been performed on crystals or liquid solutions. In all these studies the

observed data are a superposition of intramolecular and intermolecular effects which are difficult (if not impossible) to separate. The low-pressure gas-phase case provides a way of studying the effect of strictly intramolecular contributions to the relaxation process.

It is obviously difficult for a review such as this to include discussion of all relevant work in the field. We have attempted to cover the recent literature through August 1976. For the authors whose work is not included, or is incorrectly interpreted or presented, we stress the fact that this was done unintentionally and for this we offer our apologies.

The article is almost half theory (section II) and half experimental results (section III). In the theory part, the case of large molecules is examined first (section II.A) followed by cases of small and intermediate molecules (section II.B). The experimental section is classified according to the molecular system studied: aromatic hydrocarbons (III.A), azaaromatics (III.B), dicarbonyls (III.C) and monocarbonyls (III.D). In section IV, a summary and overview are given. A comparison between gas-phase and solid-state results is made, and examples are offered for the extension of radiationless transition theory to photochemistry. Along these lines we suggest several new directions which we think are important to pursue.

## II. Theory

## A. The Case of "Large" Molecules

### 1. Introduction

The "large" molecule limit is best characterized by the experimental fact that an electronically excited state of the species in question decays exponentially—in the absence of collisions—with a rate greater than the radiative rate. Consider, for example, the excitation of a particular vibrational level in the $S_1$ state of benzene, under "zero" pressure (i.e., $p < 0.1$ Torr) conditions. A plot of the emission intensity vs. time shows an exponential decay with a lifetime of $\approx$70 ns[1,2] and a fluorescence quantum yield of $\approx$0.2.[3] The fact that the fluorescence quantum yield $\phi_F \approx 0.2$, under pressure conditions where the electronically excited molecules undergo no collisions, means that four out of five molecules decay "all by themselves" from the $S_1$ state (i.e., without emitting light or transferring energy to other molecules). This intramolecular conversion of electronic into vibrational/rotational energy is referred to as a "radiationless transition". Since the molecule is isolated (no collisions occur and we forget for the moment about its interaction with the radiation field), its total energy remains constant. The energy is simply redistributed. Part or all of the $S_1$ electronic excitation is converted into vibrational motion of the nuclei as the molecule "relaxes" into a lower triplet ($T_1$) or ground electronic state ($S_0$). In the former case the radiationless transition is labeled an intersystem crossing (since the spin is changed) and in the latter case an internal conversion.

Recall that the fluorescence quantum yield for an electronically excited atom at low enough pressures is expected to be unity. When it is not we look immediately for evidence of a radiationless process such as autoionization[4] which can account for the observed decay of the initially prepared electronic state. Similarly, predissociation is the most familiar kind of radiationless transition which accounts for the less-than-unity fluorescence quantum yields of isolated diatomic molecules (such as $O_2$ excited in its Schumann–Runge bands[5]). In both of these cases the system ends up unbound; an electron is ejected from the atom, or the diatomic molecule breaks apart. In our benzene example, on the other hand, the final state following the radiationless transition is very much bound, and must await collision or emission before it is deactivated. This is a fundamental difference that sets the internal conversion and intersystem crossing processes quite apart from the autoionizations and predissociations. Also, unlike the obvious footprints of ejected electrons and atomic fragments, we shall see that it is exceedingly difficult to monitor final states in the cases of radiationless transitions which interest us.

We summarize below the several conceptual questions which we try to answer in our brief theoretical discussion of the "large" molecule limit.

(a) What are the internal (intramolecular) interactions which give rise to the exchange of energy between electrons and nuclei, i.e., that make unstable the initially prepared vibronic state (even in the absence of collisions and emission)?

(b) Given these interactions between the several low-lying electronic configurations, how is it possible to prepare the molecule in a particular vibrational level of, say, the first excited singlet?

(c) How can we understand the apparently irreversible (and simple exponential) decay of the initially prepared state under "zero"-pressure conditions? Equivalently, since the molecule almost always remains bound and has a limited number of internal degrees of freedom, why do we not see evidence for reversible exchange between the interacting states?

(d) How is the $S_1$-decay rate, and its dependence on excess vibrational energy, related to the details of molecular structure; e.g., can we learn something new about benzene, say, by quantitative comparisons between theoretical and experimental analyses of the radiationless transition?

All of these questions have, of course, been asked many times in recent literature. Accordingly we shall concern ourselves primarily with those aspects which have not been adequately stressed in earlier reviews. In section 2, for example, we discuss numerical studies of the necessary conditions for exponential decay and "irreversibility" [see (c) above]. We also summarize there the indispensable "step ladder" model for radiationless transitions in "large" molecules and briefly explain the usual assumptions about the initially prepared state [(b)]. In section 3 we treat the question of interaction energies [see (a) above] and stress how little is known about the nuclear-coordinate dependence of the electronic wave functions relevant to discussions of internal conversion and intersystem crossing processes. This leaves uncertain the precise "mechanism" of most radiationless transitions of interest. In section 4 we present a simple theory which relates the nonradiative decay rate for a particular vibronic level to the molecular vibrational structure [(d)]. Local- vs. normal-mode descriptions of the CH stretches in aromatic hydrocarbons are considered, and qualitative rules of thumb are presented to characterize "large"-molecular radiationless transitions' behavior (e.g., energy gap laws, isotope effects, "accepting mode quality", etc.).

### 2. Exponential Decay and Irreversibility

#### a. The "Step Ladder" Model

No review on radiationless transitions can begin without reference to the "step ladder" model suggested in the early work of Robinson,[6] Ross,[7] and Siebrand,[8] and immortalized by the analytical treatment of Bixon and Jortner.[9] Figure 1 depicts schematically the energy level scheme in the region of a large molecule's first singlet ($S_1$) state. $\phi_s$ denotes a particular low-lying vibrational level in $S_1$, while $\{\phi_l\}$ correspond to the large number of nearly degenerate, highly vibrationally excited levels of the lower triplet ($T_1$) or ground ($S_0$) state. In a molecule like benzene where the $S_1$–$T_1$ energy gap (separation between origins) is $\approx$8500 $cm^{-1}$, say, the density of the $\phi_l$ states at $E_{S_1}$ is given approximately by the number of ways of distributing 8500 $cm^{-1}$ over the 30 normal modes of vibration. Because of the many low-frequency stretches and bends, the number of these overtones and combinations is enormous: there are as many as $\approx 3 \times 10^5$ states per $cm^{-1}$ in the $S_1$–$T_1$ benzene case.

The states $|s\rangle = |\phi_s\rangle$ and $\{|l\rangle\} = \{|\phi_l\rangle\}$ interact through the spin–orbit coupling and nuclear kinetic energy terms discussed below in section 3. Thus they are not eigenfunctions of the full molecular Hamiltonian $H_{mol}$. Let $H_{mol}|\psi_n\rangle = E_n|\psi_n\rangle$ and write

$$|\psi_n\rangle = C_n^S|S\rangle + \sum_l C_n^l|l\rangle \quad (1)$$

Bixon and Jortner showed[9] that simple solutions could be derived for the eigenfunction coefficients ($C_n^S$, $\{C_n^l\}$) and energies ($E_n$) as soon as a few approximations were introduced: (1) the energies of the $\{\phi^l\}$ levels are taken to be uniformly spaced, i.e., $E_l = E_S + \alpha + l\epsilon$ where $l = 0, \pm 1, \pm 2, \ldots$; (2) the interactions mixing $\phi_s$ with each of the $\phi_l$'s are assumed to be uniform; $\langle S|H_{mol}|l\rangle = v$, for all $l$. From these simplifications it follows that the coefficient $C_n^S$ is given exactly by

$$(C_n^S)^2 = v^2/[(E_n - E_S)^2 + (\pi v^2/\epsilon)^2 + v^2] \quad (2)$$

with the eigenenergies satisfying

$$E_n = E_S - (\pi v^2/\epsilon)\cot[(\pi/\epsilon)(E_n - E_S - \alpha)] \quad (3)$$

According to eq 3 the $E_n$ can only be obtained by (numerical computation or) a graphical solution. It is easily shown that each new eigenenergy falls between a pair of "zero-order" $E_l$'s. Thus it was natural for Bixon and Jortner to introduce the further approximation

$$E_n = E_S + n\epsilon, \quad n = 0, \pm 1, \pm 2, \ldots \quad (4)$$

### b. Initial State Preparation

Now suppose the molecule, originally ($t = 0$) in its ground state $\phi_g$, is subjected to an exciting pulse of light whose duration is very short compared with all decay times of interest:

$$V(t) = \mu\delta(t) \quad (5)$$

Here $\mu$ is the electric dipole moment operator. Then the time-dependent wave function for $t > 0$ is given by

$$|\psi(t)\rangle = \sum_n a_n(t)|\psi_n\rangle \exp(-iE_nt/\hbar) \quad (6)$$

where, from first-order perturbation theory[15]

$$a_n(t) \approx (1/i\hbar)\int_0^t d\tau \exp[i(E_n - E_{\phi_g})\tau/\hbar]\langle\psi_n|V(\tau)|\phi_g\rangle \quad (7)$$

Taking $E_{\phi_g}$ as the zero of our energy scale, and substituting for $V(t)$ in eq 7 from eq 5, we have that $a_n(t) \approx \langle\psi_n|\mu|g\rangle/i\hbar$. Since we shall be interested in cases where $\phi_g$ and the $\{\phi_l\}$ correspond to singlet and triplet states, respectively, it is reasonable to set $\langle\phi_l|\mu|g\rangle$ equal to zero for all $l$. Using the expansion (1) for $\psi_n$, $\langle\psi_n|\mu|g\rangle$ is then given by $C_n^S\mu_{gS}$ where $\mu_{gS} \equiv \langle S|\mu|g\rangle$. That is, each molecular eigenfunction $\psi_n$ carries oscillator strength proportional to its "weight" $(C_n^S)^2$ of singlet character. From the above we can write

$$|\psi(t = 0^+)\rangle = \sum_n a_n(t = 0^+)|\psi_n\rangle \approx \frac{\mu_{gS}}{i\hbar}\sum_n C_n^S|\psi_n\rangle \quad (8)$$

as the initially prepared state of the system. But, noting that $C_n^S = \langle\psi_n|S\rangle$ (see eq 1) and that $\Sigma_n|\psi_n\rangle\langle\psi_n| = 1$, eq 8 implies immediately that $|\psi(t = 0^+)\rangle \approx (\mu_{gS}/i\hbar)|S\rangle$ "=" $|S\rangle$.

Crucial to the above result is the $\delta$-function form for the exciting light pulse. The linear combination of $\psi_n$'s given by eq 8 corresponds to a coherent superposition of all those molecular eigenstates which contain a nonzero contribution ($C_n^S = \langle\psi_n|S\rangle \neq 0$) from $|S\rangle$. Otherwise we could not invoke the completeness relation $\Sigma_n\psi_n\rangle\langle\psi_n| = 1$, i.e., $|S\rangle$ is not the initial state unless we have "collected it all up" by exciting a broad enough energy spread of $\psi_n$'s. The $\delta$-function perturbation is equivalent to an infinitely broad spread in exciting light frequencies. In actual practice, on the other hand, the coherent bandpass of the pulse is "uncertainty-principle-limited", and we must worry about whether it is indeed possible to excite all the $\psi_n$'s with $C_n^S \neq 0$ (see, for example, section 4.3 of Freed's most recent review[10]). For the "large" molecules in which we are interested, it is assumed that the interaction energies ($v$) and level spacings ($\epsilon$) are small enough so that the conditions necessary for eq 8 to hold are satisfied. Otherwise the right-hand side of eq 8 needs to be replaced by a summation which is restricted to those $\psi_n$'s whose energies lie within the bandpass of the exciting light. Through the rest of this review we shall ignore all of the subtleties involved in the preparation of the initial state. These subtleties, of which there are many, have been discussed in detail by Rhodes,[11] Freed,[10] Jortner and Mukamel,[12] Robinson,[13] and others.[14] Even though these articles contain definite predictions concerning the effects of the light source characteristics on the preparation and decay of the excited states, no experiments have been reported which clearly demonstrate these effects in "large" molecules.

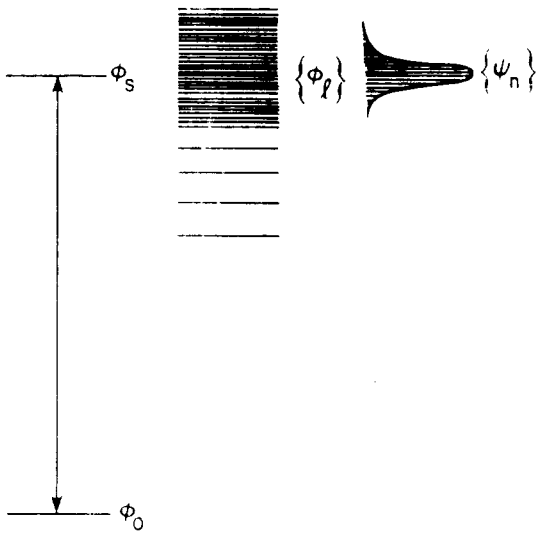


**Figure 1.** Energy-level scheme for a "large" molecule.

### c. Exponential Decay and Recurrences

Let us return to a discussion of the time development of the molecular excited state:

$$|\psi(t)\rangle \approx \frac{\mu_{gS}}{i\hbar}\sum_n C_n^S \exp(-iE_nt/\hbar)|\psi_n\rangle \quad (9)$$

Neglecting for the moment the effects of radiation and collision, we can express the time-dependent probability of finding the molecule in its initial state $|S\rangle$ as

$$P_S(t) \equiv |\langle S|\psi(t)\rangle|^2 = \left|\sum_n (C_n^S)^2 \exp(iE_nt/\hbar)\right|^2 \quad (10)$$

(In passing from eq 9 to 10 we have dropped a factor of $(\mu_{gS}/i\hbar)$ in order to leave the probability function normalized to unity.) If we can show that $P_S(t)$ falls off exponentially, then we will have demonstrated that a first-order decay proceeds independently of the familiar radiative and collisional deactivation of $|S\rangle$. This will account for the shortened lifetime ($\tau < \tau_{rad}^{S_1}$) and smaller-than-unity fluorescence quantum yield observed under low-pressure ("isolated" molecule) conditions.

Suppose we proceed as follows.[9] We substitute for $(C_n^S)^2$ and $E_n$ in eq 10, from eq 2 and 4:

$$P_S(t) \approx \left|\sum_n \left\{\frac{v^2}{n^2\epsilon^2 + \Delta^2}\exp(-in\epsilon t/\hbar)\right\}\right|^2 \quad (11)$$

Here $\Delta^2 \equiv (\pi v^2/\epsilon)^2 + v^2$. Now, when $v \gg \epsilon$ and $t \gg h/\epsilon$, the

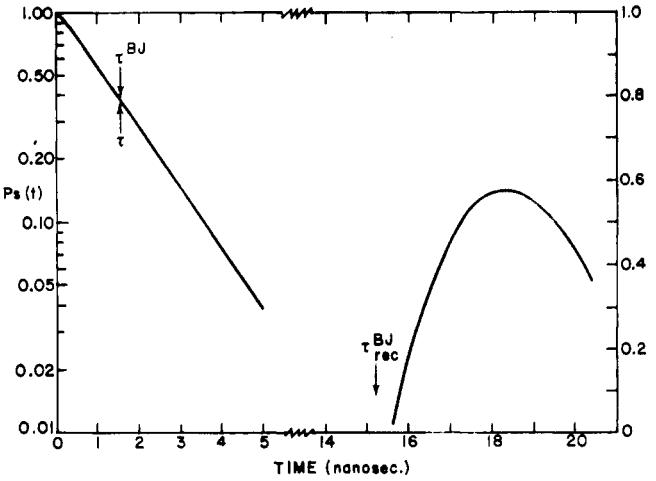


**Figure 2.** $P_S(t)$ for first case (SRF = IRF = 0) in text. The abscissa is broken into two time scales to display the initial decay (referred to the left, logarithmic ordinate scale) and the recurrence (referred to the right, linear scale).

expression in curly brackets is a slowly enough varying function of $n$ so that the sum $\Sigma_{n=-\infty}^{+\infty}$ over $n$ can be replaced by an integral $\int_{-\infty}^{+\infty}$.

$$P_S(t) \xrightarrow[v \ll \epsilon]{t \gg \hbar/\epsilon} \left| \int_{-\infty}^{+\infty} dx \left\{ \frac{v^2}{(\Delta x)^2 + \Delta^2} \cos(\epsilon x t/\hbar) \right\} \right|^2 = \exp(-k_{NR} t) \quad (12)$$

where

$$k_{NR} = (2\pi/\hbar)v^2(1/\epsilon) \quad (13)$$

Thus when the mean interaction erergy is sufficiently larger than the average level spacing $\epsilon$, and the time is short compared with $\hbar/\epsilon$, the initially prepared state will decay exponentially with a nonradiative rate given by eq 13. Note that $k_{NR} = (2\pi/\hbar)v^2(1/\epsilon)$ is the familiar "Golden Rule" result, which is most often obtained from first-order time-dependent perturbation theory.[15]

The time $\hbar/\epsilon$, beyond which $P_S(t)$ can no longer be approximated by $\exp(-k_{NR}t)$, is referred to as the "recurrence time". The reason for this is clear from inspection of the sum appearing in eq 11: it is a perfectly repeating function of time with period $2\pi\hbar/\epsilon$. Obviously, the time development observed for $P_S(t)$ will be a simple exponential if and only if the "recurrences" never have a chance to appear (at $t = 2\pi\hbar/\epsilon, 4\pi\hbar/\epsilon, \ldots$), i.e., if the molecule does not stay isolated long enough for the initial state to reappear. Recall that the density of states $(1/\epsilon)$ appropriate to the $S_1 \rightsquigarrow T_1$ transition in benzene had been estimated to be $\approx 3 \times 10^5$ cm$^{-1}$; this would imply a recurrence time on the order of $2\pi\hbar(1/\epsilon) \approx 10^{-5}$ s. Thus, only a single exponential decay is observed since, long before $t \approx 10^{-5}$ s, the excited state will have been depleted by radiative decay (and, for pressures greater than a few Torr, by collisional deactivation).

Accordingly, on the basis of the Bixon–Jortner analysis, it was concluded that *apparently irreversible* nonradiative relaxation would occur in all those polyatomic molecules for which $v \gg \epsilon$ [guaranteeing $k_{NR}^{-1} = \epsilon\hbar/2\pi v^2 = \tau_{NR} \gg \hbar/\epsilon = \tau_{recurrence}$] and $\tau_{rec} \gg \tau_{max}$, where $\tau_{max}$ is the maximum time (e.g., before collision or emission) that the excited molecule is isolated.[16] These conditions were said to characterize the "large" molecule limit. They are, however, based on a model involving several simplifications which require examination: (a) the interactions mixing the initial state $|S\rangle$ with each of the final levels $|l\rangle$ have been taken to be constant; (b) similarly, the spacings between the $|l\rangle$ levels have been assumed uniform; and (c) the spacings of the exact (i.e., molecular eigenstate) energies, which follow from a diagonalization of the Hamiltonian matrix defined by (a) and (b), are not uniform but have been taken to be so.

The above simplifications allowed for a simple, analytical theory of the excited state's time evolution. Avoiding them means that we must resort to numerical evaluations of the $\psi_n$'s, $E_n$'s and $P_S(t)$. But this is a small price to pay, now that we appreciate already the basic concepts.

### d. Numerical Studies

First consider the fact that the $E_n$'s are not uniformly spaced, *even when* $\langle S|H_{mol}|l\rangle = v$ and $|E_l - E_{l+1}| = \epsilon$ for all $l$. Suppose we take $v/\epsilon$ as small as $1/2$ and calculate $P_S(t)$ from eq 10 and 2. As shown in Figure 2, we find[17] an exponential decay characterized by a rate $1/\tau_{NR} = 2\pi v^2/\hbar\epsilon$, and a *partial* recurrence at $t \gtrsim 2\pi\hbar/\epsilon$. These results correspond to taking 51 $|l\rangle$ levels (taking more changes nothing) and choosing $v = 1.096 \times 10^{-3}$ cm$^{-1}$, $\epsilon = 2.192 \times 10^{-3}$ cm$^{-1} = 2v$, $E_S = 0.0548$ cm$^{-1}$, and $E_l = E_S + l\epsilon$ (i.e., $\alpha = 0$), $l = 0, \pm1, \pm2, \ldots, \pm 25$. Note that $P_S(t)$ is independent of $E_S$; choosing $E_S = 0.0548$ cm$^{-1}$ and $\alpha = 0$, corresponds to placing $|S\rangle$ in the middle of the $\{|l\rangle\}$ and referencing its energy to that of the lowest ($l = -25$) $|l\rangle$ state, i.e., $E_S = E_{l=0} = 25\epsilon$. Furthermore, the functional form of $P_S(t)$ depends only on the *ratio* (1.096/2.192 = 1/2) of $v$ and $\epsilon$; the actual choice of $\epsilon$ simply determines the units of time (here we have chosen $\epsilon$ so that $\tau_{NR}$ is on the order of ns).

Note in Figure 2 that the value of $P_S(t)$ at the recurrence is $\approx 0.57$ instead of unity. This follows from the fact that $P_S(2\pi\hbar/\epsilon) = 1$ requires that all the $E_n$'s be uniformly distributed according to $|E_n - E_n \pm 1| = \epsilon$ whereas, in fact, even for constant $\langle S|H_{mol}|l\rangle$ and $|E_l - E_{l\pm1}|$, the exact eigenvalue spacings are significantly smaller than $\epsilon$ in the energy region around $E_S$. (Also, for this same reason, the recurrence comes a little later than $2\pi\hbar/\epsilon$.) Nevertheless the partial recurrence at $t \gtrsim 2\pi\hbar/\epsilon$ would easily be observed were it not for the spontaneous *radiative* decay ($\tau_{rad}$ $10^{-8}$ s) which wipes it out. The actual time $t$ at which $P_S(t) = 1$ is many orders of magnitude greater than $2\pi\hbar/\epsilon$ and is not of interest here. $t = 2\pi\hbar/d$ where $d$ is the largest real number such that $E_n/d$ is an integer for all $n$, i.e., $d(\gg\epsilon)$ is the greatest common divisor for the set of energies $\{E_n\}$. It is at $t$, rather than at $t_{rec}^{BJ} = 2\pi\hbar/\epsilon$, that all the phase factors in eq 10 are restored for the first time to their initial values (so that the state $|S\rangle$ can "recur").

Suppose now we allow the zero-order energies $\{E_l\}$ to be *non*uniformly distributed. The simplest way to treat this case is by diagonalizing a matrix $H_{mol}$ whose diagonal elements are given by $E_S = 0.0537$ cm$^{-1}$ and $E_l = E_S + l\epsilon + \delta(\text{SRF})\epsilon$. Here $\epsilon = 2.192 \times 10^{-3}$ cm$^{-1}$ $(=2v)$ as before but now $\delta$ is a random number between $-1$ and $+1$. SRF is the "spacing randomization factor"[17] which gives rise to fluctuations in the level spacings. The offdiagonal elements $\langle S|H_{mol}|l\rangle$ are again taken to be constant ($v = 1.096 \times 10^{-3}$ cm$^{-1}$). $\{(C_n^S)^2, E_n\}$ and the corresponding $P_S(t)$ have been computed[17] for several different values of the SRF ranging between 0 (see Figure 2) and 10. For SRF $\lesssim$ 1, $P_S(t)$ remains virtually identical with that shown in Figure 2 (SRF = 0), i.e., $\tau_{NR} \approx 1.5$ ns, $t_{rec} \approx 15$ ns and $P_S(t_{rec}) \approx 0.6$. For SRF $>$ 1, $t_{NR}$ and $t_{rec}$ stay essentially the same, but the original decay begins to deviate from exponentiality for $t \gtrsim 2t_{NR}$ and the recurrence becomes less "clean". The results for SRF = 6 are shown in Figure 3.

Introducing nonuniformity into the $\{v_{Sl}\}$ instead of the level spacings is found to give slightly more significant changes in the excited states dynamics. Here we diagonalize $H$ matrices with $E_l = E_S + \epsilon l$ but with the interaction energies given by

$$\langle S|H_{mol}|l\rangle = v_{Sl} = \bar{v} + \delta(\text{IRF})\bar{v} \equiv \bar{v} + \Delta v_l$$

(IRF is the *interaction* randomization factor). Again, for IRF small enough ($\lesssim 1$) $P_S(t)$ is roughly the same as that shown in Figure 2 except for the initial exponential decay being a bit more sloppy. For IRF $>$ 1, however, the value of $P_S(t)$ at its quasi-recurrence ($t = 2\pi\hbar/\epsilon$) is greatly reduced. Approximate analytical expres-

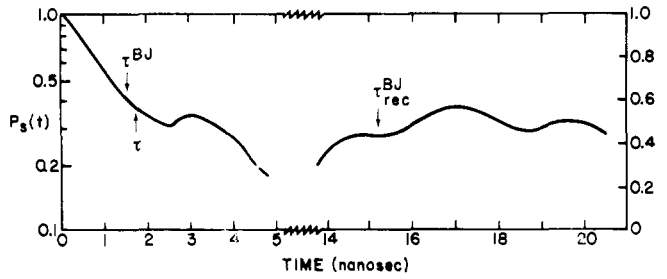


**Figure 3.** $P_S(t)$ for SRF = 6. See Figure 2 caption for explanation of ordinate scales.

sions for $P_S(2\pi\hbar/\epsilon) = 1$ have been derived and discussed by Gelbart, Heller, and Elert.[17] Also, as shown in Figure 4 for IRF = 5, the initial fall-off in $P_S(t)$ is characterized by a lifetime significantly shorter (here by a factor of 8) than those found for smaller nonuniformities in the interaction energy. The "observed" $t_{NR}$ of $\approx$0.22 ns corresponds closely to $1/[2\pi\bar{v}_{SI}{}^2/h\epsilon] = 1/[2\pi(\bar{v}^2 + \overline{\Delta v_I{}^2})/\hbar\epsilon] \ll 1/[2\pi\bar{v}^2/\hbar\epsilon] = t_{NR}{}^{BJ}$. And it is the mean square $(\bar{v}_{SI}{}^2)$ interaction energy rather than the square of the mean $(\bar{v}^2)$ which can be shown[18] analytically to provide the actual radiationless lifetime. Note also that $P_S\ (t = 2\pi\hbar/\epsilon) \lesssim 0.13$ and is essentially washed out by the "noise" in the long-time nonexponential decay.

Finally, in the cases where *both* the $v_{SI}$'s and $E_I$'s are nonuniform, it is found that the $P_S(t)$'s behave as would be expected from the computations described above. That is, for $\bar{v}$ as small as $\frac{1}{2}\epsilon$ the decays remain exponential until the IRF's (and less dramatically the SRF's) become large enough for the initial fall-off to be faster and the partial recurrence to be "wiped out". Similarly, nothing unexpected happens when the $v_{SI}$'s are taken to fall off from $1.096 \times 10^{-3}$ cm$^{-1}$ to zero on either side of $E_S$, or to decrease from $\bar{v}$ to zero as $E_I$ runs from 0 to $50\epsilon = 0.1096$ cm$^{-1}$. This latter scheme simulates the fact that Franck–Condon factors are approximately decreasing functions of quantum number mismatch in the case of almost parallel, undistorted surfaces. In this situation, where the interaction energies range from $\bar{v} = 1.096 \times 10^{-3}$ cm$^{-1}$ to 0, $v_{eff} \approx v_{"middle"} = \frac{1}{2}(1.096 \times 10^{-3}$ cm$^{-1})$ and the decay is found accordingly to be $v^2/v_{eff}{}^2 = 4$ times slower than in the constant $v_{SI}$ case.

## e. Discussion

From the above discussion it is clear that $\bar{v} \gg \epsilon$ is an unduly severe necessary condition for "large" molecule behavior. From numerical computations of the "step ladder" model's dynamics, it has in fact been established that $\bar{v}$ can actually be *smaller* than $\epsilon$. Recall that the $\bar{v} \gg \epsilon$ condition came about within the constant $v_{SI} = \bar{v}$ and $|E_I - E_{I+1}| = \epsilon$ model from requiring $t_{NR} \ll t_{rec}$ and from making the identifications $t_{NR} = h\epsilon/2\pi\bar{v}^2$ and $t_{rec} = 2\pi\hbar/\epsilon$. But the effect of fluctuations in the level spacings has been seen above to shorten $t_{NR}$ (replacing $\bar{v}^2$ by $\bar{v}_{SI}{}^2$) and to wash out the recurrence at $2\pi\hbar/\epsilon$. Thus $t_{NR}{}^{actual} \ll t_{rec}{}^{actual}$ can be satisfied *without* requiring that $\bar{v} \gg \epsilon$, thereby extending significantly the number of examples included in the "large" molecule regime. Recall, though, that the *relative* magnitudes of $\bar{v}$ and $\epsilon$ do not tell us everything we need to know for predicting that "irreversible" exponential relaxation will occur. As discussed above, we also need to have the average level spacing and root-mean-square interaction energy small enough so that $|\psi(0)\rangle = |S\rangle$ and $t_{rec}{}^{actual} \gg t_{max}$.

Numerical computations similar in spirit to those presented above have been carried out by Delory and Tric.[19] They use a randomization scheme which is somewhat different, but come to the same conclusions: (1) fluctuations in the zero-order level spacings have less of an effect on $P_S(t)$ than nonuniformities in the interaction energies; (2) the main effect of fluctuating $v_{SI}$'s is to *shorten* the initial decay and to "smear out" the recurrences. (Delory and Tric also discuss general conditions for the appearance of quantum beats[20] and present an interesting comparison between the time interference effects in the decay of coherently excited molecular eigenstates and the spatial interferences comprising the light scattering by a many-body system.) The notion of "partial recurrences" arising from randomness in the level spacings and couplings had been suggested earlier in a qualitative argument by Siebrand.[21]

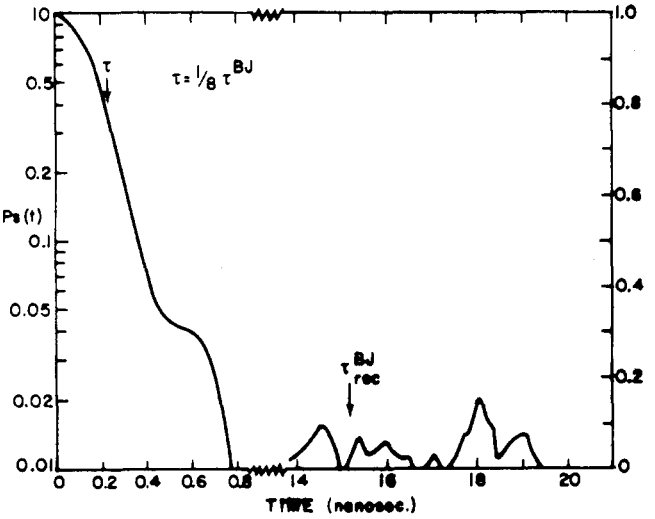


**Figure 4.** $P_S(t)$ for IRF = 5. Note that: $\tau_{calcd} \approx 2.2 \times 10^{-10}$ s $\ll t_{NR}{}^{BJ} \approx 1.5 \times 10^{-9}$ s; the initial decay (see left, logarithmic ordinate scale) is exponential over several lifetimes; and $P_S(t) \lesssim 0.1$ in the region of the recurrence (see right, linear scale).

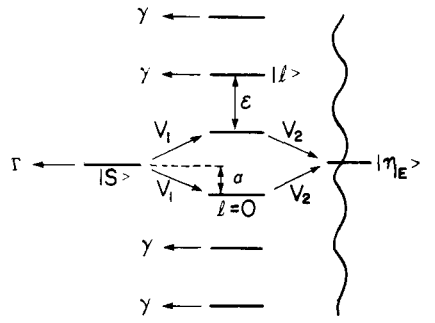


**Figure 5.** Step ladder model generalized to include coupling of the $|I\rangle$ states to a continuum, $|\eta_E\rangle$.

Also related to the above discussion is a paper by Lefebvre and Savolainen[22] in which the exact solution to a generalized Bixon–Jortner model is used to treat recurrences and to derive conditions for exponential decay. The "step ladder" scheme considered above is extended as shown in Figure 5 to include the interaction of each of the zero-order states with continua. Thus the levels acquire "widths" and interfere additionally with one another through common continua. (The continua take into account the effects of radiative emission, fragmentation and intermolecular collisions, etc.) Lefebvre and Savolainen obtain an exact expression for $P_S(t)$ in the case of arbitrary $v_1$, $v_2$, $E_S$, $\epsilon$, $\Gamma$, and $\gamma$ defining the six-parameter model displayed in Figure 5. Here $\alpha$ denotes as before the energy difference between $|S\rangle$ and the closest of the evenly ($\epsilon$) spaced $|I\rangle$ levels; $v_1$ is the interaction energy between $|S\rangle$ and $|I\rangle$; $v_2$ is the coupling of $|S\rangle$ and $|\eta_E\rangle$; and $\Gamma$ and $\gamma$ are the widths of $|S\rangle$ and $|I\rangle$, respectively, due to *independent* decays into "unbound" final states (via emission, collisional deactivation, etc.) Lefebvre and Savolainen show, for example, the effect of increasing $\gamma$ on the attenuation of partial recurrences and discuss the "sequential" vs. "nonsequential" character of the decay of $|S\rangle$ into the bound states $\{|I\rangle\}$ and the continuum $\{|\eta_E\rangle\}$. This latter question, e.g., whether or not the evolution of the excited state proceeds

stepwise according to $|S\rangle \rightarrow \{|I\rangle\} \rightarrow \{|\eta_E\rangle\}$, has been treated in detail by many investigators. We shall not be concerned with these subtleties in the present review and refer the interested reader to the several recent papers in the literature.[23-27]

### 3. The Interaction: What Is the "Mechanism"?

#### a. Introduction

We have seen above that the first excited singlet, say, of a "large enough" molecule can decay exponentially with a rate equal to $k_{rad}{}^{S_1} + k_c{}^{S_1}P + k_{NR}{}^{S_1}$. Here $k_{rad}{}^{S_1}$ is the radiative decay rate and $k_c{}^{S_1}P$ is the collisional deactivation rate at the pressure $P$. $k_{NR}{}^{S_1} = 2\pi\bar{v}_{SI}{}^2/\hbar\epsilon$, where $v_{SI}$ is the interaction energy between $S_1$ and the $I$th of the closely spaced (average density $= 1/\epsilon$) vibrational levels belonging to a lower electronic state. Now we must face the question: What *is* the interaction, i.e., what part of the full molecular Hamiltonian is it that makes nonstationary the initially prepared state? Also, equivalently, what is the right wave function for describing the initially prepared state? Attempts to answer these questions constitute the "basis set controversy" which has lurked behind much of the last 10 years' work on radiationless transition theory. As we shall see, the problem of choosing a proper representation (for describing the electronic relaxation process of interest) is essentially that of determining the correct "mechanism". This area of radiationless transition theory has been dominated by the many contributions of Siebrand and his co-workers, and it is their approach which we follow closely in the brief discussion given below.

As has been stressed by Siebrand et al.,[28] a straightforward way to determine the best representation of the states involved in the electronic relaxation process is to consider the nature of the initially prepared state. It is produced through optical excitation and hence depends on the well-known selection rules governing the interaction of molecules with electromagnetic fields: (1) electronic transitions are much (i.e., $\gtrsim 10^{10}$ times) stronger than vibrational transitions, particularly in the visible and ultraviolet parts of the spectrum with which we are concerned; and (2) spin-allowed transitions are much ($\gtrsim 10^8$) stronger than spin-forbidden transitions, especially when no "heavy atoms" are present. Also related to these guidelines are the concepts embodied in the Franck–Condon principle and the orbital-allowedness of electronic transitions, and the fact that the linear momentum (translational energy) and angular momentum (rotational energy) are essentially conserved in an isolated molecule (see, however, ref 29).

#### b. "Adiabatic" vs. "Crude" BO Basis Sets

Suppose we assert that the initially prepared state should be described by a wave function which can be written as a Born–Oppenheimer product[30] of an electronic and a vibrational part:

$$\Psi_S(qQ) = \psi_S(qQ)\chi_S(Q) \tag{14}$$

Here $q$ and $Q$ denote collectively the electronic and the vibrational coordinates, respectively. Now, as is well-known, there is an embarrassingly large number of ways to choose the separate factors in eq 14. We start by writing

$$H_{mol} = T(q) + U(qQ) + T(Q) \tag{15}$$

where the first and third terms denote the electronic and nuclear kinetic energy operations, and $U(qQ)$ is the set of Coulomb attractions and repulsions involving the electrons and nuclei. If $T(Q)$ is neglected then the allowed electronic motions are given by wave functions $\psi_n{}^{ABO}(qQ)$, including $\psi_S(qQ)$, which satisfy

$$[H_{mol} - T(Q)]\psi_n{}^{ABO}(qQ) = [T(q) + U(qQ)]\psi_n{}^{ABO}(qQ) = E_n{}^{ABO}(Q)\psi_n{}^{ABO}(qQ) \tag{16}$$

With $\psi_S(qQ)$ chosen in this way, the product wave function defined by eq 14 is found to interact with the states $\{\psi_n(qQ)\chi_n(q)\}_{n\neq S}$ through matrix elements of the form

$$\langle S|H_{mol}|n\rangle = \langle \psi_S{}^{ABO}(qQ)\chi_S(Q)|\,T(Q)\,|\psi_n{}^{ABO}(qQ)\chi_n(Q)\rangle \equiv v_{Sn}{}^{ABO} \tag{17}$$

If, on the other hand, we had proceeded from eq 14 and 15 by neglecting not just $T(Q)$ but also the $Q$ dependence of $U(qQ)$, then the electronic wave functions would satisfy

$$[H_{mol} - T(Q) - \{U(qQ) - U(qQ_0)\}]\psi_n{}^{CBO}(qQ_0) = [T(q) + U(qQ_0)]\psi_n{}^{CBO}(qQ_0) = E_n{}^{CBO}(Q_0)\psi_n{}^{CBO}(qQ_0) \tag{16a}$$

Here $Q_0$ denotes a particular choice of positions at which the nuclei are fixed. With $\psi_S(qQ)$ chosen as a solution to (16a) the interaction matrix elements are now given by

$$\langle S|H_{mol}|n\rangle = \langle \psi_S{}^{CBO}(qQ_0)\chi_S(Q)|\{U(qQ) - U(qQ_0)\}|\psi_n{}^{CBO}(qQ_0)\chi_n(Q)\rangle \equiv v_{Sn}{}^{CBO} \tag{17a}$$

Note that $T(Q)$ makes no contribution to $v_{Sn}{}^{CBO}$ since it is proportional to $\partial^2/\partial Q^2$ whereas the $\psi^{CBO}$'s are independent of $Q$ and are orthogonal to one another.

The superscript "CBO" used above refers to "*crude* Born–Oppenheimer"; "ABO" denotes similarly "*abiabatic* Born–Oppenheimer". The "crudeness" of the CBO wave functions corresponds to the fact that the electrons have not been allowed to "adiabatically" follow the vibrations of the nuclei. That is, the potential energy of the electrons is taken to be $U(qQ_0)$ (see eq 16a which defines $H_{el}{}^{CBO} = T(q) + U(qQ_0)$) even when the nuclei have undergone large displacements from $Q_0$! This constraint is responsible for negative charge centers (due to atomic core electrons) building up (at $Q_0$) away from the actual ($Q$) nuclear positions, thereby giving rise to vibrational constants which are much poorer[31,32] than those obtained within the ABO approximation. It has been argued further by Freed[10] that transition probabilities between a pair of electronic states are much more sensitive to errors in the wave function than are single-state properties and that it is therefore particularly appropriate to use the ABO (rather than CBO) in the evaluation of radiationless transition rates. Equivalently, as Henry and Siebrand[28] have stressed, a single choice of $Q_0$ must fail in general to properly describe the potential energy surface for one or the other of the two electronic states involved. Early calculations[33] which discussed the possible inappropriateness of ABO wave functions have been undermined by several more recent investigations.[34-36] (See, however, the general arguments offered by Lefebvre.[37]) Henceforth we shall describe all product states within the ABO, rather than the CBO, approximation.

#### c. Spin–Orbit Coupling

Before proceeding further let us consider still another way to choose the interaction, i.e., to describe the initial state. Up until now we have made no explicit mention of spin-dependent terms in the molecular Hamiltonian. On the basis of the second selection rule discussed earlier (namely that spin-allowed transitions are much stronger than those which involve a change in spin), it is natural to assert that the optically prepared state is a singlet-state eigenfunction of $H_{mol}$ (as given by eq 15) and that this state is made nonstationary by the relativistic spin–orbit (so) coupling. Then we would write

$$v_{sn}{}^{so} = \langle \Psi_{S_1}|H_{so}|\Psi_n\rangle \tag{17b}$$

In the Born–Oppenheimer approximation this interaction energy reduces to

$$v_{sn}{}^{so} = \langle {}^{\mu}\psi_{S_1}\chi_{S_1}|H_{so}|{}^{\nu}\psi_n\chi_n\rangle \tag{17c}$$

where $\mu$ and $\nu$ denote the spin multiplicities of the electronic

wave functions ($\mu$ = singlet in the above example). Note that $v_{sn}^{SO} = 0$ when $\mu = \nu$ = singlet, whereas if we evaluate eq 17 and 17a in the pure spin approximation, $v_{sn}^{ABO} = 0 = v_{sn}^{CBO}$ when $\mu \neq \nu$. That is, if the basis set including $s$ and $\{n\}$ diagonalizes $T(Q)$, then only intersystem crossings are possible for initial singlets, whereas if it diagonalizes $H_{so}$ it is the nuclear kinetic energy which drives the radiationless transition.

It should be clear at this point that the interaction matrix element $v_{sn}$ is extremely sensitive to the representation chosen for the initially prepared state. As mentioned earlier, this choice is dictated by the selection rules for optical excitation. Consider first the case of internal conversion ($S_1 \rightsquigarrow S_0$ say) where the existence of spin contamination is expected to have a negligible effect on the intramolecular couplings (provided only light nuclei are involved so that the spin–orbit interactions are weak). Suppose that there are no higher electronic states $\psi_m$ close to $S_1$ which have large transition dipole moments with $S_0$. Then the selection rules 1 and 2 allow us to write the initial state as a singlet pure-spin (singlet $S_1$) ABO function, and similarly for the $n$ states. The interaction matrix element is given accordingly by eq 17. In the case of *intersystem crossing* the situation is more complicated since neither the $H_{so}$ *nor* $T(Q)$ interactions can be neglected. As we shall see below, the coupling energy of eq 17b is only one of several contributions to the $v_{sn}$ which governs the intersystem crossing rate.

## d. Internal Conversion

Let us consider in detail the interaction matrix element given by eq 17 for internal conversion. Writing the nuclear kinetic energy as $T(Q) = -\sum_k \hbar^2/2\mu_k)\partial^2/\partial Q_k{}^2$ (where $Q_k$ denotes the $k$th normal coordinate, having reduced mass $\mu_k$), and using the "chain" rule for differentiation of a product, eq 17 can be reduced to

$$v_{sn}^{ABO} = -\sum_k (\hbar^2/\mu_k) \int_Q \chi_s(Q) \times \left\langle \psi_s(qQ) \middle| \frac{\partial}{\partial Q_k} \middle| \psi_n(qQ) \right\rangle \frac{\partial}{\partial Q_k} \chi_n(Q)\, dQ \quad (18)$$

Here we have neglected terms which involve the *second* derivative of the electronic wave functions with respect to nuclear displacements ($Q_k$). Now it has been common practice to neglect further (see, however, discussion at the end of this section) the $\{Q_i\}$ dependence of the "electronic factor" in eq 18,

$$\left\langle \psi_s(qQ) \middle| \frac{\partial}{\partial Q_k} \middle| \psi_n(qQ) \right\rangle \equiv \beta_{el}{}^{IC}{}_{(k)}(\{Q_i\}) \approx \beta_{el}{}^{IC}{}_{(k)} \quad (19)$$

so that $v_{sn}$ becomes proportional to products of vibrational overlap integrals:

$$v_{sn}\Big|_{(18)} \rightarrow -\sum_k \left\{ [\hbar^2 \beta_{el}{}^{IC}{}_{(k)}/\mu_k] \left\langle \chi_k{}^{(S)} \middle| \frac{\partial}{\partial Q_k} \middle| \chi_k{}^{(n)} \right\rangle \times \prod_{i \neq k} \langle \chi_i{}^{(S)} | \chi_i{}^{(n)} \rangle \right\} \quad (20)$$

Here we have simply written out the vibrational wave function for each electronic state as a product of harmonic oscillator wave functions, one for each normal mode: $\chi_s\ (Q = \{Q_i\}) = \Pi_i \chi_i{}^{(S)}\ (Q_i)$, and similarly for $\chi_n$. When the sum in eq 20 is dominated by a single term, the corresponding "$k$" is referred to as the "promoting mode", insofar as the electronic factor $\beta_{el}{}^{IC}{}_{(k)}$ (see eq 19) is largest for this particular cordinate. $\partial/\partial Q_k$ "induces" the radiationless transition much as $Q_k$ promotes radiative allowedness in the familiar Herzberg–Teller theory of absorption and emission.[39] The remaining ($i \neq k$) vibrational degrees of freedom are referred to as "accepting modes" and serve simply to provide a sink for the electronic energy.

Much as we shall find for the intersystem crossing case, the main stumbling block in the quantitative calculation of internal conversion matrix elements is the evaluation of the appropriate nuclear-coordinate-dependent electronic wave functions. Also, very little data on $S_1 \rightsquigarrow S_0$ rates are available since this process does not compete effectively enough (at least at *low* excess energies (see end of section A.4)) with emission and with the $S_1 \rightsquigarrow T_1$ process. Whereas $S_2 \rightsquigarrow S_1$ processes, for example, can be so fast that line-broadening effects are observable, there are many new theoretical and experimental complications which preclude simple analyses of these internal conversion decays. These considerations are discussed in section A.4, as well as throughout the "Experimental" part of this review.

## e. Intersystem Crossing

Consider now the interaction matrix element for the case of intersystem crossing, $S_1 \rightsquigarrow T_1$, for example. On the basis of the optical selection rules (1) and (2) mentioned earlier (see also the discussion of initial state preparation in section 2) we take as our representation of $|S\rangle$ the pure-spin adiabatic Born-Oppenheimer state ${}^1\psi_{S_1}(qQ)\chi_{S_1}(Q)$. The left superscript denotes the fact that the initial state has pure singlet character. The "final" states, on the other hand, are triplet states which have been mixed by $H_{so}$ and $T(Q)$ with other pure-spin product states *lying outside* the $S_1$ energy region. To first order in the interactions, then,

$$|n\rangle \approx |{}^3\Psi_{T_1}\rangle + \sum_i \frac{\langle {}^1\Psi_i | H_{so} | {}^3\Psi_{T_1} \rangle}{E_i - E_{T_1}} |{}^1\Psi_i\rangle + \sum_j \frac{\langle {}^3\Psi_j | T(Q) | {}^3\Psi_{T_1} \rangle}{E_j - E_{T_1}} |{}^3\Psi_j\rangle \quad (21)$$

where $i$ runs over all singlet states (excluding $S_1$) and $j$ over all triplets (excluding $T_1$). The intersystem crossing matrix element can be written accordingly as

$$\langle S | H_{so} + T(Q) | n \rangle \approx \langle {}^1\Psi_{S_1} | H_{so} | {}^3\Psi_{T_1} \rangle \langle {}^1\Psi_{S_1} | H_{so} | {}^3\Psi_i \rangle \langle {}^3\Psi_i | T | {}^3\Psi_{T_1} \rangle + + \sum_i \frac{\langle {}^1\Psi_{S_1} | T | {}^1\Psi_i \rangle \langle {}^1\Psi_i | H_{so} | {}^3\Psi_{T_1} \rangle}{E_i - E_{T_1}} \quad (22)$$

(In the above, ${}^1\Psi_{S_1} \equiv {}^1\psi_{S_1}(qQ(X_{S_1}(Q)$, and so on.)

Note that the leading term in eq 22 is precisely that given by eq 17c; it corresponds to the "direct" spin–orbit coupling "mechanism" for intersystem crossing. It is large ($\gtrsim 50$ cm$^{-1}$) for $\pi,\sigma^*$ or $n,\pi^*$ states coupled to $\pi,\pi^*$ states, but small ($\lesssim 1$ cm$^{-1}$) when only $\pi,\pi^*$'s are involved.[38a] The additional terms in eq 22 are identical with those which have been treated in considerable detail by Siebrand and co-workers.[28,38] They simplify things by introducing the following approximations.

(a) Each of the promoting modes (arising, say, in the $T(Q)$ matrix elements discussed above) is assumed to undergo no (frequency or equilibrium position) changes in passing from the initial to final electronic state; this is equivalert to neglecting the small extent to which promoting modes can also act as accepting modes. In this limit, for example, eq 20 for the internal conversion matrix element reduces, for the case of no initial ($S_1$) excitation of the promoting modes, to

$$v_{sn}{}^{IC} \approx + \sum_k \left( \frac{\hbar^3 \omega_k}{2\mu_k} \right)^{1/2} \beta_{el}{}^{IC}{}_{(k)} \langle \chi^{(S)} | \chi^{(n)} \rangle \quad (23)$$

where $\omega_k$ is the $k$th vibration's frequency.

(b) $\langle {}^1\psi_i(qQ)\chi_i(Q) | H_{so} | {}^3\psi_j(qQ)\chi_j(Q) \rangle$, where $i$ and $j$ refer to an arbitrary pair of electronic states with "opposite" spin multiciplicity, is expanded about a suitably chosen nuclear equilibrium configuration $Q = 0$ and all terms quadratic or higher order in $Q$ are neglected.

(c) A correction factor $p_k$ is introduced into eq 23 to account approximately for the dependence of $\beta_{el}{}^{IC}{}_{(k)}$ on $Q$. $p_k$ is the ratio of the left- to the right-hand side of eq 19: Orlandi and Siebrand[35]

have carried out model calculations which suggest that $p_k$ is, in many cases, on the order of 1–10.

(d) The intermediate states included by the sum over $i$ in eq 22 are divided into $\pi\pi$ and $\pi\sigma$ states. The energy denominators appropriate to the $\pi\sigma$ states are approximated by the electronic origin differences, so that closure may be applied to the vibrational wave functions:

$$\sum_i \langle \chi_{S_1} | \chi_i \rangle \langle \chi_i | \chi_{T_1} \rangle = \langle \chi_{S_1} | \chi_{T_1} \rangle \tag{24}$$

This means that the corresponding terms in eq 22 are proportional to $\langle \chi_{S_1} | \chi_{T_1} \rangle$ and that the remaining sum over $i$ refers only to electronic labels. The contributions from the $\pi\pi$ states, on the other hand, are assumed to be dominated by a single state ("resonance") with energy $E_i \approx E_{T_1}$; recall that $E_{T_1} \approx E_{S_1}$ refers to the electronic-*plus*-vibrational erergy in the interaction region.

Siebrand et al have shown that the above simplifications lead, in the case of zero-point energy only in the initial state's vibrational degrees of freedom, to an intersystem crossing interaction matrix element which can be written as a sum of five terms:[28,38] $v^{ISC} = v^{(1)} + v^{(2)} + v^{(3)} + v^{(4)} + v^{(5)}$. $v^{(1)}$ and $v^{(2)}$ correspond to the leading term and first correction in the expansion (see (b) above) of $\langle {}^1\psi_{S_1} | H_{so} | {}^3\psi_{T_1} \rangle$ about $Q = 0$. $v^{(3)}$ arises from the second-order terms in eq 22 for which $E_i \approx E_{T_1}$, e.g., from the $\pi\sigma$ intermediate states; although these states have high energies (big energy denominators) they can still dominate the sum over $i$ because of their large (one-center integral) spin–orbit interactions. The $\pi\pi$-intermediate states in eq 22 give rise to $v^{(4)}$ and $v^{(5)}$ which are related to one another as $v^{(2)}$ relates to $v^{(1)}$; i.e., they come from the leading term and first correction (linear in $Q$) in the expansion of $\langle {}^1\psi_i | H_{so} | {}^3\psi_{T_1} \rangle$ about $Q = 0$.

The central theme, clarified and stressed throughout the work of Siebrand and co-workers,[28,38] is that each of the terms in $v^{ISC} = \sum_{i=1}^{5} v^{(i)}$ corresponds to a different "mechanism" for the intersystem crossing, each implying different isomeric deuterium effects (i.e., rate constant dependence on the *particular positions* of a *fixed* number of D substituents), temperature dependences, and triplet sublevel preference of the ISC process. $v^{(1)}$ is the *direct* spin–orbit contribution which is negligible in many instances involving $\pi\pi^*$ interactions in aromatic hydrocarbons, but dominant in others involving $n\pi^*$–$\pi\pi^*$ coupling in heterocyclics.[39a] $v^{(1)}$ is expected to show no isomeric effect. $v^{(2)}$, the vibronically induced ("indirect") spin–orbit contribution, is expected[38] to exhibit less of an isomeric effect than $v^{(3)}$ since the latter is proportional to $(\omega_k/\mu_k)^{1/2}$ rather than $(1/\mu_k\omega_k)^{1/2}$ and is "promoted" by out-of-plane modes rather than CC stretches. The "resonance" mechanism implied by $v^{(4)}$ and $v^{(5)}$, on the other hand, involves much more complicated dependence on the D-substituent positions, making unambiguous predictions impossible. They can be shown,[38] though, to lead to the same alignment of triplet spin-sublevels as do $v^{(1)}$ and $v^{(2)}$.

For a detailed discussion of the experimental determination of intersystem crossing "mechanisms", the reader is referred to the work of Siebrand et al. (and to the papers cited therein). Metz, Friedrich, and Hohlneicher[40] have also discussed this question. They expand the interaction energy through second order, obtain an expression which is essentially identical with eq 22 above, and present calculations for the $T_1 \rightsquigarrow S_0$ decay in naphthalene.

### f. Factorization of $v$

Before closing this section we consider briefly the problem of factorizing matrix elements of the form given by eq 18. The common procedure which we followed at first, in order to obtain eq 19 was to simply neglect the nuclear coordinate dependence of

$$\langle \psi_S(qQ) | \frac{\partial}{\partial Q_k} | \psi_n(qQ) \rangle = \langle \psi_S(qQ) | \frac{\partial U(qQ)}{\partial Q_k} | \psi_n(qQ) \rangle / [E_S(Q) - E_n(Q)] \tag{25}$$

(Equation 25 follows directly from differentiating eq 16 with respect to $Q_k$, multiplying by $\psi_S(qQ)$ and integrating over all $q$.) We mentioned a bit later that Orlandi and Siebrand[35] have shown how the $Q$ dependence of the energy denominator in eq 25 leads to a multiplicative correction factor, $p_k$. Nitzan and Jortner[41] have similarly taken into account the variation of $[E_S(Q) - E_n(Q)]$ with $Q$, but have also estimated the $Q$ dependence of the *numerator* in eq 25. They conclude that the corrections due to the numerator's $Q$ dependence are dominant, the individual magnitudes varying with electronic energy gap, vibrational frequencies, and displacements (between "$S$" and "$n$") of normal mode equilibrium positions. It is argued[41] that the absolute value of radiationless decay rates is increased by orders of magnitude above that predicted from the approximate eq 23 while isotope effect and *relative* rate calculations (see section A.4) should be essentially unmodified.

Most recently, Freed and Lin[42] have suggested a quite different approach to the problem of the electronic factor's $Q$ dependence. They suggest that it is indeed possible to factorize the interaction matrix elements in eq 18 but that the $\langle \psi_S(qQ) | \partial/\partial Q_k | \psi_n(qQ) \rangle$ term in the $Q$ integral should *not* be expanded about an equilibrium position. Because of the energy conservation constraint, the most important $\chi_n(Q)$ may have classical turning points which are quite far from $Q_{eq}^{(S)} \approx Q_{eq}^{(n)}$. Thus Freed and Lin introduce the notion of the "$Q$-centroid" (in analogy with the familiar "$r$-centroid" in *radiative* transition theory) defined by the value $Q = Q_0$ which gives the fastest convergence for the $k$th term in eq 18, when $\langle \psi_S(qQ) | \partial/\partial Q_k | \psi_n(qQ) \rangle$ is expanded in powers of $Q - Q_0$. $Q_0$ determined in this way is found to depend on $k$ and on the initial and final vibrational wave functions (as well as, of course, on the electronic and normal-mode structure of the molecule). The $Q_{0,i}$'s in $Q_0$ (recall that $Q_0$ denotes the full set of $3N - 6$ nuclear coordinates evaluated as the "centroid") which correspond to the best accepting modes show the largest deviations from the $Q_{e,i}^{(s,n)}$'s. Since this set often includes nontotally symmetric modes, the $Q$-centroid configuration ($Q_0$) can have lower symmetry than the equilibrium geometry ($Q_{eq}$). Freed and Lin[42] discuss how such a situation can significantly affect the role of electronic symmetry and of promoting modes in the elucidation of "mechanism". They consider in particular the possibility that a direct spin–orbit coupling term $v^{(1)}$ from above, which vanishes when evaluated at $Q = Q_{eq}^{(s,n)}$, can be dominant for $Q = Q_0$; the promoting modes become "irrelevant" in this case. These arguments, while extremely interesting, are still in a speculative stage and need to be pursued further. We shall return to them briefly in the following section where we discuss examples of the apparent breakdown of the factorization of molecular interaction energies into electronic and vibrational parts.

## 4. *The "Golden Rule" Rate*

### a. General Discussion

In section A.2 the Bixon–Jortner model was solved in the "large" molecule limit and shown to give a nonradiative decay rate having the form $k_{NR} = 2\pi v^2/\hbar\epsilon$ where $v$ and $\epsilon$ are the constant interaction energy and level spacing. We also discussed there the way in which numerical studies lead, in the case of realistically fluctuating $v_{sl}$'s and $E$'s, to a similar result: $k_{NR} = 2\pi\bar{v}_{sl}^2/\hbar\bar{\epsilon}$. ($1/\bar{\epsilon}$ is the average density of $l$ states at $E_S$.) In the present section we treat an equivalent representation of the nonradiative rate which is more useful for application to particular molecules of interest.

Suppose we start again with the molecule initially prepared

in the zero-order state $|S\rangle$ having energy $E_S$. Let $\{v_{sl}\}$ denote as before its set of interaction energies with the "final" closely spaced states having energies $\{E_l\}$. Then, a first-order application of time-dependent perturbation theory[15] shows that the initial state will decay exponentially with a rate given by the familiar "Golden Rule" sum:[43]

$$k_{s\to l} = \frac{2\pi}{\hbar}\sum_l \overline{v_{sl}}^2 \delta(E_s - E_l) \tag{26}$$

Note that eq 26 reduces to $k = (2\pi/\hbar)v_{sl}^2\Sigma_l\delta(E_s - E_l) \equiv (2\pi/\hbar)v_{sl}^2\rho_l(E_S)$ when $v_{sl}^2$ is slowly enough varying to be replaced by its average value. [$\rho_l(E_S)$, the density of $l$ states near $|S\rangle$, is equal to $\Sigma_l\delta(E_S - E_l)$ in the sense that integration of either quantity over a unit energy interval about $E_S$ gives the number of $l$ states per $cm^{-1}$ at $E_S$.]

Now, we saw in the preceding section that the interaction energy, $v_{sl}$, is in general given by a complicated sum of electronic factors and vibrational overlap integrals. We discussed further how the relative importance of these several contributions ("mechanisms") depends on the many (often unknown) particulars of molecular structure. Nevertheless, in order to illustrate many of the broader features of the radiationless decay rate, we introduce at this point the following simplification: we assume that $v_{sl}$ can be written as a *single* product of an electronic factor, $\beta_{sl}$, say, and a vibrational overlap integral. $v_{sl}$ actually does reduce to this form in the case of intersystem crossing dominated by the direct spin–orbit coupling mechanism (see "$v^{(1)}$" from section A.3), i.e., $v^{ISC} \approx \langle\psi_S(qQ_0)\cdot\chi_S(Q)|H_{so}(qQ_0)|\psi_T(qQ_0)\chi_T(Q)\rangle = \langle\psi_S|H_{so}|\psi_T\rangle\langle\chi_S|\chi_T\rangle$] or for internal conversion where only a single promoting mode contributes [$v^{IC} \approx +(\hbar^3\omega_k/2\mu_k)^{1/2}\beta_{el}{}^{IC}{}_{(k)}\langle\chi_{S_1}|\chi_{S_1}|\chi_{S_2}\rangle$, as in eq 23]. Later, in this section we shall discuss examples of the breakdown of this assumption. But, in the meantime, its use will lead to much simplification and to qualitatively correct rationalizations of several characteristic properties of "large" molecule nonradiative decay. In this approximation, then, eq 26 can be rewritten as

$$k_{sl}(\mathbf{m}) = (2\pi/\hbar)\beta_{sl}^2\sum_{\mathbf{n}}|\langle\mathbf{m}|\mathbf{n}\rangle|^2\delta(\Delta E_{sl} + \sum_i m_i\hbar\omega_i^{(s)} - \sum_i n_i\hbar\omega_i^{(l)}) \tag{27}$$

Here $\mathbf{m}$ and $\mathbf{n}$ denote the sets of $3N - 6$ quantum numbers specifying the vibrational excitation in the $|s\rangle$ and $|l\rangle$ states, respectively. $\Delta E_{sl}$ is the energy difference between the zero-point ($\mathbf{m} = 0 = \mathbf{n}$) levels of the initial and final electronic states, and $\omega_i$ is the fundamental frequency of the $i$th vibrational degree of freedom.

Now, just to get started (we shall treat the more general case soon enough), suppose that all the $m_i$'s are zero and that mode 1 undergoes only geometry (not frequency) changes between the $s$ and $l$ potential surfaces, while the rest of the modes stay the same. Then the vibrational quantum numbers for these latter modes must remain zero, and eq 27 becomes

$$k_{sl}(0) = (2\pi/\hbar)\beta_{sl}^2\sum_{n_1}|\langle 0|n_1\rangle|^2\delta(\Delta E_{sl} - n_1\hbar\omega_1) \tag{28}$$

where $\langle 0|n_1\rangle$ is the vibrational overlap integral for the displaced oscillator (with frequency $\omega_1$) corresponding to normal mode 1, and $\Delta E_{sl}$ is the energy available to this mode in the final electronic state. Expressions 26–28 for $k_{sl}$ would, of course, be troublesome if the energy-conserving $\delta$ functions were "real" or, equivalently, if the sum over final states were truly discrete. Recall though that a time-independent, first-order rate constant does not arise unless the set of closely spaced $l$ levels can be treated like a continuum. Indeed it was precisely the replacement of a sum by an integral in section A.2 (see eq 11–13) that led to simple exponential decays. Similarly, in the conventional perturbation theory derivation[15] of the "Golden Rule", the $\delta$ functions appear (as approximations to $\sin^2\{(E_s - E_l)t/2\hbar\}/\pi\{E_s - E_l)\cdot t/2\hbar\}^2$) *only after* it is assumed that the final states behave like a continuum.

Thus it is proper in the "large" molecule limit to replace the sum over $n_1$ by an integral in eq 28:

$$k_{sl}(0) \to \frac{2\pi}{\hbar}\beta_{sl}^2\int_0^\infty dn_1|\langle 0|n_1\rangle|^2\delta\left[\hbar\omega_1\left(\frac{\Delta E_{sl}}{\hbar\omega_1} - n_1\right)\right]$$
$$= \left(\frac{2\pi}{\omega_1}\right)\frac{\beta_{sl}^2}{\hbar^2}\{|\langle 0|n_1\rangle|^2\}n_1 = \Delta E_{sl}/\hbar\omega_1 \equiv \gamma$$
$$= \left(\frac{2\pi}{\omega_1}\right)\frac{\beta_{sl}^2}{\hbar^2}\frac{e^{-x_1}x_1^\gamma}{\Gamma(1+\gamma)} \tag{29}$$

$\Gamma$ denotes the usual gamma function[44] and $x_1 \equiv (M_1\omega_1/2\hbar)(Q_{eq}{}^S - Q_{eq}{}^l)^2$ is a dimensionless measure of the shift in equilibrium positions for normal mode 1; $M_1$ is the corresponding reduced mass. The last identity in eq 29 follows from the fact that $|\langle 0|n\rangle|^2 = e^{-x}x^n/n!$ for a displaced ($\Delta Q \neq 0$) but undistorted ($\Delta\omega = 0$) harmonic oscillator, and $n! \to \Gamma(1+n)$ as $n$ becomes nonintegral. (That is, the gamma-function, $\Gamma(y)$, defined for *all real* $y$, has the very special property that its value at the integer $n$ is $(n-1)!$.)

### b. Energy Gap Law and Isotope Effects

When the "energy gap" $\Delta E_{sl}$ is large enough compared with the vibrational quantum $\hbar\omega_1$, the gamma function $\Gamma(1+\gamma)$ can be well approximated[44] by $(2\pi)^{1/2}\exp[\gamma(\ln\gamma - 1)]$, from which it follows that the rate in eq 29 can be written as [noting that $x_1{}^\gamma = \exp(\gamma\ln x_1)$]

$$k_{sl}(0) \approx \left(\frac{2\pi\hbar\omega_1}{\Delta E_{sl}}\right)^{1/2}\left(\frac{\beta_{sl}^2}{\hbar^2\omega_1}\right)e^{-x_1}e^{-\Omega(\Delta E_{sl}/\hbar\omega_1)} \tag{30}$$

where

$$\Omega \equiv \ln(\Delta E_{sl}/x_1\hbar\omega_1) - 1 \tag{30a}$$

Note that $x_1 \ll 1$ and the quantity $\Omega$ is only weakly dependent on $\Delta E_{sl}$ and $\hbar\omega_1$, thus we have the now familiar result, first clarified by Siebrand,[45] that the radiationless transition rate is an exponentially decreasing function of energy gap. A semilogarithmic plot of the observed $T_1 \rightsquigarrow S_0$ decay rate vs. the triplet energy ($\Delta E_{T_1S_0}$) is indeed linear for a wide range of aromatic hydrocarbons.[45]

The nonradiative rates are found to decrease upon deuteration by factors of 3–20. This can also be understood from eq 39. Recall that mode 1 is the only vibrational degree of freedom which appears there, simply because it is the only one which we have allowed to act as "acceptor"; all the other oscillators have been assumed identical in both electronic states and have thus been constrained to keep their quantum numbers fixed ($n_{i\neq 1} = m_{i\neq 1} = 0$). In the aromatic hydrocarbons, the best accepting mode by far is the CH stretch, largely (see below) because of its high frequency. The changes ($\Delta Q_{eq}$, $\Delta\omega$) in the CC vibrations, for example, while bigger than those for the CH stretch, are not sufficient to counter the effect of a much smaller frequency (which forces final state quantum numbers to be large, and thus to be weighted by small Franck–Condon factors). Accordingly, the $\omega_1$ in eq 30 corresponds to $\omega_{CH\ stretch}$. This frequency decreases by a factor of $(2)^{1/2} = 1.414$ upon deuteration since $\mu$ is doubled and $\omega = (1/2\pi)^{1/2}k^{1/2}\mu^{1/2}$. $\Omega$ is independent of the isotopic substitution while the factors $1/\omega_1$ and $e^{-x_1}$ are weakly dependent on it. The main effect of deuteration comes from the decrease in the exponential factor, $\exp[-\Omega\Delta E_{sl}/\hbar\omega_1]$. That is, deuteration changes the "dimensionless energy gap" $\Delta E_{sl}/\hbar\omega_1$, which is the number of $\omega_1$ quanta needed to "absorb" the electronic excitation.

Both the "energy gap law" and deuterium effect mentioned above have a simple interpretation even without reference to

eq 30. The bigger the energy gap, the larger the density of interacting states in the region of the initial state. But at the same time there is a greater amount of electronic excitation which must be "accepted" by the vibrations. And the larger the difference in vibrational quantum numbers, the smaller the vibrational overlaps. That is, since the oscillators are almost the same (as far as equilibrium position, frequency and anharmonicity, etc., are concerned) $|\langle 0|n\rangle|^2$ is a rapidly decreasing function of $n$. The fact that $k_{NR}(0)$ decreases rapidly with increasing $\Delta E_{sl}$ means that the density-of-states increase is easily offset by the Franck–Condon factor decrease. The CH stretch is the dominant accepting mode since its especially high frequency ($\gtrsim$50% higher than all the others) allows it to take up a lot of energy without its quantum number getting too high. Upon deuteration its frequency is reduced by 30%, resulting in a dramatic decrease in Franck–Condon factors for the energy-conserving final states.

We should mention here a couple of exceptions to the "normal" isotope effect discussed above. When the energy gap is small enough (e.g., in the case of a nearly degenerate second triplet, $T_2$, in the region of $S_1$) deuteration is found to *increase* the radiationless decay rate. This "inverse" isotope effect has been treated by Sharf and Silbey[46] and more recently by Metz.[47] Also, as we shall see below, the increase in decay rate as $S_1$ is excited with successively more quanta in a particular vibration; e.g., the CC-skeletal stretch in the aromatic hydrocarbons is greatest when this vibration is the best "accepting mode". Furthermore, the accepting quality of the CC stretch increases with electronic gap. Ordinarily the high-frequency CH stretches are the dominant accepting mode. But, for a large enough energy gap, deuteration allows the CC vibration to compete at short wavelength excitation since its frequency is comparable with the *CD* stretch's. Then the relative rate increase is so great as to offset the "normal" isotope effect.

### c. Contact with Literature

The derivation and interpretation of eq 30, of course, involved many oversimplifications: we neglected the contribution of all vibrations but the CH stretch, "pulled out" an electronic factor from the interaction energy and then overlooked its isotope dependence, etc. Nevertheless, this result illustrates many basic features of the "large" molecule radiationless decay rate, and it is appropriate here, before going into more details, to remark on work in the literature which is directly related to the above discussion.

(a) The replacement of sums by integrals in the "Golden Rule" expressions[26-28] and the subsequent evaluations of Franck–Condon factors involving nonintegral vibrational quantum numbers were first treated explicitly in the middle-to-late 60's by Siebrand.[45a-e] He generalized the $|\langle 0|n_1\rangle|_{n_1\to\gamma}$ appearing in eq 29 to allow for frequency changes and anharmonicity in addition to the shift in equilibrium position included above. Furthermore he provided for $N$-fold degeneracy in the accepting mode, as was required by his use of "local" CH stretches rather than the usual "normal" modes. (Later in this section when we treat the calculation of *relative* radiationless decay rates in benzene, we shall discuss the local- vs. normal-mode description of CH vibrations in the aromatic hydrocarbons.) Using a semiempirical expression for the generalized Franck–Condon factor in eq 29 he was able to correlate a great deal of data relating to the "energy gap law" and deuterium effect. Throughout his series of papers[45a-e] he also gives a discussion of the earlier work of Robinson and Frosch[6] and Ross and co-workers[7] which provided the roots for many of his ideas and those we have outlined above.

(b) In the late 60's, Lin and Bersohn[48] and Englman and Jortner[49] introduced a "many-phonon" theory of the radiationless transition Golden Rule rate, which formalism was borrowed from the work of Kubo and Toyozawa[50] and other solid-state physicists[51] on the spectra of trapped electrons and localized impurities in crystals. The point of departure in this approach is to introduce the Fourier-integral representation of the $\delta$ function in eq 38, i.e., $\delta(E) = 1/\hbar\delta(\omega) \equiv (1/2\pi\hbar)\int_{-\infty}^{+\infty} dt\, e^{i\omega t}$. Then it follows immediately that $k_{sl}(0)$ can be written as

$$k_{sl}(0) = (\beta_{el}^2/\hbar^2)\int_{-\infty}^{+\infty} dt\, e^{it\Delta E_{sl}/\hbar} f_1(t) \tag{31}$$

where

$$f_1(t) = \sum_{n_1} |\langle 0|n_1\rangle|^2 \exp(-it\omega_1 n_1) \tag{32}$$

The sum over $n_1$ in eq 32 can be evaluated in closed form for the case of harmonic oscillator wave functions. In the case of no frequency change, for example, $f_1(t)$ can be expressed exactly as $\exp(-x_1)\exp[x_1\exp(i\omega_1 t)]$ where $x_1$ is the dimensionless geometry change defined earlier. Evaluating[250] the integral in eq 31 within the saddle point approximation,[49,52-58] which is valid for $\Delta E_{sl}$ large enough compared with $\hbar\omega_1$, it is found that

$$\int_{-\infty}^{+\infty} dt \cdots \approx \frac{1}{\omega_1} e^{-x_1}\left(\frac{2\pi\hbar\omega_1}{\Delta E_{sl}}\right)^{1/2} \exp[-\Omega(\Delta E_{sl}/\hbar\omega_1)] \tag{33}$$

where $\Omega = \ln(\Delta E_{sl}/\hbar\omega_1 x_1) - 1$ as in eq 30a. Thus a result is obtained for $k_{sl}(0)$ *which is identical with eq 30.* This intimate connection between the many-phonon theory and the nonintegral quantum approach was first discussed by Siebrand[53] and Fischer.[54]

Recall that our earlier comment following eq 26 about how the sum over energy-conserving $\delta$ functions becomes $\rho_l(E_s)$ after an average of the slowly varying $v_{sl}^2$'s is pulled out of the Golden Rule sum. Avoiding this approximation we can either replace the discrete sum by a continuous one or, equivalently (as we have seen above), follow the procedure of the many-phonon formalism. It is in this sense that $|\langle 0|n_1\rangle|^2_{n_1\to\gamma}$ or equivalently, $\int_{-\infty}^{+} dt \ldots$ in eq 31, has come to be referred to as the "density of-states-weighted Franck–Condon factor". As mentioned earlier Siebrand[45] has treated semiempirical generalized $|\langle 0|n_1\rangle|^2_{n_1\to\gamma}$'s which allow for many accepting modes with anharmonicity, frequency changes, etc. Similarly, Freed and Jortner,[55] Fischer,[56] Freed, Heller, Prais, and Gelbart,[57,58] and Metz[59] have extended the many-phonon formalism to include the effects of many, displaced and distorted, accepting modes. Anharmonicity has proven to be the most difficult feature to treat simply and properly, and we shall discuss this point in some detail below.

(c) Christie and Craig[60] have "smoothed out" in a still different way the Golden Rule sum over rapidly varying Franck–Condon factors and energy conserving $\delta$ functions. They rewrite the sum in terms of its Laplace (rather than Fourier) integral and fit the latter to a carefully chosen approximation whose transform gives a smooth energy dependence for the rate. This method is again equivalent to (a) and (b) above, but it has not yet been thoroughly tested for particular molecules.

### d. Relative Rate Calculations

The calculation of *relative* radiationless decay rates, e.g., the change in rate as the excess vibrational energy in the initial electronic state is varied, has occupied the attention of many workers. Assuming that the overall interaction energies $\{v_{sl}\}$ can be factored into single products of electronic and vibrational overlaps, the ratio of decay rates reduces to a ratio of Franck–Condon sums. Thus one is spared the problems of evaluating the elusive $\beta_{sl}^2$. More explicitly, let us return to eq 27 and consider the case where: (a) all the $m_i$'s are zero *except* for $m_1$ (i.e., we excite successively higher overtones of the first vibrational mode, in the initial electronic state); and (b) all oscillators *but the first three* are constrained not to undergo changes in frequency,

anharmonicity, or equilibrium position in passing from initial to final electronic state (thus these oscillators must have the same quantum numbers before and after the radiationless transition). Henceforth "2" refers to the *best* accepting mode, "1" is the optically excited vibration ($m_1 \neq 0$) and "3" describes the remaining degree of freedom which is capable of taking up electronic energy.

Then, proceeding in analogy with the arguments leading earlier from eq 27 to eq 28 we can write immediately

$$k_{sl}(m_1) = \frac{2\pi}{\omega_1{}^l} \times \frac{\beta_{sl}{}^2}{\hbar^2} \sum_{n_1} |\langle m_1|n_1\rangle|^2 \sum_{n_3} |\langle 0|n_3\rangle|^2 |\langle 0|n_2\rangle|^2_{n_2=\gamma} \quad (34)$$

The nonintegral quantum number $\gamma$ is defined by $\Delta E(n_1,n_3)/\hbar\omega_2{}^l$ where $\Delta E(n_1,n_3) = \Delta E_{sl} + m_1\hbar\omega_1{}^s - n_1\hbar\omega_1{}^l - n_3\hbar\omega_3{}^l$ is the energy available to "2" in the lower ($l$) state. $\omega_i{}^s$ denotes the frequency of the $i$th vibration in the electronic state $s$, and so on. As will be discussed in exhaustive detail in the second half of this review, many experiments have been performed in which a molecule (benzene, say) is excited to its first singlet with successively more quanta in a particular vibration (the first, say). The corresponding radiationless decay rates are measured; when referenced to the decay rate of the zero-point level, they are given by

$$\frac{k_{sl}(m_1 \neq 0)}{k_{sl}(0)} = \frac{\sum_{n_1} \langle m_1|n_1\rangle|^2 \sum_{n_3} |\langle 0|n_3\rangle|^2 |\langle 0|n_2\rangle|_{n_2=\gamma(m_1)}}{\sum_{n_1} |\langle 0|n_1\rangle|^2 \sum_{n_3} |\langle 0|n_3\rangle|^2 |\langle 0|n_2\rangle|_{n_2=\gamma(0)}} \quad (35)$$

The Franck–Condon factors corresponding to *integral* quantum numbers $|\langle m|n\rangle|^2$ can be written as closed-form functions of $m$ and $n$, even in the general case where the oscillator involved is anharmonic and undergoes simultaneous geometry and frequency changes. The generalizations required for the evaluation of $|\langle 0|n_2\rangle|^2$ for *non*integral $n_2 = \gamma$ have been worked out by Kühn, Heller, and Gelbart.[61] [Recall that we presented before only the simplest such example, i.e., $|\langle 0|n\rangle|^2_{n\to\gamma} = \{e^{-x}x^n/n!\}_{n\to\gamma} = e^{-x}x^\gamma/\Gamma(\gamma+1)$ for the case of a harmonic oscillator undergoing only a shift in equilibrium position.] Thus for each value of $m_1$ the double sum over $n_1$ and $n_3$ in eq 35 can be computed straightforwardly, and a prediction of the relative rates obtained. One "only" needs to know the energy gap $\Delta E_{sl}$ and the frequencies, equilibrium positions, and anharmonicities of each of the accepting modes in each of the electronic states $s$ and $l$.

One of the problems that arises immediately, of course, is that, even for the much-studied benzene molecule, insufficient information is available on the vibrational structure. If we treat, for example, the $S_1 \rightsquigarrow T_1$ intersystem crossing, we need to know normal mode frequencies in the lowest triplet. (For $S_1$ these data are well known from analyses of vibrational progressions in the absorption spectra. No such direct, gas-phase measurement is possible in the case of $T_1$.) Evaluations of eq 35 have beer carried out in which the optically excited mode ("1") is the totally symmetric CC stretch, "2" is the high-frequency CH stretch, and "3" is the 521-$cm^{-1}$ ($S_1$) out-of-plane bend.

Table I shows the relative rates for several cases of initial excitation in both modes "1" *and* "3". The numbers given in the first column are the experimental[62] radiationless decay rates *relative* to that of the zero-point level. The third column gives the results of theoretical evaluation of eq 35; all three vibrations are treated as harmonic, with the following frequencies and geometry chances: $\omega_1{}^i = 923\ cm^{-1}$; $\omega_2{}^i = 3130\ cm^{-1}$; $\omega_6{}^i = 521\ cm^{-1}$; $\Delta\omega_1 \equiv \omega_1{}^f - \omega_1{}^i = +25\ cm^{-1}$; $\Delta\omega_2 = 0$; $\Delta\omega_6 = +50\ cm^{-1}$; $x_1 = 0.025$; $x_2 = 0.002$; $x_6 = 0$. ("i" and "f" refer to the initial ($S_1$) and final ($T_1$) electronic states in benzere, for which the energy gap $\Delta E_{sl}$ is roughly 8000 $cm^{-1}$; the results are quite insensitive to 20–30% changes in $\Delta E_{sl}$.) The second column in Table I shows the relative rates obtained[57,58] by use of the many-phonon theory and saddle-point approximation. This latter treatment, while giving essentially identical results with those calculated from eq 35, is not as easily extended to include frequency changes and anharmonicities in the best accepting modes.

**TABLE I. Comparison of $[k(1^n6^m2^0)/k(1^06^02^0)]$'s for $S_1 \rightarrow T_1$ in Benzene**

| | Rate, relative to zero-point level[a] | | |
|---|---|---|---|
| Level | (1) | (2) | (3) |
| $1^06^1$ | 1.19 | 1.14 | 1.15 |
| $1^16^0$ | 1.22 | 1.27 | 1.29 |
| $1^06^2$ | 1.27 | 1.32 | 1.33 |
| $1^16^1$ | 1.42 | 1.45 | 1.49 |
| $1^26^0$ | 1.73 | 1.62 | 1.69 |
| $1^16^2$ | 1.64 | 1.67 | 1.73 |
| $1^26^1$ | 1.94 | 1.84 | 1.94 |
| $1^36^0$ | 2.42 | 2.06 | 2.19 |
| $1^26^2$ | 2.67 | 2.12 | 2.25 |

[a] Obtained from: (1) experiment [K. G. Spears and S. A. Rice, *J. Chem. Phys.*, **55**, 5561 (1971)] (uncertainties are ≈10–15%); (2) the saddle point approximation;[57] and (3) the present calculation, i.e., eq 35. All three vibrations are treated as harmonic, with geometry changes and frequencies as in Table VIII of ref 57: $\omega_1{}^i = 923\ cm^{-1}$, $\omega_2{}^i = 3130\ cm^{-1}$, $\omega_6{}^i = 521\ cm^{-1}$; $X_1 = 0.025$, $X_2 = 0.002$, $X_6 = 0$; $\Delta\omega_1 \equiv \omega_1{}^f - \omega_1{}^i = +25\ cm^{-1}$, $\Delta\omega_2 = 0$, $\Delta\omega_6 = +50\ cm^{-1}$. Finally, $\Delta E_{sl} = 8200\ cm^{-1}$.

As mentioned earlier, and discussed elsewhere,[61] there is considerable uncertainty associated with the $x$'s and $\Delta\omega$'s for the $S_1 \rightsquigarrow T_1$ transition in benzene. Of course, $x \equiv 0$ for the nontotally symmetric modes (assuming that the molecule has $D_{6h}$ symmetry in both $S_1$ and $T_1$) while $x_1$ and $x_2$ are known to at best 50%. The frequency changes are still more uncertain; the magnitudes of the $\Delta\omega$'s deduced spectroscopically for modes 1, 2, and 3 could easily be off by tens of $cm^{-1}$. Accordingly, it is highly ambiguous which choices of the $x$'s and $\Delta\omega$'s are appropriate for evaluations of relative radiationless decay rates. Several years ago[57,58] it was found that the relative rate calculations were quite sensitive to small changes (i.e., within the above quoted uncertainties) in the $x$'s and $\Delta\omega$'s, and that only a very special choice of, say, $\Delta\omega_1$ and $\Delta\omega_3$ gave results in agreement with experiment. In this vein it was suggested that relative rate calculations could be used in conjunction with the measured values of $k_{sl}(m_1)/k_{sl}(0)$ to deduce the otherwise unknown $\Delta\omega_1$ and $\Delta\omega_3$. Subsequently it was shown[61] however, that the relative rate calculations were sensitive as well to $\Delta\omega_2$ (the frequency change in the best mode) and to anharmonicities in the vibrational motions. Thus there proves to be no unique choice for these parameters which accounts for the experimental data. This situation is, of course, exacerbated by the fact that the measured relative rates are themselves uncertain to as much as 10–15%.

Table II shows a compilation of ($\nu_{CC}$, $\nu_{CH}$, $\nu_{bend}$) parameter sets which give $[k(1^m)/k(0)]$'s in agreement with experiment. In the evaluations of eq 35 the vibrations were again taken to be harmonic: the $\omega^i$'s are known (and given above), the $\omega^f$'s (unknown) were varied within a few percent (10's of $cm^{-1}$) of the $\omega^i$'s, and the $x$'s within a factor of 2 about their estimated values. Note that no choices with $\Delta\omega_1 < 0$ gave agreement with experiment. Furthermore, it is found that even quite large parameter changes in a nonoptical, poor acceptor ($\nu_{bend}$ in this base) will not sensibly influence the relative rates. This fact is also established by looking at the effect of $\nu_{CC}$ parameter changes when $\nu_{CC}$ is not optically excited. That is, even though these changes influence strongly the $1^m2^03^0$ relative rates, they have virtually no effect on the $1^02^03^m$ progression. So it is sufficient to take only the

**TABLE II. Compilation of ($\nu_1$, $\nu_2$, $\nu_6$) Parameter Sets Which Give $[k(1^m)/k(0)]$'s in Agreement with Experiment [a]**

| $\Delta\omega_1$, cm$^{-1}$ | $X_1$ | $\Delta\omega_2$, cm$^{-1}$ | $X_2$ | $\frac{k(1^1)}{k(0)}$ | $\frac{k(1^2)}{k(0)}$ | $\frac{k(1^3)}{k(0)}$ |
|---|---|---|---|---|---|---|
| +25 | 0.025 | 0 | 0.002 | 1.29 | 1.69 | 2.19 |
| +25 | 0.060 | +10 | 0.002 | 1.36 | 1.82 | 2.42 |
| +50 | 0.025 | +10 | 0.002 | 1.30 | 1.72 | 2.31 |
| +50 | 0.038 | +20 | 0.002 | 1.29 | 1.69 | 2.22 |
| +25 | 0.025 | −9 | 0.001 | 1.20 | 1.70 | 2.90 |
| +25 | 0.025 | −22 | 0.003 | 1.30 | 1.80 | 2.60 |
| Experiment | | | | 1.2–1.4 | 1.6–2.0 | 2.1–2.8 |

[a] The vibrations are taken to be harmonic: $\omega^i$'s are known (see Table I caption), $\omega^f$'s (unknown) are varied within a few percent of the $\omega^i$'s, and $X$'s are within about a factor of 2. The $1^m$ relative rates are insensitive to $\nu_6$'s parameters, which latter are chosen as in Table I.

parameters of the optical and the *best* acceptors into account, while neglecting other modes. However, there are still several parameter sets which give comparably good agreement with experiment.

The qualitative effects of parameter changes in any mode can be straightforwardly understood in terms of its acceptor quality. Each mode competes for the available vibrational energy in the final state: the acceptor quality is a measure of its relative ability to do so. In general, an increase of the acceptor quality of a nonoptical mode will cause the decay rates to vary more slowly with increasing excitation. Conversely any improvement of the optical mode acceptor quality will enhance corresponding relative rates. [The increase in nonradiative rates can itself be explained by the fact that (in general) the more initial excitation a mode has the more easily it can change its vibrational quantum number in the radiationless transition (i.e., its acceptor quality increases).] The larger the $\nu_{CH}$ displacement, for example, the better its acceptor quality. The same holds for distortions, as long as $\omega^f > \omega^i$ ($\Delta\omega > 0$). That is, for $\Delta\omega_2 \gtrless 0$, a larger displacement and/or distortion in $\nu_2$ leads to smaller increases in the $\nu_1$ relative rates. In the limit where $\nu_2$ dominates $\nu_1$, further changes in its acceptor quality have no effect. For $\omega^f < \omega^i$ ($\Delta\omega < 0$) the most striking feature in plots of $[k(1^m)/k(0)]$ vs. $\Delta\omega_2$ is a sharp peak (maximum) in the relative rates as $\Delta\omega_2$ becomes large enough (10–30 cm$^{-1}$). Negative frequency changes cannot be expected to have a monotonic effect; a smaller vibrational frequency in the final electronic state tends to lower the acceptor quality (larger quantum number changes are necessary to conserve energy), while a further larger distortion can enhance it (less orthogonality of vibrational wave functions). So there are certain negative frequency changes that can make the $\nu_{CH}$ mode a worse acceptor, thus leading to an increase in the corresponding $\nu_{CC}$ relative rates.

### e. "Local" vs. "Normal" Modes

Consider now the effect of vibrational anharmonicity. This was first treated in a series of papers by Siebrand[45] in the late 1960's. Although these papers were widely read and quoted, the concept of "local" vs. "normal" molecular vibrations, introduced there for the first time, was largely overlooked by most workers in the field. Since this concept is important for our present discussion (and, in fact, for all of vibrational spectroscopy, intramolecular energy transfer and dissociation!) we shall review it briefly here.

As is well known, the familiar normal mode description of molecular vibrations is rigorous only in the limit of infinitesimally small nuclear displacements. Once any normal mode is excited with a few quanta, however, it begins to exchange energy with the other normal modes. At this point it must be questioned whether these normal modes still provide the "best" description of the vibrational degrees of freedom—"best" in the sense that the nuclear potential energy is most nearly separable. If, for example, a molecule like benzene were dissociated by heating or by laser light absorption, it is a *single* H atom (rather than all six) which would appear. Clearly it is not a single, symmetry adapted CH normal mode which is excited in this case, but rather a single "local" CH stretch. Such a picture is confirmed by the analyses of long progressions in the overtone spectra of benzene. The strongest of these is virtually identical with the vibrational spectrum of the diatomic radical CH, and is thus assigned to the "local" CH stretch in $C_6H_6$. Siebrand and Henry[63] and their co-workers, and more recently Wallace[64] and Albrecht et al.,[65] have presented very compelling analyses of the infrared spectra of a large number of hydrocarbons which suggest strongly the advantages of "local" mode descriptions for nuclear motion in these systems. We shall not treat this question further here except insofar as it relates to the calculations of radiationless transition rates.

As mentioned earlier, the "local" mode concept has been largely neglected in the radiationless transitions literature. In Siebrand's early papers,[45] it is suggested that the 24 non-CH-stretch vibrational degrees of freedom be described by the usual normal modes, with only the remaining (six) CH stretches regarded as local modes (i.e., bond length changes). Consider again our fundamental equation (35). To make contact with Siebrand's discussions, we shall use here his "$v$" instead of our "$\gamma$". Equation 35 involves the evaluations of double sums over $n_1$ and $n_3$, where the general term is $|\langle m_1|n_1\rangle|^2|\langle 0|n_3\rangle|^2|\langle 0|n_2 \rightarrow v\rangle|^2$; here $v \equiv (1/\hbar\omega_2{}^f)(\Delta E_{if} + m_i\hbar\omega_1{}^i - n_1\hbar\omega_1{}^f - n_3\hbar\omega_3{}^f - \hbar\omega_p{}^f)$. In the case discussed earlier, $|\langle 0|v\rangle|^2$ is the Franck–Condon factor for a *single* oscillator (the $A_{1g}$ CH-normal mode) which is harmonic with $x \neq 0$ but $\beta = 1$. That is, we have

$$|\langle 0|n_2\rangle|^2 = e^{-x}\frac{x^{n_2}}{n_2!} \xrightarrow{n_2 \rightarrow v} e^{-x}\frac{x^v}{\Gamma(1+v)} \qquad (36)$$

and the corresponding calculation of relative rates (via eq 35) is that reported in Table I.

Now suppose that we choose to describe the CH stretches by *local* rather than normal modes. In the latter case, only one of the six modes (the $A_{1g}$ CH stretch) served as an acceptor; the other five (a $B_{1u}$, two $E_{1g}$'s, and two $E_{2u}$'s) do not have the right symmetry ($A_{1g}$) to change their $Q_{eq}$. In the local mode case, on the other hand, *all six* CH stretches undergo the same bond length change and serve as acceptors. Thus we must generalize $|\langle 0|n_2\rangle|^2 = |\langle 0|v\rangle|^2$ according to

$$|\langle 0|v\rangle|^2 = \sum_{v_1}{}' \cdots \sum_{v_6}{}' \prod_{k=1}^{6} |\langle 0|v_k\rangle|^2 \qquad (37)$$

Here the $\Sigma_{v_1}{}' \ldots \Sigma_{v_6}{}'$ summation runs over all $v_1, \ldots, v_6$ such that $\Sigma_{k=1}^{6} v_k = v$; hence the primes on the summations. If each CH bond stretch is harmonic with $\bar{x} \neq 0$ and $\bar{\beta} = 1$, then eq 37 becomes (see eq 26–29 in Siebrands first paper[45a])

$$e^{-6\bar{x}}\bar{x}^v\left(\sum_{v_1}{}' \cdots \sum_{v_6}{}' \prod_{k=1}^{6}\frac{1}{v_k!}\right) = e^{-6\bar{x}}\bar{x}^v\left(\frac{6^v}{v!}\right) = e^{-6\bar{x}}\frac{(6\bar{x})^v}{\Gamma(1+v)} \qquad (38)$$

According to the local mode theory, then, this is the function of $v$ which should be used, instead of eq 36, for $|\langle 0|v\rangle|^2$ in eq 35. But $\Delta Q_{\nu_2} = (6)^{1/2}\Delta\nu_{CH} \Rightarrow x = 6\bar{x}$, so that there is no difference in this case between the local- and normal-mode formulations; i.e., eq 36 and eq 38 are identical.

For the case of CH bond stretches which involve $\bar{x} \neq 0$ *and* $\bar{\beta} = 1$ (i.e., frequency changes) and/or anharmonicity, it is no longer straightforward to evaluate the generalized Franck–Condon factor given by eq 38. Siebrand has discussed, however, two approximate evaluations.

(a) In the second paper[45b] of his series Siebrand derives the following, semiempirical result (we write $\gamma$ for his $v$):

$$|\langle 0|\gamma\rangle|^2 = F(0)\left(\frac{\lambda\gamma}{N_C}\right)^{\gamma}\Gamma(N_H+\gamma)/\Gamma(\gamma+1)\Gamma(N_H) \quad (39)$$

Here $\lambda$ is an experimentally determined[45b,c] constant which phenomenologically takes into account the anharmonicity and geometry and frequency changes associated with the CH bond-stretch. $N_H$ and $N_C$ are the number of H and C atoms, respectively, in the molecule under study.

(b) In a later paper,[45d] treating in particular the nonradiative decay of the first singlet ($S_1$) of benzene, it is argued that the sum in eq 37 is dominated by those six sets of $v_1, \ldots, v_6$ which correspond to all $v$ quanta in a single bond stretch and none in the others. Thus

$$(37) \approx 6(|\langle 0|0\rangle|^2)^5|\langle 0|\gamma\rangle|^2 = f|\langle 0|\gamma\rangle|^2_{\text{single oscillator}} \quad (40)$$

Here $f \equiv 6(|\langle 0|0\rangle|^2)^5$, being $\gamma$-independent, will cancel out in the calculation of relative rates. Using approximation 40, then, results in a theory, still based on eq 35, according to which $|\langle 0|n_2\rangle|^2_{n_2\to\gamma}$ simply corresponds to a nonintegral occupation-number Franck–Condon factor for a single *local* (vs. normal) mode oscillator.

As far as we are aware there are no published calculations which employ the local mode description to treat the effect of anharmonicity on relative rate calculations. In fact, all the literature on the vibrational quantum-number dependence of radiationless decay rates has been explicitly referenced to a *normal* mode description. Apart from Siebrand's series of papers[45a-d] the first studies of anharmonic Franck–Condon factors were offered by Burland and Robinson[66] and by Fischer and coworkers.[67,68] These calculations treated anharmonicities only through cubic and quartic terms in the individual oscillator potentials. Shimakura et al.[69] introduced the explicit use of Morse functions to describe the oscillator potentials, but they too neglected to treat the effect of anharmonicity on the vibrational quantum number dependence, i.e., on the *relative* rates. (Metz[59] has recertly proposed a scheme for calculating relative rates within the generating-function-saddle-point-integral framework which is not in principle restricted to the harmonic approximation, even though its application thus far still is.) Also, as mentioned above, all of these studies are based on the normal vs. local mode description of the molecular vibrations. Possibly the only exception is the discussion by Guttman and Rice[70] of their measured relative rates for the deuterated benzenes. Here, however, the use of local vs. normal modes was not introduced to treat anharmonicity, but rather to handle conveniently the successive breakings of vibrational symmetry as the molecule is deuterated one D at a time.

Kühn et al.[61] have determined in particular the effect of anharmonicity in the $\nu_1$ and $\nu_2$ modes on the relative rates for $S_1 \to T_1$ and $S_1 \to S_0$ decays in benzene. They analytically evaluated the Franck–Condon factor $|\langle 0|n_2\rangle|^2_{n_2\to\gamma}$ appearing in eq 35 for the case of a Morse oscillator, the integral occupation-number Franck–Condon factor, $|\langle m_1|n_1\rangle|^2$, for the optically excited $\nu_1$ mode is much more straightforward to compute. Recall that each Morse oscillator is characterized by the potential energy $U(Q) = D[1 - \exp\{-\alpha(Q - Q_{eq})^2\}]^2$ with bound state energies $E_n = \hbar\omega(n + \frac{1}{2}) - \kappa(n + \frac{1}{2})^2$. Here $\kappa = (\hbar\omega)^2/4D$, where $D$ is the dissociation erergy, and $\omega = \alpha(2D/M)^{1/2}$ the "fundamental frequency". (M is the mass associated with the normal coordinate.)

The computations of Kühn et al.[61] demonstrate that even though the $S_1 \rightsquigarrow T_1$ radiationless decays are essentially unaffected by $\nu_1$ anharmonicity, they *do* depend somewhat on the $\nu_2$ anharmonicity. Taking the $\kappa$ and $\alpha$ values reported by Burland and Robinson[66] for $\nu_2$ in the ground electronic state, it is found that: (a) the absolute magnitude of the decay rates is increased by as much as a factor of 10; and (b) the observed *relative* rates

**TABLE III. $k_{vib}(0)$ and $[k(1^m)/k(0)]$ ($m$ = 1–5) for $S_1 \to S_0$ in Benzene, with and without $\Delta\omega_2 \neq 0$, $\kappa_2$, $\alpha_2 \neq 0$, and Local Modes[a]**

| | | Rel rates $k(1^m)/k(0)$, $m$ = | | | | |
|---|---|---|---|---|---|---|
| | $k_{vib}(0)$ | 1 | 2 | 3 | 4 | 5 |
| | (a) Harmonic Case | | | | | |
| (1) | $0.91 \times 10^{-24}$ | 10 | 63 | 307 | 1254 | 4588 |
| (2) | $0.14 \times 10^{-23}$ | 6.7 | 29 | 9 | 367 | 1139 |
| | (b) Morse $\nu_2$ (normal modes) | | | | | |
| (3) | $0.29 \times 10^{-19}$ | 3.5 | 10 | 24 | 55 | 118 |
| (4) | $0.65 \times 10^{-18}$ | 2.8 | 6.6 | 14 | 28 | 53 |
| | (c) Morse $\nu_2$ (local modes) | | | | | |
| (5) | $0.16 \times 10^{-17}$ | 1.7 | 2.7 | 4.0 | 5.7 | |
| (6) | $0.47 \times 10^{-16}$ | 2.0 | 3.6 | 6.1 | 9.8 | |

[a] The parameter sets for the six reported calculations are (with $\omega_1^i$ = 923 cm$^{-1}$, $\omega_1^f$ = 990 cm$^{-1}$, $\omega_2^i$ = 3130 cm$^{-1}$, and $X_1$ = 1.3 *in all but the sixth*): (1) $\omega_2^f$ = 3130 cm$^{-1}$, $X_2$ = 0.06, i.e., $\Delta\omega_2 = 0$, $\kappa_2, \alpha_2 = 0$ as in earlier calculations; (2) $\omega_2^f$ = 3063 cm$^{-1}$, $X_2$ = 0.036; (3) $\omega_2^f$ = 3063 cm$^{-1}$, $\Delta Q_2$ = −0.028 Å, $\kappa_2$, $\alpha_2$ = 9.2 cm$^{-1}$ 0.714 Å$^{-1}$; (4) 3063 cm$^{-1}$, −0.028 Å, 12.6 cm$^{-1}$, 0.834 Å$^{-1}$; (5) $\omega_2^f$ = 3063 cm$^{-1}$, $\Delta Q_2$ = −0.028 Å/(6)$^{1/2}$ ≈ −0.01 Å, $\kappa$ = (9.2 cm$^{-1}$)(6) ≈ 55 cm$^{-1}$, $\alpha$ = +714 Å$^{-1}$) (6)$^{1/2}$ ≈ 1.8 Å$^{-1}$; (6) $\omega_2^i$ = 3273 cm$^{-1}$, $\omega_2^f$ = 3183 cm$^{-1}$, $\Delta Q_2 \approx -0.01$ Å, $\kappa \approx 55$ cm$^{-1}$, $\alpha \approx 1.8$ Å$^{-1}$.

can be fit by choosing somewhat different sets of geometry and frequency changes from those displayed in Table II. This latter result points up again the ambiguities, mentioned earlier, which surround the theoretical interpretation of relative rates.

Consider now the $S_1 \rightsquigarrow S_0$ transition. Since so much more electronic energy is converted here into vibrational excitation than in the $S_1 \rightsquigarrow T_1$ case, it is reasonable to expect larger anharmonicity effects. The possible implication of the $S_1 \rightsquigarrow S_0$ internal conversion in the nonradiative decay of the first excited singlet of benzene has been discussed elsewhere (see, for example, ref 58). A well-known (but not yet understood) property of this first excited state is the relatively sharp onset of diffuseness in the high resolution absorption spectrum.[71] Thus line broadening for the $1^n6^m$ levels with vibrational energy in excess of ≈3000 cm$^{-1}$ and the corresponding cut-off in fluorescence[72] indicate the onset of a fast nonradiative decay channel ("channel 3"). Rough theoretical estimates[58] suggest that, because of the huge energy gap involved, the ratio of $S_1 \rightsquigarrow S_0$ to $S_1 \rightsquigarrow T_1$ decay rates for the $S_1$ zero-point level might be as small as $10^{-9}$. It is for this reason, of course, that the nonradiative relaxation of the first singlet is commonly treated as an intersystem crossing. Because the rate of $S_1 \rightsquigarrow S_0$ internal conversion increases much faster with vibrational excitation, however, this process could conceivably become competitive with the faster but essentially constant (within a factor of 2) $S_1 \rightsquigarrow T_1$.

The $\nu_1$, $\nu_2$, and $\nu_3$ frequency and geometry changes are well established experimentally[73] for the $S_1 \rightsquigarrow S_0$ transition. Within the normal mode description, the anharmonicities are also known.[66] Table III shows the results obtained by Kühn et al. for the relative nonradiative $1^m$ rates and for the absolute magnitude of the zero-point level. $k_{vib}$ is given by

$$\frac{2\pi}{\hbar\omega_2^f}\sum_{n_1}|\langle m_1|n_1\rangle|^2 \times \sum_{n_3}|\langle 0|n_3\rangle|^2|\langle 0|n_2\rangle|^2_{n_2\to\gamma} \equiv k_{vib}(m_1) \quad (41)$$

i.e., it is the actual decay rate divided by the square of the "electronic factor" which later has been assumed independent of vibrational excitation. In (a) are compared the results for the harmonic approximation with and without the frequency shift in $\nu_2$; previous calculations had taken $\Delta\omega_2 = 0$. It is seen that the distortion in $\nu_2$ leads to a slightly higher $k_{vib}$, but at the same time to a slower increase in the relative $1^m$ rates. This effect, caused by the enhancement of the acceptor quality of $\nu_2$, can be seen

even more clearly when a Morse potential in $\nu_2$ is involved (see (b)). ($\Delta Q_2 = (Q_{eq}^{S_1} - Q_{eq}^{S_0})_2 = -0.028$, as determined in the early work of Craig.[74]) $k_{vib}$ becomes larger by as much as four to five orders of magnitude but the relative rates are less steep. Because of the problems mentioned earlier regarding the calculation of the electronic matrix elements, a direct comparison of these computations with experimental lifetime measurements is not possible. Qualitatively it is obvious, though, that inclusion of the Morse potential enhances (compared to the harmonic case) the $S_1 \rightsquigarrow S_0$ rates much more than the $S_1 \rightsquigarrow T_1$. Taking the estimate given by Prais et al.[58] for the relation between the vibrationless IC and ISC rates (harmonic value) of $\approx 10^{-9}$, we see that even the enhancement due to the anharmonicity in $\nu_2$ will at best make the IC rate "only" a 1000 times smaller than the ISC rate (for excess energies around $m_1 = 5$). For the IC rate to be much higher than the ISC rate, and to thereby account for the diffuseness of these levels and the fluorescence cut-off, it is necessary to include the concept of excitation dependent electronic matrix elements as discussed below.

First, though, we consider how the effect of anharmonicity on absolute and relative rates is changed when the CH stretches are treated as *local* rather than normal modes. As explained earlier, we can do so by evaluating eq 39 or 40 for $|\langle 0|\gamma\rangle|^2$. Using eq 40 is more appropriate for the present discussion since it involves an a priori (instead of empirical) calculation of the anharmonic Franck–Condon factor. Recall that the evaluation of $|\langle 0|\gamma\rangle|^2_{(40)}$ proceeds exactly as before; that is, the analytical expression for $|\langle 0|n_2\rangle|^2_{Morse}$ is simply generalized to nonintegral $n_2(\rightarrow\gamma)$, except that the anharmonicity and geometry and frequency changes are now those of a single CH-bond stretch, rather than those of the $A_{1g}$ CH-normal mode. Thus[63] $\Delta Q_2 \rightarrow \Delta Q_2^{normal}/(6)^{1/2}$, $\kappa_2 \rightarrow \kappa_2(6)$ and $\alpha_2 \rightarrow \alpha_2(6)^{1/2}$. ($f \equiv 6(|\langle 0|0\rangle|^2)^5 \approx 6$ since $|\langle 0|0\rangle|^2 \approx 1$.) The results for the absolute and relative $S_1 \rightsquigarrow S_0$ rates are shown in part (c) of Table III: the first entry corresponds to taking the initial and final oscillator frequencies equal to those of the $A_{1g}$ CH-*normal* mode; the second to choosing the *local* mode values suggested by Lawetz, Siebrand, and Orlandi.[75] These results are consistent with entries 3 and 4 in part (b) which show that an increase in $\kappa,\alpha$ implies a larger absolute rate and a smaller increase in relative rates. In the local mode case (entries 5 and 6) the huge $\kappa,\alpha$ increase is partially offset by the smaller $\Delta Q$.

[The effect of anharmonicity on the $S_1 \rightsquigarrow T_1$ transition was mentioned earlier (in our discussion of the normal mode description) to be small. Preliminary calculations within the *local* mode formulation (see above, and ref 61) support this conclusion.]

From Table III and the above few paragraphs, it is clear that $S_1 \rightsquigarrow S_0$ internal conversion cannot account for the superfast "channel 3" in benzene, even when a full account is taken of anharmonicity and geometry and frequency changes. Related calculations by Prais et al.[58] and Lawetz et al.[75] have led to similar conclusions. In the case of the aliphatic ketones and naphthalenes, on the other hand, Gillispie and Lim[76] and Beddard et al.[77] (see also Fischer et al.[78]) have argued that the sharp decreases observed for fluorescence lifetimes and quantum yields might indeed be explained by the fast increases in $S_1 \rightsquigarrow S_0$ relative rate. As discussed by Kühn et al.[61] and by Freed,[10] the "benzene problem" must lie with the assumption (see beginning of this section) that the overall interaction energy $v_{sl}$ can be written as a single product of an electronic factor $\beta_{sl}$ and a vibrational overlap integral.

Prais et al.[58] and Freed and Lin[42] have argued in particular that the observed "channel 3" behavior in benzene is qualitatively consistent with the hypothesis that the $S_1 \rightsquigarrow S_0$ decay is additionally enhanced by a sharp increase in the *electronic* factor as $\nu_1$ is excited. The geometry change $x_1^{S_1-S_0}$ is especially large in benzene, and we have seen as a result that excitation of $\nu_1$ in $S_1$ makes the $\nu_1$ vibration a much better accepting mode, competitive with $\nu_2$. It has also been argued that this means the electronic factor is no longer weakly dependent on $Q\nu_1$ since the $Q$ centroid (see end of section 3) for that mode begins to deviate considerably from the equilibrium position, tending toward a surface crossing. It is this $m_1$ dependence of the $Q$ centroid which accounts for the sharp increase in $\beta_{el}$ with $m_1$. In the fully deuterated molecule this effect should be even more pronounced since $\nu_1$ competes still more effectively with $\nu_2$ as an acceptor. Experiment bears this out: diffuseness sets in faster as the $\nu_1$ progression is excited. More work on the nature of "channel 3" and the breakdown of the factorization approximation is needed before firmer conclusions can be reached. For further discussion of this point, see ref 58, 61, 10, and 42.

Recall that $S_1 \rightsquigarrow S_0$ is suspected[58,75-78] of taking over the $S_1$ radiationless decay of large molecules since its relative rates increase so much faster with vibrational excitation than do $S_1 \rightsquigarrow T_1$'s. This is because relative rate increases are more dramatic for larger energy gaps (and/or larger geometry and frequency changes[251]). An interesting new view of this possibility has been advanced by Lim and Fischer and their co-workers.[80,82] In naphthalene,[81] for example, the nonradiative decay rate of the first singlet state increased linearly with energy as long as the exciting wavelength is long enough; progressions are seen in the totally symmetric skeletal vibrations. At shorter wavelengths the optical excitation prepares naphthalene in its $S_2$ singlet. $S_2$ then undergoes rapid internal conversion to give $S_1$, which carries most of its vibrational energy in the high-frequency CH stretches. At these shorter wavelengths the relative rate increase in $S_1$ is expected to be different from that at the longer wavelengths since the CH stretches undergo different changes in anharmonicity, geometry, and frequency than do the CC skeletal vibrations. In fact, the radiationless rate increase, which began as a linear function of excess energy becomes exponential in the region above $S_2$. This suggests that a much larger energy gap might be involved, as would be the case if $S_1$ were beginning to relax into $S_0$ instead of $T_1$. Indeed, in the same optical wavelength region where the $S_1 \rightsquigarrow T_1$ process appears to be overtaken by $S_1 \rightsquigarrow S_0$, the measured triplet yield is found to drop off significantly.

It should already be clear that the benzene example, which we have considered in detail earlier in this section, provides insights into several general features of intramolecular radiationless transitions in large polyatomics. In particular, the conclusions concerning the dependence of relative rate increases on deuteration, energy gap, anharmonicity, and geometry and frequency changes are expected to carry over to other molecules. We have already referred in this context to many studies on the deuterated, halogenated, and otherwise (e.g., methyl-, amine-) substituted benzenes and naphthalenes, etc. Later, in the discussion of experimental results, we shall make mention of several more theoretical features of the radiationless decay processes.

## B. The Case of Smaller than "Large" Molecules

### 1. General Remarks

#### a. Introduction

Recall that the hallmarks of radiationless transitions in "large" molecules include the following: (a) In the zero pressure limit, the decay of an electronically excited state S is exponential with a rate exceeding $k_{rad}^S$. (b) Pressure dependence appears only when $P$ is high enough for vibrational relaxation to take place within S. As an introduction to the "small" and "intermediate" molecule cases, we consider the following experimental data for sulfur dioxide ($SO_2$) and methylglyoxal ($CH_3COCOOH$), respectively.

*$SO_2$.* When $SO_2$ is excited (bandpass $\approx 3$ cm$^{-1}$, pulse duration $\approx 10^{-7}$ s) in the region of 3400–2500 Å at low pressures (1–50 mTorr), the emission intensity is found in general to be biexponential.[83] The short and long lifetimes observed are $\approx$50–600

$\mu$s and are dramatically dependent on pressure: $(1/\tau) \approx (1/\tau)_{P=0} + k_c P$. Here $k_c$, the collisional quenching rate constant, is on the order of (and greater than) the gas kinetic value. The radiative lifetime estimated from the integrated absorption coefficient for the 3400–2500-Å transition is as short as $10^{-7}$ s. The $P \rightarrow 0$ fluorescence quantum yield is unity. Thus we have a situation where the emission rate is orders of magnitude *slower* than what would be expected from the pure radiative decay ($k^S_{rad}$), even though $\phi_F = 1$. Also, the pressure quenching of fluorescence is orders of magnitude *faster* than typical collisional deactivation of electronically excited states. Similar results are found for $NO_2$[84] and (to a lesser extent) $CS_2$.[85]

*$CH_3COCOOH$.* Here again the emission decay following short-pulse ($\lesssim 10^{-8}$ s), narrow bandpass ($\lesssim 5$ cm$^{-1}$) excitation at low pressures ($\lesssim 1$ Torr) is biexponential;[86,87] $I(t) = I^0_{fast} \exp(-\lambda_f t) + I^0_{slow} \exp(-\lambda_s t)$. For $P \lesssim 0.1$ Torr, the fast rate $\lambda_f$ is independent of pressure, but increases with excitation energy. $\lambda_s$ varies with $P$ according to $\lambda_s = (\lambda_s)_{P=0} + k_c P$ where $k_c$ is slightly higher than the gas kinetic rate. At higher pressures ($P > 2$ Torr) the slow decay component vanishes and $I(t) \rightarrow I_f \exp(-\lambda_f t)$. In this $P$ region $\lambda_f$ acquires pressure dependence, increasing or decreasing according to the temperature and exciting wavelength. For $P > 200$ Torr, $\lambda_f$ is constant for all wavelengths and pressures. Finally, $\lambda_f$ is always two orders of magnitude faster than the pure radiative rate. Similar behavior is observed for the homologous dicarbonyls $CH_3COCOCH_3$ (biacetyl) and HCOCOH (glyoxal).[86]

The data cited in the above examples provide prototypes for the "small" molecule "lifetime lengthening" and "intermediate"-case "reversible radiationless transitions" which have been well documented in the recent literature. The details of the experimental observations for these and other systems are discussed in later sections of this review. Numerous theoretical treatments have been offered to account for these effects; virtually all of them have employed either the damping matrix (effective Hamiltonian) formalism, or Green's function (resolvent operator) techniques.[10] These two methods make most people a little nervous. Also, as we shall argue, their rigor and detail are somewhat inappropriate to the present state of knowledge about molecular vibrational structure and interelectronic interactions. In the present section, then, we discuss simple qualitative theories of "small"- and "intermediate"- case behavior which explain a wide variety of observed results (those cited above). We emphasize that the apparently anomalous features mentioned above are just as natural as those characterizing the "large" molecule case. Contact is made with many of the expressions derived in the more formal, sophisticated theories, and references to more detailed discussions of these effects are given. We start with a very brief treatment of the $SO_2$ example, and then focus on methylglyoxal.

### b. "Small" Molecules

The anomalously long-lived fluorescence and large quenching cross sections in $SO_2$ ($NO_2$, $CS_2$, etc.) can be readily accounted for in the molecular eigenstates picture. Recall from section A.2 that the interactions $v_{sl}$ between the emitting state $|S\rangle$ (the first excited singlet, say) and the nonemitting states $\{|l\rangle\}$ (e.g., vibrationally excited triplet levels) can be diagonalized to give linear combinations

$$|\psi_n\rangle = C_n^S|S\rangle + \sum_l C_n'|l\rangle \qquad (42)$$

which are eigenfunctions of the full molecular Hamiltonian. We discussed there also how coherent excitation leads to an initial state

$$|\psi(0)\rangle = \sum_{(E_n \text{ in } \Delta E)} \langle \psi_n|\mu|g\rangle |\psi_n\rangle = \mu_{gS} \sum_{(\Delta E)} C_n^S|\psi_n\rangle \qquad (43)$$

where the sum is over all molecular eigenstates whose energies $E_n$ lie within the exciting light's bandpass $\Delta E$. If $\Delta E$ is big enough to include all states $|\psi_n\rangle$ which have $\langle S|\psi_n\rangle \equiv C_n^S \neq 0$, then $|\psi(0)\rangle = \mu_{gs}\Sigma_n|\psi_n\rangle\langle\psi_n|S\rangle = \mu_{gS}|S\rangle$ "=" $|S\rangle$. This is a hallmark of the statistical limit.

In triatomics such as $SO_2$, on the other hand, the interaction energies $v_{sl}$ are often larger than hundreds of cm$^{-1}$; this arises from Renner effects involving the ground (≈bent) and excited (≈linear) electronic states. Also, the $\{|\psi_n\rangle\}$ are spaced widely enough apart so that under typical laboratory conditions the sum in eq 43 includes only one or a small number of the molecular states for which $\langle S|\psi_n\rangle \neq 0$. Each of these carries oscillator strength porportional to $|\langle\psi_n|\mu|g\rangle|^2 = \mu_{gS}^2|C_n^S|^2$ and each $|C_n^S|^2 \ll 1$. Thus the $|\psi_n\rangle$ fluorescence lifetimes are expected to be much longer than that which would be calculated from the integrated absorption coefficient. The oscillator strength ($\mu_{gS}^2$) associated with $|S\rangle$ has been "spread out" over a large number of molecular states. This accounts as well for the appearance of many "new" (and unassigned) lines in the high-resolution spectrum. In the absence of large interelectronic perturbations only regular progressions in $S$ would be observed. Also, because the nonemitting states $\{|l\rangle\}$ include highly vibrationally excited levels of the ground electronic state, we expect the $|\psi_n\rangle$'s given by eq 42 to be collisionally deactivated at a gas kinetic rate.[88] In the limit of "zero" pressure, however, the fluorescence quantum yields associated with excitation of the $|\psi_n\rangle$ states would be unity; i.e., there is no radiationless transition.

The above arguments are confirmed by Brus and McDonald in their comprehensive studies of $SO_2$ excited state dynamics.[83] They also treat in detail the interelectronic perturbations involving the low-lying singlets and discuss many of the more subtle features of the emission kinetics (which we have only hinted at above). Theoretical formulations of the "small" molecule case had been provided earlier by several authors.[16b,85,89] We do not pursue this theory further here since it is less germane to our overview of radiationless transitions than is the "intermediate" case discussed below.

## 2. *"Intermediate" Molecules*

### a. Weak Coupling

The excited state dynamics in methylglyoxal serve as an excellent prototype for the "reversible radiationless transitions" which have recently interested many investigators.[90] We have outlined briefly in section 2 above the experimentally observed behavior for such a system. Let us rationalize these results as follows. Suppose for the moment that each vibrational level of $S_1$ interacts weakly with a single $T_1^*$ level. Here the asterisk reminds us that the $T_1$ level, lying in the energy region of $S_1$, is vibrationally excited. (We will allow later for an arbitrary number of $T_1^*$ levels.) Then the molecular eigenfunctions corresponding to such a pair can be written as

$$|\psi_1\rangle = (1-\epsilon)^{1/2}|S_1\rangle + \epsilon^{1/2}|T_1^*\rangle$$
$$|\psi_2\rangle = \epsilon^{1/2}|S_1\rangle - (1-\epsilon)^{1/2}|T_1^*\rangle \qquad (44)$$

where, from first-order perturbation theory, $\epsilon^{1/2} = v/(E_{S_1} - E_{T_1^*}) \ll 1$. As discussed in section A.2, it is possible to prepare the system initially in the state $|S_1\rangle$, since the $|T_1^*\rangle$ states do not carry oscillator strength and the exciting light bandpass is broad enough. Thus $|\psi(0)\rangle = |S_1\rangle$. But this initial state does not decay exponentially. Instead the excited state emission is a superposition of the radiative decays of the molecular eigenstates $|\psi_1\rangle$ and $|\psi_2\rangle$ (plus some oscillatory terms which are of negligible amplitude in the weak coupling limit; see later discussion).

Note that the electric dipole transition moments associated with $|\psi_1\rangle$ and $|\psi_2\rangle$ are $\langle g|\mu|\psi_1\rangle = (1-\epsilon)^{1/2}\mu_{gS}$ and $\langle g|\mu|\psi_2\rangle = \epsilon^{1/2}\mu_{gS}$, respectively. This follows from eq 44 and from the fact that $\langle g|\mu|T_1^*\rangle \equiv 0$. Since radiative rates are proportional

to the square of dipole transition moments, $|\psi_1\rangle$ will decay with a rate $(1-\epsilon)k_{rad}^{S_1} + k_{NR}^{S_1}$, and $|\psi_2\rangle$ with a rate $\epsilon k_{rad}^{S_1} + k_{NR}^{T_1^*}$. Each of the nonradiative rates can be written as the sum of a zero pressure contribution and a collisional deactivation term: $k_{NR} = (k_{NR})_{P\to 0} + k_c P$. The zero pressure $k_{NR}$ for $S_1$ is associated here with $S_1 \rightsquigarrow S_0$ internal conversion, say, while $k_{NR}^{T_1^*}{}_{P\to 0}$ corresponds to $T_1 \rightsquigarrow S_0$ intersystem crossing. Thus we have, following pulse excitation of $|S_1\rangle$, that the emission intensity will fall off according to

$$I(t) = I_f^0 \exp(-\lambda_f t) + I_s^0 \exp(-\lambda_s t) \tag{45}$$

where

$$\lambda_f = (1-\epsilon)k_{rad}^{S_1} + (k_{NR}^{S_1})_{P\to 0} + k_c^{S_1} P \tag{45a}$$

$$\lambda_s = \epsilon k_{rad}^{S_1} + (k_{NR}^{T_1^*})_{P\to 0} + k_c^{T_1^*} P \tag{45b}$$

and

$$I_s^0/I_f^0 = \epsilon/(1-\epsilon) \tag{45c}$$

Now $k_c^{S_1} \ll k_c^{T_1^*}$ since the collisional deactivation rate constant is expected to be much greater in the $T_1^*$ state than in $S_1$. This follows from the fact that $\psi_2$ fluorescence is quenched as soon as the molecule is relaxed out of its narrow ($\lesssim 1$ cm$^{-1}$) $S_1$–$T_1$ interaction zone into the region of *pure* (and hence nonemitting) triplet. Also, because the $S_0$–$S_1$ and $S_0$–$T_1$ energy gaps are comparable in the dicarbonyls,[86,87] $(k_{NR}^{S_1 \rightsquigarrow S_0})_{P\to 0} \gg (k_{NR}^{T_1 \rightsquigarrow S_0})_{P\to 0}$. Finally, $\epsilon \ll 1$ means that $(1-\epsilon)k_{rad}^{S_1} \gg \epsilon k_{rad}^{S_1}$. Thus we expect that the $\psi_1$ decay rate ($\lambda_f$) will be essentially independent of pressure, whereas the $\psi_2$ rate ($\lambda_s$) will be dominated by the $k_c^{T_1^*} P$ term. The actual pressure dependence observed for $\lambda_s$ by Coveleskie and Yardley[87] can be fit to our eq 45b where $[\epsilon k_{rad}^{S_1} + (k_{NR}^{T_1^*})_{P\to 0}] \approx 2.5 \times 10^5$ s$^{-1}$ and $k_c^{T_1^*} \approx 5.3 \times 10^7$ s$^{-1}$ Torr$^{-1}$. A similar experiment, with methylglyoxal pressure fixed at 7 mTorr and argon pressure varying up to 100 mTorr, also gives a linear plot but with smaller slope ($\approx 2.1 \times 10^7$ s$^{-1}$ Torr$^{-1}$), corresponding to the fact that argon is less efficient a quencher than methylglyoxal. Note that $k_c^{T_1^*}$'s on the order of $2\text{–}5 \times 10^7$ s$^{-1}$ Torr$^{-1}$ are considerably larger than gas kinetic values, which is not unreasonable for collisional relaxation in the triplet. As we have mentioned above and as van der Werf et al.[86] have stressed, collisions in $T_1$ can be very weak and long-ranged since they quench emission by simply carrying off enough energy to remove the molecule from its interaction region with $S_1$.

According to eq 45c the ratio of initial intensities for the slow and fast emissions is $\epsilon/(1-\epsilon)$, and hence very small compared with unity. As $P$ increases, this ratio remains constant while $\lambda_s$ increases; for $P$ large enough, then, we expect that $|\psi_2\rangle (\approx |T_1^*\rangle)$ is collisionally relaxed so fast that its emission is quenched. In this case only $|\psi_1\rangle$ emission is observable and $I(t)$ will be given by a single exponential. This is displayed in Coveleskie and Yardley's[87] Figure 4 where $I(t)$ is shown on a semilog plot for a methylglyoxal pressure of 70 mTorr with added argon pressures up to 2.45 Torr. Total pressures of a couple Torr are apparently sufficient to relax $|\psi_2\rangle$ before it has a chance to emit.

Pressure of a few Torr, however, are *not* sufficient to vibrationally relax $|\psi_1\rangle$ ($\approx |S_1\rangle$). Thus we expect that the fast emission rates ($\lambda_f$) will depend on the wavelength of the exciting light, i.e., on the particular vibrational level to which $|S_1\rangle$ corresponds. [Recall that $\psi_f \approx (1-\psi)k_{rad}^{S_1} + (k_{NR}^{S_1 \rightsquigarrow S_0})_{P\to 0}$. $\lambda_f$ is found[86,87] to be as big as $10^7\text{–}10^8$ s$^{-1}$, whereas $k_{rad}^{S_1}$ is estimated from integrated absorption coefficients to be at least two orders of magnitude smaller.] At total pressures of 5 Torr (0.1 Torr methylglyoxal, 5 Torr argon), $\lambda_f \approx k_{NR}^{S_1}$ is indeed found to depend on excitation wavelength; see Figure 3 in Coveleskie and Yardley.[87]

It is only at much higher pressures ($\gtrsim 100$ Torr) that $\lambda_f$ acquires $P$ dependence. At these higher pressures there are enough collisions per second to begin driving the initially excited vibrational level of $S_1$ into its neighbors. Figure 2 of Coveleskie and Yardley[87] shows the dependence of $\lambda_f$ on pressure for exciting wavelengths of $\lambda$ 4492 Å and 4193 Å. $\lambda$ 4492 Å corresponds to excitation of $S_1$ at its origin, whereas 4193 Å involves an excess vibrational energy of $\approx 2000$ cm$^{-1}$. Thus, for example, in the 4492-Å case, thermal equilibrium drives the optically prepared $S_1$ level into neighbors which have higher vibrational energy. Hence we expect the $\lambda_s$ rate for 4492 Å to increase with pressure. This is precisely what is seen. And, similarly, the $\lambda_s$ rate for 4193 Å is found to *decrease* with pressure. Only for pressures greater than $\approx$ 200 Torr is the $S_1$ state thermally equilibrated. For $P > 200$ Torr, then $\lambda_f$ depends only on temperature (which fixes the mean excess vibrational energy in $S_1$), and not on pressure or exciting wavelength.

### b. Contact with Literature

The weak coupling ($\epsilon \ll 1$) mixed-state theory which we have used above to explain the observed methylglyoxal fluorescence behavior is surely not general, and involves much oversimplification. Its basis is heuristic rather than rigorous. Nevertheless, it is qualitatively consistent with the more sophisticated and detailed theories[10] which have been based on the Green's function and damping matrix methods. Consider, for example, the discussion by Nitzan, Jortner, and Rentzepis[91] in which the above two-state model is treated by effective Hamiltonian methods. They study, essentially exactly, the emission dynamics of an excited molecule in which an emitting state ($S$) interacts with a single nonemitting state ($I$). The $S$ and $I$ states each have widths ($\gamma_S$ and $\gamma_I$) corresponding to radiative ($k_r$), nonradiative ($k_{NR}$) and collisional ($k_c P$) deactivation. They show that in the weak coupling limit ($v_{sI} \ll E_S - E_I$) where $\gamma_I, \gamma_S \ll E_S - E_I$, the emission is biexponential. [See their eq 3.17a,b and 3.18, p 379.] Their additional term, arising from the fact that the mixed states do not quite decay independently, is a damped oscillatory term $[\approx 2\epsilon \exp\{-[\gamma_I + \gamma_S/2]t\} \cos(\Delta E t)]$ of negligible amplitude in the weak coupling limit.] $\gamma_f$ is shown to be $\approx \gamma_S \leftrightarrow k_{rad}^{S_1} + (k_{NR}^{S_1})_{P\to 0}$, while $\gamma_s \approx \gamma_I + \epsilon\gamma_S$ where $\epsilon = v_{sI}^2/(E_S - E_I)^2$ as before. Writing the width $\gamma_I$ as $(k_{NR}^{T_1^*})_{P\to 0} + k_c^{T_1^*} P$, we see that these expressions for $\gamma_s$ and $\gamma_f$ have essentially the same form as our eq 45a,b. The ratio of initial intensities for the slow and fast emissions is similarly found to be $\approx \epsilon$, in agreement with our eq 45c.

### c. Strong Coupling

Having established contact between our heuristic theory and a more rigorous approach, it is interesting to note here that Nitzan et al.[91] have generalized their treatment of the weak coupling limit to include an arbitrary number of $T_1$ states. This extension makes the model more realistic and yet leads to essentially the same emission dynamics. Instead of a single slow decay, one simply has many of them. The longer lived emission is thus multiexponential in general, but $\lambda_f$ and $(\lambda_s)_{av}$ are still characterized by the same pressure dependences, etc. Nitzan et al. have also treated the case where $\gamma_S, \gamma_I$ are not necessarily small compared with $E_S - E_I$, and have discussed the possibility of interference effects in the overall decay of $|\psi(0)\rangle = |S\rangle$. Similarly, they (and Tric and co-workers[92]) have used the damping matrix (effective Hamiltonian) method to study various cases of the *strong* coupling $[v_{sI}^2 \ll (E_S - E_I)^2 + (\gamma_S - \gamma_I)^2/4]$ limit.

The work of Tric et al.[92] is important, especially since it has been used quite extensively for interpreting nonexponential decays in a wide variety of molecular vapors (see experimental sections below). Recall that in the heuristic discussion presented above, the quasi-stationary states defined by eq 44 were assumed to decay independently. Accordingly the decay of the

optically prepared state ($|S_1\rangle$) was simply given by a sum of exponentials. As mentioned in the preceding paragraph, however, a more rigorous treatment shows that there are also damped oscillatory contributions of the form $2\epsilon \exp\{-\frac{1}{2}(\gamma_I + \gamma_S)t\} \cos(\Delta E t)$; here $\Delta E$ is the energy difference between the quasi-stationary states of $\psi_1$ and $\psi_2$. In the general case where an arbitrary number of $T_1$ levels is involved, there is, of course, a similar contribution for each possible pair of states. *But, in the weak coupling limit, the amplitude of these "interference" terms is negligible.* In the case of *strong coupling,* on the other hand, these contributions have a magnitude which is comparable or greater than that of the independent decay terms. Lahmani, Tramer, and Tric[92a] refer to these interference and independent decay terms as the "coherent" and "incoherent" contributions, respectively. Suppose we write the emission intensity in a form analogous to eq 10 from section A.2, but now the molecular (quasi-stationary) energies have *complex* energies $E_n = \epsilon_n - i\gamma_n/2$ and we have (neglecting, in over simplification, the nonhermiticity of the effective Hamiltonian)

$$I(t) = \left| \sum_n (C_n^S)^2 \exp(iE_n t/\hbar) \right|^2 = \sum_n (C_n^S)^4 \exp(-\gamma_n t)$$

$$+ 2 \sum_n \sum_m (C_n^S)^2 (C_m^S)^2 \exp[-\tfrac{1}{2}(\gamma_n + \gamma_m)t] \cos(E_n - E_m)t$$

[Recall that $(C_n^S)^2$ gives the amount of $S$ in the $n$th quasi-stationary state.] Lahmani et al.[92a] stress the fact that $I(t)$ is dominated by the coherent terms in the strong coupling limit when enough $T_1$ levels ($N$ in number) are involved. The $\Sigma_n \Sigma_m$ terms decay roughly exponentially on a time scale $\Delta^{-1}$ where $\Delta = 2\pi v^2 \rho/\hbar$; this is the "phase dismatching" time for the interfering $\{n\}$ states which are spread out over an energy range $\Delta$. At longer times $t \ll \Delta^{-1}$, the decay (amplitude proportional to $1/N$) is governed by the incoherent (independent decay) terms $\exp(-\gamma_n t)$ characterized by the slower rates $\gamma_n$. Thus the strong coupling analysis would attribute the fast decay in biexponential emissions to an interference effect involving the quasi-stationary states, whereas the weak coupling theory attributes it to the independent decays.

The strong coupling limit has been used[87] to analyze the methylglyoxal data described above. As we have seen, the relationships between laboratory observables and model parameters are quite different from those discussed for the weak coupling case. Essentially identical data for the homologous dicarbonyl, biacetyl, have also been interpreted[86] in terms of a strong coupling situation. The relevant level spacings, interaction energies, and widths have been estimated from comparisons between the experimental data and the theoretical expressions characterizing this limit. Here, for example, the pressure-independent terms in $\lambda_f$, instead of being thought of as (see eq 45a) $k_{rad}^{S_1} + (k_{NR}^{S_1})_{P\to 0}$, are interpreted as $k_{rad}^{S_1} + 2\pi v_{S_1T_1} \rho_{T_1}$ ($\equiv \Delta$) where $\rho_{T_1}$ is the density of $T_1$ levels strongly coupled through $v_{S_1T_1}^2$ to $S_1$. Similarly, $\lambda_s \leftrightarrow (1/N)k_{rad}^{S_1} + (k_{NR}^{T_1*})_{P\to 0} + k_c^{T_1*} P$, as opposed to eq 45b's $\lambda_s = \epsilon k_{rad}^{S_1} + \ldots$; and $I_s^0/I_f^0 \approx (1/N)$, *vs* $\approx \epsilon$. (Here $N$ is the number of strongly coupled $T_1$ levels.)

But we have shown earlier that it is possible to similarly analyze the dicarbonyl emissions in terms of a *weak* coupling model. From this we must conclude that *both* limits can account qualitatively for the "reversible" dynamics of the excited states, and that ambiguity remains. Neither of the two limits should be taken to have quantitative significance until independent information is obtained about the relative magnitudes of level spacings, interaction energies, and widths. Indeed, it is most conceivable that bits of both are simultaneously operative in the actual molecules of interest.

### c. Kinetic Model

Another quite different approach to the analysis of these pressure-dependent, excited-state dynamics is the purely classical kinetic scheme used by Ashpole et al.,[93] Baba et al.,[94] van der Werf et al.,[95] and Coveleskie and Yardley.[87] In the case of $CH_3COCOOH$, for example, one writes

(a) $S_1 \xrightarrow{k_{rad}^{S_1}} S_0 + h\nu$ fluorescence

(b) $S_1 \xrightarrow{k_{NR}^{S_1}} S_0$ irreversible NR decay

(c) $S_1 \underset{k_b}{\overset{k_f}{\rightleftharpoons}} T_1^*$ "reversible" intersystem crossing

(d) $T_1^* \xrightarrow{k_{NR}^{T_1*}} S_0$ irreversible NR decay

(e) $T_1^* + M \xrightarrow{k_c^{T_1*}M} T_1$ collisional deactivation

This scheme can be shown to lead directly to biexponential decay for the emission according to

$$I(t) = I_+^0 \exp(-\lambda_+ t) + I_-^0 \exp(-\lambda_- t) \qquad (46)$$

with

$$\lambda_\pm = \tfrac{1}{2}\{k_f + k_b + k_s + k_I \pm [(k_f - k_b + k_s - k_I)^2 + 2k_f k_b]^{1/2}\} \qquad (46a,b)$$

and

$$I_-^0/I_+^0 = (\lambda_+ - k_f - k_s)/(k_f + k_s - \lambda_-) \qquad (46c)$$

Here $k_s = k_{NR}^{S_1} + k_{rad}^{S_1}$ and $k_I \equiv k_{NR}^{T_1} + k_c^{T_1*} M$.

The unusual feature in the above kinetic scheme is, of course, the assignment of first-order rate constants $k_f$ and $k_b$ to describe the "forward" and "backward" exchange between $S_1$ and $T_1^*$ *in the isolated molecule.* As Lahmani et al. have themselves pointed out, this assignment can only be made "tentatively",[92] since collisions are not being invoked to establish the $S_1 \rightleftharpoons T_1^*$ equilibrium. Coveleskie and Yardley[87] have used the above parameterization of the biexponential emission to interpret their methylglyoxal data. Indeed they infer the following values for the various rate constants: $k_f \approx 5 \times 10^7\ s^{-1}$; $k_b \approx 1 \times 10^7\ s^{-1}$; $k_c^{T_1*}$ (methylglyoxal) $\approx 6\text{–}7 \times 10^7\ s^{-1}$; and $k_c$(argon) $\approx 2\text{–}3 \times 10^7\ s^{-1}$ (both $k_s$ and $k_{NR}^{T_1}$ are at least an order of magnitude smaller). Note that this interpretation is quite different from that provided by the weak coupling theory discussed earlier.

Lahmani et al.[92] have presented an analysis in which the predictions of the above kinetic scheme are compared in detail with those derived from their effective Hamiltonian treatment of the strong coupling limit. They establish approximate correspondences between the rate constants in the kinetic scheme and the level spacings, interaction energies, and widths in the quantum mechanical formulation. In a sense this justifies the use of the kinetic scheme in parameterizing the nonexponentiality and pressure dependence of emission in "intermediate" molecules. As Soep et al.[96] suggest, for example, "the reverse crossing followed by emission has the same physical meaning as the anomalously long fluorescence due to the nonnegligible singlet character of the molecular quasi-stationary levels." We feel nevertheless that the various quantum mechanical formulations (weak and strong coupling limits, etc.) offer a more conceptually sound interpretation of the excited-state dynamics. The emphasis on "forward" and "backward" rate constants and "reversible"

$$(S_1 \underset{k_b}{\overset{k_f}{\rightleftharpoons}} T_1^*)$$

radiationless transitions, in the absence of collisions, can be misleading and can obscure the actual time development of the prepared state. Rather, the "intermediate" behavior (e.g., nonexponential and pressure dependent decays) can be better and more simply described by the level spacings, interaction energies, and widths which appear naturally in the quantum

mechanical formulations. In any case, as we have already mentioned above, enough ambiguity remains about the relative magnitudes of these parameters in actual molecules of interest so that no single interpretation should be taken too seriously.

### d. Pressure-Dependent Quantum Yields

Actually, the original use of the concept of "reversible" radiationless transitions arose in discussions of the pressure-dependent quantum yields observed for triplet states following flash excitation of higher singlets in the aromatic hydrocarbons.[93] Similar experimental results have been reported most recently for biacetyl.[86,97] Moss and Yardley,[97] for example, excite the first singlet of biacetyl at low pressures with a pulsed source (having $\approx$50-cm$^{-1}$ bandpass). The ensuing phosphorescence is time resolved, and its decay rate is found to be constant as the pressure and exciting wavelength are varied (1 Torr $\leq P \leq$ 200 Torr, 4400 Å $\leq \lambda \leq$ 3650 Å). The phosphorescence *intensity* (i.e., quantum yield) *is* $P$ and $\lambda$ dependent.

These results are readily explained as follows. At all pressures studied, the vibrational relaxation in $T_1$ is fast enough (compared to the radiative lifetimes of the excited triplet levels) so that all phosphorescence takes place from a thermally relaxed triplet having a characteristic decay time. As for the $P$ and $\lambda$ dependence of the phosphorescence quantum yield $\phi_P$, we need simply allow for the possibility that $T_1^* \rightsquigarrow S_0$ intersystem crossing competes with $T_1^* \rightsquigarrow T_1$ vibrational relaxation. The excess energy associated with $T_1$ increases as $\lambda$ becomes shorter. Since $T_1^* \rightsquigarrow S_0$ ISC rates are known to increase with $T_1^*$ energy, we expect $\phi_P$ (the amount of $T_1$ emission), at low enough pressures, to decrease as the wavelength of the exciting light becomes shorter. Note that for high enough pressure (fast enough vibrational relaxation) $\phi_P$ is expected to be independent of $\lambda$. Similarly, for long enough $\lambda$ (small enough $k_{NR}^{T^* \rightsquigarrow S_0}$) $\phi_P$ should become independent of pressure. Thus we can write

$$\phi_P(P,\lambda) = [k_c^{T_1^*}(\lambda)P/\{k_c^{T_1^*}(\lambda)P + k_{NR}^{T_1^* \rightsquigarrow S_0}(\lambda)\}]\phi_P^{P\to\infty} \quad (47)$$

which indeed accounts for the observed phosphorescence behavior.[97]

A similar analysis has been applied[98,99] to interpret the pressure-dependent triplet yields of the naphthalenes and anthracenes. As mentioned above, these data had at first been analyzed by Ashpole et al.[93] in terms of a "reversible" intersystem crossing ($S_1 \rightleftharpoons T_1^*$, $k_f$, $k_b$). In a more recent discussion,[98] however, the low-pressure falloff of the triplet quantum yield $\phi_T$ is explained by means of the vibrational relaxation mechanism outlined above. More explicitly, an equation identical with eq 47 can be written for $\phi_T$. Again $k_{NR}^{T_1^* \rightsquigarrow S_0}$ increases with energy in $T_1^*$, whereas increasing $P$ leads to more efficient removal of vibrational excitation in $T_1$. Thus the high-pressure limit (i.e., thermal equilibration in $T_1$ before intersystem crossing) gives the maximum triplet yield.

Fluorescence dynamics can be similarly accounted for. Heller and Freed,[99] in fact, have developed a simple but general stochastic theory which emphasizes the competing effects of (1) thermal equilibrium within an electronic state and (2) the dependence of nonradiative electronic relaxation rates on vibrational level. This scheme has been applied by Beddard et al.[98] to account quantitatively for their observed pressure dependence of fluorescence decay rates and quantum yields in naphthalene, benz[*a*]anthracene, chrysene, and pyrene.

In attempting above to present a simple overview of the "intermediate" case of radiationless transition behavior, we have short changed some rigor as well as a large body of theoretical work on the subject. As mentioned earlier, the recent review by Freed[10] contains an especially comprehensive discussion as well as references to much of the original literature. In particular we cite here the important contributions to the "intermediate" case made by Jortner and Mukamal[12] and by Langhoff and Robinson.[13b,100] Much of this work was addressed to the problem of unravelling irregular features in optical absorption spectra due to $S_2$–$S_1$ perturbations. These theoretical questions are certainly as interesting as the gas-phase emission dynamics on which we chose to focus in the above discussion. Similarly, we discussed almost exclusively the dicarbonyls, whereas considerable attention in the literature has been given as well to the diazanaphthalenes[101] etc. Since these other examples involve conceptual problems which are qualitatively similar to those offered by the dicarbonyls, we shall not treat them further except in the experimental sections.

## III. Experimental Studies

## A. Aromatic Hydrocarbons

### 1. Benzene and Fluorinated Benzenes

The first study of the fluorescence decay characteristics of *benzene* vapor, at pressures low enough so that collisions are not important, was performed by Selinger and Ware.[1] In this study benzene vapor at a pressure of 0.1 Torr was excited with a bandwidth of 20 Å to the band maxima of the transitions $B_0^0(6_1^0)$, $A_0^0(6_0^1)$ and $A_1^0(6_0^1 1_0^1)$. Single exponential decay curves were obtained with lifetimes of 90 ± 4, 80 ± 3, and 68 ± 2 ns, respectively.

At about the same time Parmenter and Schuyler[102] determined the absolute quantum yields of fluorescence for the same three vibronic levels studied by Selinger and Ware.[1] These yields were found to be as follows: $\phi_F(0) = 0.22$, $\phi_F(6_0^1) = 0.27$ and $\phi_F(6_0^1 1_0^1) = 0.25$. In a subsequent article Selinger and Ware[103] have extended their measurements on benzene and have included benzene-$d_6$. The experimental conditions were the same as in the previous study[1] while an additional level, $6_0^1 1_0^2$, was excited.

The lifetimes obtained were coupled with the quantum yield data by Parmenter and Schuyler[102] to obtain radiative $k_F$, and nonradiative, $k_{NR}$, rate constants. The experimentally observed ratio of radiative rate constants was determined to be $k_F(6_0^0)$: $k_F(6_0^1)$:$k_F(6_0^1 1_0^1)$ = 1:1.4:1.5 to be compared with the ratio predicted by the Herzberg–Teller theory,[104,105] of 1:2:2, assuming that all three transitions are totally induced by $6(e_{2g})$. Better agreement was found by assuming (as has been suggested by studies of Parmenter and co-workers) that the $6_0^0$ transition is only 65% induced by $6(e_{eg})$.

The $k_{NR}$ was also found to vary upon different vibronic excitation. The $k_{NR}$ was determined as $8.7 \times 10^6$ s$^{-1}$ ($6^0$), $9.1 \times 10^6$ s$^{-1}$ ($6^1$), and $11.0 \times 10^6$ s$^{-1}$ ($6^1 1^1$). The observed increase in the nonradiative rate with excess energy was ascribed to an enhancement of the S $\rightsquigarrow$ T intersystem crossing. By studying $C_6D_6$ the authors found a significant deuterium effect on the fluorescence lifetimes. The ratio $\tau_F(C_6D_6)/\tau_F(C_6H_6)$ was determined as 1.82 ($6^0$), 1.56 ($6^1$), 1.23 ($6^1 1^1$), and 1.38($6^1 1^2$). This normal ($\tau_F^D/\tau_F^H > 1$) isotope effect was interpreted as due to a reduction of $k_{NR}$ upon deuteration.

Selinger and Ware have also examined the pressure dependence of the fluorescence lifetimes of $C_6H_6$ and $C_6D_6$ using isopentane as the collisional partner. A small decrease in lifetime was found for isopentane pressures higher than 50 mTorr. This result was considered as an indication of some kind of collisionally induced nonradiative process. In the absence of quantum yield data at these pressures no more definite conclusions could be reached.

By calculating density of states and through use of the experimental data on $k_{NR}$, Ware et al.[106] concluded that all the studied vibronic levels of $^1B_{2u}(S_1)$ state lie in the statistical limit.

An even more extensive study of benzene vapor under "isolated molecule" conditions was conducted by Spears and Rice.[62]

In this study measurements of the lifetimes of 22 vibronic states of benzene and the relative quantum yields of fluorescence for transitions originating from these states have been reported. An excitation bandwidth of about 1 Å was used. From the observed lifetimes and quantum yields, nonradiative lifetimes have been obtained.

The following general conclusions were reached:

(a) Often states with nearly the same excess vibrational energy have different nonradiative lifetimes.

(b) There appears to be a monotonic dependence of the nonradiative lifetime on the number of quanta in a vibrational progression.

(c) The rate of change of lifetime with energy within one progression is quasilinear over the energy range 0–3300 $cm^{-1}$. Regarding the particular vibronic levels being excited, states forming progressions in the totally symmetric C–C stretching mode $1(a_{1g})$ have nonradiative lifetimes that depend only on the excess energy above the $^1B_{2u}$ origin, e.g., as in the $1^n$, $6^11^n$, $6^21^n$, and $6^110^21^n$ progressions. Furthermore, adding energy in the in-plane carbon bending mode $6(e_{2g})$ does not change this behavior (see the 0, $6^1$, and $6^2$ states). On the other hand, when there is vibrational energy in an out-of-plane mode [$10(e_{1g})$, $11(a_{2u})$], the lifetime of the state is shorter than expected solely on the basis of the energy content and the correlation deduced from the behavior of states with only $1(a_{1g})$ and $6(e_{2g})$ vibrations excited. Progressions in the out-of-plane mode $16(e_{2u})$ have lifetimes that decrease more rapidly with excess energy than do states having progressions in $1(a_{1g})$, but the decrement in lifetime per quantum of vibrational energy is about the same for the different progressions.

An interpretation of the results on the variation of the nonradiative lifetime with excess energy was attempted using the theoretical model of Gelbart, Spears, Freed, Jortner, and Rice.[107] The nonradiative process operating was considered to be the $^1B_{2u} \rightsquigarrow {}^3B_{1u}$ intersystem crossing. As the number of quanta in the totally symmetric $1(a_{1g})$ C–C stretching mode increased from 0 to 1, 2 and 3, the calculated nonradiative rates increased by factors of 1.2, 1.4, and 1.6, respectively, to be compared with the experimental values (arising from the $6_1^0 1_0^n$ excitation) of ~1.3, ~1.8, and ~2.5, respectively. The results of Spears and Rice on the variation of the radiative lifetime with vibrational excitation are somewhat different from those of Selinger and Ware.[103]

Using their lifetime measurements and with the help of an analysis of the expected radiative lifetime, Spears and Rice determined that the $7^1$ and $6^11^3$ states of benzene, with energies 3080 and 3290 $cm^{-1}$ above the origin, respectively, have faster nonradiative decay rates than expected from the trends defined by the properties of the lower energy states. The same may be true for the $6^21^2$ state. The possibility of the opening of a new nonradiative channel, possibly a photochemical one, was discussed, along with speculations about the possible effects of angular momentum conservation on its efficiency.

Finally the authors found a pressure dependence of the observed lifetime to pressures as low as $6 \times 10^{-3}$ Torr. A model was then proposed where the low-pressure quenching of the $6^1$ state proceeds through hard-sphere collisions capable of redistributing the vibrational energy to populate a new state not possessing a $\nu_6'$ quantum.

The onset of a new nonradiative decay channel (channel III) in benzene for excess energies higher than 3000 $cm^{-1}$ has also been observed by Callomon et al.[71] These authors studied the widths of the absorption lines of benzene under high resolution and found that many but not all of the bands with $E_{vib} \geq 1000$ $cm^{-1}$ becomes diffuse. Two different possibilities have been considered regarding the nature of this nonradiative process: (a) predissociation:

$$C_6H_6 + h\nu \rightarrow C_6H_5(^2A_1 \text{ or } ^2B_1) + H(^2S) \quad \text{(i)}$$

$$C_6H_6 + h\nu \rightarrow C_6H_4 + H_2(^1\Sigma_g^+) \quad \text{(ii)}$$

and (b) coupling to an unidentified state of benzene. Since no hydrogen formation was detected by prolonged irradiation, the possibility of predissociation was excluded. Concerning the unidentified state, the possibilities considered were an $^{1,3}E_g(\pi,\pi^*)$ state, an $^3E_{2u}(\sigma,\pi^*)$ state or the state of a valence isomer of benzene.

The question of the importance of valence isomerization as the channel III process has been discussed by Phillips.[108] It was suggested that the quantum yields of formation of valence isomers, as revealed by 1,2 shifts in substituted benzenes, cannot account for the total value of the nonradiative process.

The effect of rotational excitation on the electronic relaxation of the $S_1$ state of benzene has also been discussed by Parmenter and Schuh.[109] In this study the authors used narrow band exciting light (0.3–0.5 Å) and measured the relative quantum yields of resonance fluorescence generated when this narrow band light is swept through the rotational envelopes of four $S_1 \rightarrow S_0$ absorption bands. It was found that within a 10% uncertainty the fluorescence yields are independent of the position of the exciting light within an absorption band. Thus in benzene it appears that neither the radiative decay nor the intersystem crossing to the triplet state displays large sensitivity to molecular rotation, at least when excited state relaxation proceeds from rotational distributions of moderate diversity.

The measurements of Spears and Rice[62] on benzene have been extended by Abramson et al.[110] to include the fully *deuterated benzene* and *monofluorobenzene*. The lifetimes and quantum yields of fluorescence from 22 vibronic states of $C_6D_6$ and 59 vibronic states of $C_6H_5F$ have been determined under "isolated molecule" conditions.The nonradiative lifetime vs. excess energy pattern for $C_6D_6$ is very similar to the one observed for $C_6H_6$. The isotropic substitution of D or H does not seem to affect the relative nonradiative lifetimes of the $6^n$ progression. However, progressions in $1(a_{1g})$ have a greater effect in $C_6D_6$ than in $C_6H_6$. The relative magnitude of this change increases with excess vibrational energy; i.e., the $6^21^n$ progression shows a higher rate of change of $\tau_{NR}$ with vibrational excitation than the $6^01^n$ or $6^11^n$.

Nakamura[111] has reported measurements of the quantum yield of fluorescence of $C_6H_5F$ vapor (pressure $\geq$ 1 Torr, 3-Å bandwidth). It was found that $\phi_F$ is almost constant for excitation wavelengths greater than ~258 nm, but declines rapidly as the excitation wavelength decreases. At 254 nm, $\phi_F$ is about one-half the value for $\lambda > 258$ nm, where the value of $\phi_F$ is $0.22 \pm 0.04$. This general behavior is also observed by Abramson et al.[110] (0.5 Torr and 0.68-Å bandwidth). Regarding the nonradiative lifetimes of individual vibronic levels, Abramson et al.[110] found that the lifetimes of states in the progressions $(6a)^n$, (6a is a ring deformation) and $(6b)^n$ (6b is an in-plane ring deformation) change in a fashion similar to the change observed in the $6^n$ progression of $C_6H_6$. The progression $1^n$ in $C_6H_5F$ has a smaller value of $\Delta\tau_{NR}$/quantum than does the comparable progression in $C_6H_6$. All other vibronic states of $C_6H_5F$ studied, which include vibrational modes of all possible symmetries, show behavior in progressions similar to that described for the cases of $(6a)^n$, $(6b)^n$, and $1^n$. It appears that there is a remarkable uniformity of the dependence of $\tau_{NR}$ on excess number of vibrational quanta.

Since both $C_6H_6$ and $C_6D_6$ have a $D_{6h}$ symmetry, the transition $^1B_{2u}(S_1) \leftarrow {}^1A_{1g}(S_0)$ is vibronically induced and only a few vibrational modes of appropriate symmetry are prominent in the spectrum. Partial deuteration of $C_6H_6$ reduces the molecular symmetry and progressions in more vibrations appear in the spectrum. In addition, replacement of an H by a D atom leads to a large change in the highest frequency stretching mode which, along with the change in the number of totally symmetric vibrations, alters the competition between acceptor modes. For

these reasons several *partially deuterated benzenes* were studied by Guttman and Rice.[112] Specifically, benzene-$d_1$ ($C_{2v}$), *p*-benzene-$d_2$ ($D_{2h}$), *m*-benzene-$d_2$ ($C_{2v}$), and $C_6HD_5$ ($C_{2v}$) were studied.

The data on the deuterated benzenes show clear, fairly smooth trends. The fluorescence lifetimes, quantum yields, and nonradiative lifetimes all increase upon deuteration. Only $C_6H_5D$ falls slightly out of line in the sense that some of its states have quantum yields and nonradiative lifetimes slightly less than those of $C_6H_6$. Regarding the nonradiative lifetimes, it is possible, as in the case of $C_6H_6$ and $C_6D_6$, to draw relatively good straight lines through those points representing progressions in $\nu_1$ for the same number of quanta of the $\nu_6$ vibrations. Thus, the lifetimes of $6^0$, $6^01^1$, $6^01^2$, $6^01^3$ levels fall on a straight line as do the lifetimes for $6^1$, $6^11^1$, $6^11^2$, and $6^2$, $6^21^1$, $6^21^2$. In general, there is a smooth, general increase in the relative nonradiative rates with increasing deuteration.

Guttman and Rice have used the theoretical model of Heller, Freed, and Gelbart[57] in order to interpret the relative rates of nonradiative decay from selected vibronic levels of these partially deuterated benzenes. The important nonradiative process was always assumed to be that of $S_1 \rightsquigarrow T_1$ intersystem crossing, $^1B_{3u} \rightsquigarrow {}^3B_{2u}$ ($D_{2h}$) or $^1B_1 \rightsquigarrow {}^3A_1$ ($C_{2v}$). Considering the vibrational modes of $C_6H_{6-x}D_x$, the authors noted that since the CH and CD stretching motions are of much higher frequency than the rest of the vibrations, the $\nu_2$ ($a_{1g}$ C–H stretching) mode in $C_6H_6$ can be considered as proportional to the number of H and D atoms participating in a particular mode, scaled relative to the corresponding origin shifts in $C_6H_6$ and $C_6D_6$. The normal modes in the two electronic states were assumed parallel and no account was taken of the change of the number of totally symmetric (accepting) modes upon partial deuteration. Comparison of the calculated and experimental results shows that the agreement is fairly good but not as good as for $C_6D_6$.[9] Some of the comparisons, such as for the $6^01^n$ progression, show very good agreement, while others seem to disagree by a little more than the experimental error. An appropriate choice for the change in frequency of $6(e_{2g})$, ($\Delta\omega_6$), between $S_1$ and $T_1$ for each deuterated benzene might have improved the agreement. Discussing the various assumptions that have been used in these calculations, the authors concluded that probably the most severe one is the neglect of the extra accepting modes that result from breaking the symmetry upon deuteration.

This effect of the increase of the number of accepting modes upon reduction in symmetry was discussed further in a study[113] of *p*-$C_6H_4F_2$ ($D_{2h}$) and *m*-$C_6H_4F_2$ ($C_{2v}$). The measured quantum yield of the vibrationless level pumped by the 0,0 transition is 0.29 in *m*-$C_6H_4F_2$ and ~1.0 in *p*-$C_6H_4F_2$. The fluorescence lifetimes of levels of *p*-$C_6H_4F_2$ are generally longer than those of *m*-$C_6H_4F_2$. The larger excess energy dependence of $k_{NR}$ for *m*-$C_6H_4F_2$ ($C_{2v}$) than for *p*-$C_6H_4F_2$ ($D_{2h}$) was explained on the basis of the Heller, Freed, and Gelbart[57] model. Reducing the symmetry of $C_6H_6$ from $D_{6h}$ to $C_{2v}$, by fluorine substitution, increases the number of totally symmetric high frequency C–H stretches from one to three. In this case the lower frequency optical modes (C–C stretching) will be less efficient in competing for the excess energy with the three high-frequency C–H stretches acting as accepting modes. Reducing the symmetry from $D_{6h}$ to $D_{2h}$, on the other hand, does not increase the number of totally symmetric high-frequency C–H stretches; there is only one such mode to serve as an accepting mode. Therefore a larger increase in nonradiative rate constant with excess energy is expected in this case. In fact, the excess energy dependence of $k_{NR}$ in the case of *p*-$C_6H_4F_2$ ($D_{2h}$) is higher than that of $C_6H_6$ ($D_{6h}$). This fact was attributed to larger origin and frequency shifts in the former case. From the above discussion then one would expect that $(k_{S\rightsquigarrow T}(m_a)/k_{S\rightsquigarrow T}(0))_{C_{2v}}/(k_{S\rightsquigarrow T}(m_a)/k_{S\rightsquigarrow T}(0))_{D_{2h}} < 1$, as is observed.

The fluorescence lifetimes of $C_6H_5F$, $C_6H_5F$, and $C_6F_6$ in the gas phase have also been measured by Loper and Lee.[114]

Wettack and co-workers[115,116] studied the electronic and vibrational energy transfer from specific vibronic levels of the first excited singlet states of benzene and fluorobenzene to a variety of acceptor molecules. In the case of benzene the vibrational energy transfer cross section, $\sigma_v^2$, was found to increase linearly with excess energy for a variety of quenchers (acetone-$h_6$ and -$d_6$, isopropyl alcohol, methyl ester, and propanol). As the excess energy varies from 0 to 2300 $cm^{-1}$, $\sigma_v^2$ varies from 4 to 47 $Å^2$. The electronic energy transfer from benzene (0, $6^1$, $6^11^1$, $6^11^2$ levels) to acetone was found to depend only slightly on vibronic level, with the $6^1$ level showing the smallest cross section. The cross sections are approximately 50% of gas kinetic values. In the case of fluorobenzene both $\sigma_e^2$ and $\sigma_v^2$ values are larger than in the case of benzene, the former approaching hard-sphere gas kinetic values.

## 2. Aniline

From the various derivatives of benzene, *aniline* has received considerable attention. This is because aniline combines several interesting features. The $NH_2$ group lowers the symmetry of the benzene ring, and the effect of the reduced symmetry can be studied. Also, the amino group may be expected to change the nature of the electronic states by the intramolecular charge transfer interaction and the electronic matrix element (spin–orbit coupling) responsible for the nonradiative transition. Finally, the influence of the large amplitude amino group inversion mode, absent in benzene, can also be investigated.

One of the earliest studies of radiationless transitions from approximately single vibronic levels was that of von Weyssenhoff and Kraus[117] on aniline. Aniline vapor has a well-resolved vibronic absorption spectrum in the region of the first excited singlet transition. An absorption continuum underlies the structured spectrum. In this study, aniline vapor (~0.3 Torr) was excited with light (bandwidth 2.7 Å) in the range 300–275 nm. Lifetimes and relative quantum yields were measured directly, while absolute quantum yields were estimated from literature data. In the analysis of the data the only nonradiative process depopulating the first singlet was assumed to be intersystem crossing. The following observations were made.

(a) The observed lifetime ($1/\tau = k_F + k_{ISC}$) shows a sharp minimum for every major peak in the absorption spectrum.

(b) The fluorescence quantum yield shows maxima for every major peak in the absorption spectrum.

(c) The intersystem crossing rate constant, $k_{ISC}$, essentially follows the reciprocal lifetime pattern, while the radiative rate constant, $k_F$, follows the opposite pattern; however, the fluctuations of $k_F$ are smaller.

The above observations were explained in the following way. In aniline, the $S_1 \leftarrow S_0$ transition is allowed and hence $k_F$ shows relatively small variation with excitation energy. Symmetry selection rules then could apply to the intersystem crossing process which proceeds via spin–orbit and vibronic coupling simultaneously. The authors suggested that intersystem crossing is symmetry forbidden for just those vibronic modes which correspond to the discrete bands in the absorption spectrum. The reason why the intersystem crossing shows these selection rules was rationalized the following way. Aniline ($C_{2v}$) has an $A_1$ ground and a $B_2$ first excited singlet state. There are two triplets below the $^1B_2$ state; the lowest one is a $^3A_1$ and the higher one is a $^3B_2$ state. First-order spin–orbit coupling between $^1B_2$ ($S_1$) and $^3A_1$) is allowed, and therefore it will be unspecific to vibronic symmetry species. This $S_1 \leftrightarrow T_1$ coupling is not expected to be very efficient because of the large energy gap between the two states (~7200 $cm^{-1}$). On the other hand, the transition $^1B_2$ ($S_1$) $\rightsquigarrow {}^3B_2(T_2)$, which would be favorable because of the small energy gap, is forbidden in first order, but it can be induced by second-order processes involving both spin–orbit

and vibronic coupling. The vibration required for this coupling is one of symmetry species $b_2$. In aniline, the major absorption peaks are due to either totally symmetric, $a_1$, modes or $b_1$ modes. If the molecule is excited selectively to one of these modes or a combination of them, vibronic coupling should be small according to the above selection rules, and hence $k_{ISC}$ should be at a minimum and this would explain the experimental findings.

Because of the existence of the underlying continuum in the absorption spectrum of aniline, which is stronger at higher energies,[118] one might expect to observe nonexponential decays depending on the position of the excitation. The experimental technique employed by von Weyssenhoff and Kraus,[117] phase shift technique at a single modulation frequency, cannot detect nonexponential decay. Ware and Garcia[119] have reinvestigated aniline using the time correlated single photon counting technique. Several approximately single vibronic levels of the $^1B_2(S_1)$ state were excited at a pressure of ~0.3 Torr. The decay was found to be strictly a single exponential for both 0.8 and 2.0 Å bandwidth excitation into either the strong bands or into some of the valleys between strong bands. The lifetime varied from 4 to 7 ns in the energy range studied. No significant variation (~4%) was for the radiative rate constant as it is expected since the $^1B_2(S_1) \leftarrow {}^1A_1(S_0)$ transition is allowed. The nonradiative rate constant $k_{NR}$ appears to increase when one or two quanta are excited in modes 6a, 1, or 12. This does not appear to happen when one quantum of the inversion mode *I* involving the $NH_2$ group is excited. The $I^2$ level could not be measured with certainty. Ware and Garcia reported little variation of $k_{NR}$ measured in the valleys between peaks as a function of excess energy up to 35 000 $cm^{-1}$. The lifetimes are in good agreement with those of von Weyssenhoff and Kraus.[117] Beyond 35 000 $cm^{-1}$ the plot slowly turns up but the total range of $k_{NR}$ is only from $1.0 \times 10^8$ to $1.4 \times 10^8$ $s^{-1}$. The values for these valley measurements, which represent the best estimates possible for the decay properties of the continuum excited off the main peaks, are significantly higher than either the uncorrected or corrected (for the presence of the continuum) values for the single levels excited. No definite conclusion could be reached on the origin of this observation or of the continuum itself. On the other hand, as Ware and Garcia point out, the structure in the $k_{NR}$ observed by von Weyssenhoff and Kraus[117] could be just the result of the superposition of a structured spectrum on a continuum and not a result of selection rules.

Comparing aniline to benzene, one might have expected that because of the reduction of symmetry ($D_{6h} \rightarrow C_{2v}$) and of the resulting increase in the number of totally symmetric accepting modes, $k_{NR}(1)/k_{NR}(0)$ will be higher in benzene (see also $C_6H_5F$[110]). This behavior was not observed in aniline. The absolute of $k_{NR}$ is also much greater for all levels of aniline compared with those of benzene in the same energy range.

Aniline has also been the subject of an extensive study by Scheps et al.[120] In this study 37 levels of aniline-$h_7$ along with levels of aniline-*N,N*-$d_2$, aniline-$d_5$, and aniline-$d_7$ were investigated. The dependence of the nonradiative lifetime on the excess energy in aniline-$h_7$ was found to behave qualitatively similar to that in benzene for states that do not involve excitation of the inversion mode, *I*, of the amino group. As has been observed also by Ware and Garcia,[119] the decrement in lifetime per quantum of vibration of the optical mode is larger in aniline than in fluorobenzene which in turn shows a smaller decrement than benzene. As we mentioned earlier, from just symmetry considerations one may have expected the opposite behavior. Scheps et al.[120] ascribe the observed energy dependence behavior of aniline vs. fluorobenzene to the smaller $\Delta E_{S_1-T_1}$ of aniline (7200 $cm^{-1}$) than in fluorobenzene (8250 $cm^{-1}$) which results to a lower density of states of the accepting modes.

When the inversion mode, *I*, was excited a different behavior was found, that is, in aniline-$h_7$, $\tau_{NR}(I^1) > \tau_{NR}(I^0)$, contrary to what is generally expected about the excess energy dependence of $\tau_{NR}$. This finding is also in agreement with the results of Ware and Garcia.[119] This anomaly was not observed in the deuterated anilines. In aniline-$h_7$ the nonradiative lifetimes of the higher members of the inversion mode progression were found to lie in a line with the $I^1$ level as origin. This "anomalous" behavior of the inversion mode was interpreted on the basis that the triplet manifold to which intersystem crossing occurs, namely, $^3A_1(T_1)$ is nonplanar, while the $^1B_2(S_1)$ state is nearly planar. The large geometry change accompanying the $^1B_2$(planar) $\rightsquigarrow {}^3A_1$ (nonplanar) process were accommodated within the HFG model[57] by simply factoring out the Franck–Condon factor for the mode that suffers the large change and calculating it by an appropriate method. The inversion mode was represented by a parameterized double minimum potential, and since the saddle point approximation used by HFG is not valid when the inversion mode is acting as an accepting mode, Scheps et al. used a convolution integral approach in the evaluation of the corresponding overlap factor. The calculations confirmed qualitatively the notion that a significant portion of the electronic energy is dumped into the inversion mode of the $^3A_1$ state. The anomalous experimental trend of $\tau_{NR}(I)$ in aniline was also reproduced, although the authors could not find a single set of parameters that can reproduce the experimental results for all four studied compounds.

Unlike von Weyssenhoff and Kraus,[117] Scheps et al. believe that $S_1(^1B_2) \rightsquigarrow {}^3B_2(T_2)$ intersystem crossing in aniline, although it might be present, is not rate determining. This conclusion is based on the fact that in the limit of large excess energies in aniline-$h_7$ where we expect a large increase in the density of states (at 2600 $cm^{-1}$ above the $^1B_2$ origin), there is still a linear dependence of $\tau_{NR}$ on $\Delta E_{excess}$, although nonlinearity is expected if there were two competing nonradiative channels $S_1 \rightsquigarrow T_1$ and $S_1 \rightsquigarrow T_2$.

### 3. Other Benzene Derivatives

Regarding other studies on benzene derivatives, Rockley and Phillips[80] have measured the fluorescence lifetimes and quantum yields of dilute vapors (0.25 Torr) of *p-fluorotoluene* (PFT) and *p-fluorobenzotrifluoride* (PFBT), as a function of the excitation energy. The radiative rate constant, $k_F$, of PFT shows a pronounced decrease for excess energies greater than about 2500 $cm^{-1}$. In the case of PFBT, $k_F$ decreases linearly with excess energy. $k_{NR}$ increases with excess energy and this increase is more pronounced for PFT. The fast increase in $k_{NR}$ observed in PFT was attributed by the authors to large frequency changes in the optical mode between the singlet and triplet states. In contrast to benzene, where excess energy greater than 3100 $cm^{-1}$ seems to open a new nonradiative channel, no such behavior was observed for *p*-fluorotoluene even for excess energies of 5000 $cm^{-1}$.

Phillips and co-workers[121] also studied the effects of collisions on the electronic relaxation of PFT vapor. When the pressure is lower than 0.5 Torr, no variation in the spectral and dynamic parameters is observed as a function of pressure for a variety of wavelengths. Above this pressure of PFT, or of added pentane, vibrational relaxation is in competition with electronic relaxation, resulting in fluorescence spectral changes, fluorescence quantum yield changes, and nonexponential fluorescence decay curves. Slight differences in spectra for different excitation wavelengths show that even with saturated vapor pressure of cyclohexane present, complete thermal equilibrium prior to emission is not quite reached. The data on vibrational relaxation were analyzed according to a stochastic model by Freed and Heller[99] as modified by Beddard et al.[98] Addition of 2-pentanone was found to quench by electronic energy transfer, and the data showed a slightly less efficient energy transfer for excitation of *p*-fluorotoluene to higher vibrational levels.

Data on the rate constants for radiative and nonradiative decay of a variety of substituted benzenes in the low-pressure vapor phase were obtained by Rockley and Phillips[122,123] or taken from the literature and discussed in reference to current theories. The energy dependence of the radiative rate constant, $k_F$, was discussed in terms of the model of Fleming et al.[124] Although there is some qualitative agreement between the predictions of the model and the experiment, no quantitative fit was found. The smooth variation of $k_F$ with excess energy for 1,4-fluoro(methyl)benzene was ascribed to vibrational redistribution.

### 4. Naphthalene

*Naphthalene* has been studied by many research groups and a large amount of information has been gathered. Comparison of results obtained by different groups on the other hand is not always possible because of different experimental conditions.

One of the early studies of radiationless transitions in naphthalene vapor was that of Uy and Lim.[125] In this study the fluorescence quantum yield of naphthalene-$h_8$ and -$d_8$ (0.1 Torr) has been studied as a function of the exciting light energy (excitation bandwidth 10 Å). Several general conclusions were reached: (a) it was found that the emission from different vibrational levels of $S_1$ shows large variations in quantum yield, with the emission from a $b_{1g}$ level at 433 $cm^{-1}$ (419 $cm^{-1}$ for $d_8$) above the zero-point level showing the highest yield; (b) the quantum yield of fluorescence from several vibrational levels (the $b_{1g}$ mode of frequency 433 $cm^{-1}$, in particular) of $S_1$ is greater for naphthalene-$h_8$ than for naphthalene-$d_8$ (an *inverse deuterium effect*); (c) the quantum yield of fluorescence decreases rather smoothly with increasing excitation energy in the spectral region covering the second and the third electronic absorption bands of the molecule; (d) in the spectral region of the second and third absorption bands, the fluorescence yield of $d_8$ is greater than that of $h_8$ and the ratio of the two yields increases smoothly with increasing excitation energy.

The rapid decrease in the fluorescence quantum yield with increasing excitation energy in $S_2$ and $S_3$ and the normal isotope effect under the same conditions were ascribed to an enhanced intersystem crossing due to the increasing number of triplets below the singlet manifold, as the excitation energy increases. Increased vibronic interactions and more favorable Franck–Condon factors were also thought to contribute. The inverse deuterium effect obtained for $b_{1g}$ levels of $S_1$ was rationalized by postulating that besides an $S_1(^1B_{3u}^-) \rightsquigarrow T_1(^3B_{2u}^+)$ intersystem crossing process, a vibronically induced intersystem crossing to the higher triplet $^3B_{3u}$ along the $b_{1g}$ normal mode coordinate can take place. An intersystem crossing between states with small energy gap would then lead to an inverse deuterium effect according to an analysis by Sharf and Silbey.[46]

Laor and Ludwig[126] have studied the fluorescence lifetimes of naphthalene vapor ($7 \times 10^{-2}$ Torr, 50 Å bandwidth) as a function of the excitation energy. It was found that the inverse of the lifetime, $1/\tau$, is a linear function of the excitation energy within the first ($S_1$) and second ($S_2$) singlet states. This dependence becomes nearly exponential near the position of the third ($S_3$) singlet state. The linear plot of $1/\tau$ vs. $\Delta E$ has the same slope in $S_2$ as in $S_1$. No break in the $1/\tau$ vs. $\Delta E$ curve has been observed by Laor and Ludwig. This fact coupled with the fact that, in accord with previous studies of naphthalene,[127] excitation of $S_2$ leads to emission from higher vibrational levels of $S_1$, was considered as an indication that the fluorescence lifetime is determined by the same relaxation process for excitation in both $S_1$ and $S_2$ states. The nearly exponential increase of $1/\tau$ with $\Delta E$ in the region of $S_3$ was not interpreted. In the absence of fluorescence quantum yield data under the same conditions, it was not possible to decide if the lifetime is determined by the radiative or the nonradiative decay. Regarding the linear variation of $1/\tau$ within the $S_1$ state, the authors were able to rationalize a linear variation of the radiative rate constant with $\Delta E$ using a simple model based on the Herzberg–Teller theory. This model is expected to be valid if only one mode is excited with increasing quantum number. The requirement for excitation of predominantly one vibration was hardly met in this study.

Both fluorescence lifetimes and quantum yields of naphthalene vapor (0.1 Torr, 50 Å excitation bandwidth) were measured by Lim and Uy[128] (their quantum yields were found later to be in error by a constant factor[81a]). The combination of the two measurements allowed the decomposition of the total decay constant to radiative and nonradiative decay constants. The radiative rate constant was found to increase more or less linearly with excess energy. The linear dependence of the radiative rate constant on excess energy ($\Delta E$) was explained on the basis of a model using the Herzberg–Teller theory. Instead of assuming the excitation of a single mode, as in the model of Laor and Ludwig,[126] it was assumed that for molecules of the size of naphthalene the excess energy is distributed very rapidly over all normal coordinates. The most probable distribution then is determined by Bose statistics. The nonradiative decay rate was also found to increase with increasing $\Delta E$, initially approximately linearly and at still higher $\Delta E$, nearly exponentially. This behavior was interpreted at that time as due to intersystem crossing to at least two triplet states of widely different energies. At low excess energies intersystem crossing from $S_1$ was suggested to favor a higher triplet $T_j$ because of more favorable Franck–Condon factors. The intersystem crossing to $T_j$ with a small energy gap is then responsible for the linear variation of $k_{NR}$ vs. $\Delta E$. At higher excess energies the intersystem crossing process $S_1 \rightsquigarrow T_1$ involving a large energy gap was proposed to dominate giving the exponential dependence.

The question of possible reversibility of the intersystem crossing in naphthalene has been investigated by Soep et al.[96] Porter and co-workers[93] found that the triplet yield of naphthalene depends on the pressure of added gas, the yield decreasing almost to zero as the pressure is reduced. This behavior was explained on the basis of a kinetic model involving a reversible intersystem crossing process from the isoenergetic nonrelaxed triplet vibronic level to the initially excited singlet level. Soep et al. studied in particular (a) the transient triplet–triplet absorption spectra, originating from nonrelaxed triplet levels (in resonance with the excited singlet level), (b) the effect of collisions on the kinetics of the buildup and decay of the triplet–triplet absorption of the relaxed and nonrelaxed triplet, and (c) the kinetics of the fluorescence decay, as a function of the gas pressure at different exciting wavelengths. The triplet–triplet absorption studies showed that ISC occurs even in the absence of collisions. A reversible ISC would have resulted in a biexponential fluorescence decay (see the section on intermediate coupling). The long component would correspond to the inverse ISC and should be equal to the decay of the triplet–triplet absorption observed at the same pressure. At a pressure of $p =$ 0.1 Torr this lifetime should be about 2.5 $\mu$s. No such long component could be observed in the fluorescence decay, and the authors estimated that if the long component is present its preexponential factor should be smaller by about a factor of 3 $\times 10^4$ than the preexponential factor of the short component. The intersystem crossing process in naphthalene appears therefore to be practically irreversible.

Naphthalene-$h_8$ along with naphthalene-$d_8$ has been reinvestigated by Lim and co-workers.[81a,129] Both lifetimes and quantum yields have been obtained. Owing to calibration errors, the previously reported quantum yields[128] were found to be smaller than they should be by a factor of about 4. The following important general conclusions were made.

(a) The nonradiative decay probability increases first slowly, then very rapidly, as the excess energy is varied over a range of 20 000 $cm^{-1}$.

(b) A plot of the nonradiative decay rate vs. excess energy exhibits a break at photon energy corresponding to the second excited singlet state ($S_2$) of the molecule.

(c) In the low excess energy region, where the decay rate slowly increases as the excess vibrational energy increases, the isotopic ratio of the fluorescence yield or lifetime is small. The onset of the large normal isotope effect seems to coincide with the onset of the sharp increase in the nonradiative decay rate.

The break of the $k_{NR}$ vs. $\Delta E$ curve and the energy dependence of the isotope effect have been given an interesting new interpretation along the following lines: The ratio of the nonradiative rate constants of the radiationless transition $u \rightarrow l$ starting from the vibronic level $|m\rangle$ or the vibrationless level $|0\rangle$ of the state $u$, is given approximately by the ratio of the corresponding Franck–Condon factors

$$\frac{k_{u\rightarrow l}(m)}{k_{u\rightarrow l}(0)} \sim \frac{|\langle m|n\rangle|^2}{|\langle 0|n_0\rangle|^2}$$

where $n$ is a vibronic level of the lower state $l$. The magnitude of this ratio is expected to increase with increasing value of $n_0$. This will come about either by increasing the energy gap between the states involved in the nonradiative transition or by decreasing the frequency of the accepting mode (C–H stretching) by deuteration. From these arguments one would expect that the excess energy dependence of the internal conversion process $S_1 \rightsquigarrow S_0$ (large energy gap) is greater than that for the $S_1 \rightsquigarrow T_1$ intersystem crossing process (smaller gap). Also, this dependence is expected to be greater for the deuterated compound.

The above experimental findings were then explained on the basis of a model involving competing intersystem crossing dominating at small excess energies and internal conversion dominating at large excess energies. The small isotope effect in the low excess energy region is not consistent with internal conversion. The isotope effect on $S_1 \rightsquigarrow S_0$ internal conversion is expected to be large when the excess energy is small. On the other hand, a large isotope effect at high energies is not compatible with the intersystem crossing since intersystem crossing, with small isotope effect at zero excess energy, should exhibit a smaller or even inverse effect at high excess energies. The appearance of a maximum in the isotope effect seems to support further the proposal of two competing processes. The change in slope of the $k_{NR}$ vs. $\Delta E$ curve at the threshold of the $S_2$ state was explained by considering the fact that the vibrational levels of $S_1$ produced by direct absorption are determined by the Franck–Condon factors of the $S_1 \leftarrow S_0$ process. On the other hand, the vibrational distribution in $S_1$ produced by the $S_2 \rightsquigarrow S_1$ internal conversion (emission in naphthalene always originates from the $S_1$ state) is determined by the overlap integrals of the $S_2 \rightsquigarrow S_1$ radiationless transition.

The proposal that at high excess energies the important nonradiative process in naphthalene is $S_1 \rightsquigarrow S_0$ internal conversion has been tested by Hsieh and Lim[81c] through an energy transfer experiment. In this experiment 0.07 Torr of naphthalene was mixed with 0.1 Torr of biacetyl, and the excitation energy dependence of the naphthalene triplet formation was determined by measuring the phosphorescence of biacetyl sensitized by the triplet of naphthalene. Under the conditions of the experiment, both the spectrum and the fluorescence lifetime of naphthalene were found to be the same as those of naphthalene vapor (0.07 Torr). This was considered as an indication that singlet–singlet energy transfer does not contribute significantly to the sensitization of the biacetyl phosphorescence. The results showed that the relative quantum yield of the sensitized biacetyl phosphorescence first increases, then remains nearly constant, and finally decreases rapidly as the excess vibrational energy of naphthalene is increased to about 18 000 $cm^{-1}$. The point where the biacetyl phosphorescence starts decreasing coincides with the point of sharp increase of $k_{NR}$ of naphthalene. This decrease of biacetyl phosphorescence at high excess energies is compatible with the proposed enhanced $S_1 \rightsquigarrow S_0$ internal conversion in naphthalene. This, of course, will be true if the higher triplets of biacetyl formed by the energy transfer process do not have efficient photophysical or photochemical quenching mechanisms that tend to decrease the phosphorescence yield. As we will discuss in detail later, recent evidence by Moss and Yardley[97] indicates that the phosphorescence yield of biacetyl indeed decreases with decreasing excitation wavelength.

Knight et al.[130] have also studied the lifetimes of single vibronic levels of naphthalene-$h_8$ and -$d_8$ under collision-free conditions in the vapor. Special emphasis has been put in this study on the vibronic purity (single vibronic level excitation) of the prepared state. As a criterion of this purity was taken the exponentiality of the observed fluorescence decay. Broad-band excitation of many sequence bands gave nonexponential decays while in most cases sufficiently narrow bandwidth (ca. 6 $cm^{-1}$) gave exponential decays. This result is of special importance in reference to the use of nonexponentiality (see section on heterocyclics and carbonyls) as an indication of an intermediate coupling case. The mean fluorescence lifetime of the prepared state was found to decrease with increasing vibrational energy content, but not as a smooth function of energy. Using relative quantum yield data for $8(b_{1g})^1$ and $0^0$ measured by Bloridau and Stockburger,[131] the authors concluded that the ratio of the lifetimes of the above states can be explained entirely in terms of the differing radiative pathways for electronic relaxation. The authors estimated different values for $\phi_F$ and presented arguments against the validity of the reported values for the $0_0^0$ state determined by Lim and Uy.[128] The authors also report that the lifetimes of naphthalene-$d_8$ are throughout longer than the lifetimes for the corresponding $h_8$ states. The small inverse isotope effect reported by Uy and Lim[125] was not found in this study. Regarding the nonradiative activity of the different vibronic states, it appears that the $8(a_g)$ mode enhances the nonradiative decay. The $a_g$ modes could assist the nonradiative process by a Franck–Condon factor or by acting vibronically on their own.

The fluorescence lifetimes and quantum yields of naphthalene vapor have also been measured as a function of exciting wavelength and of pressure of added foreign gas by Porter and co-workers.[98,132] The fluorescence lifetimes and quantum yields, in accord with the previously mentioned studies, decrease with increasing excitation energy. This effect was attributed to internal conversion from high vibronic levels of $S_1$ to the ground state. Earlier calculations by the same group[77] of the relative rates for intersystem crossing and internal conversion have suggested the dominance of internal conversion at high energies. An interesting behavior was observed as a function of pressure. For short wavelength excitation (<305 nm), the lifetimes and quantum yields increase with pressure while for long-wavelength excitation (>305 nm) they decrease with increasing pressure. The result for short $\lambda$ excitation is a normal effect and is easily understood in terms of the stabilization effect of collisions (vibrational relaxation). The long-wavelength result could be partially due to collisional activation of the initial state on "going up to a Boltzmann distribution". It was proposed that collisional vibrational redistribution to singlet vibrational levels with large intersystem crossing rates is responsible for the observed behavior. To test this hypothesis the authors attempted to fit the lifetime measurements with a step-ladder model proposed by Freed and Heller.[99] This model assumes that the molecule can be replaced by one $N$-fold degenerate oscillator. Collisions induce transitions to adjacent levels only, and the decay rate of each level is assumed to increase linearly with quantum number. The model was found successful in predicting both the increase in lifetime at high excess energies and the decrease in lifetime at low excess energy.

Schlag and co-workers have studied naphthalene over a smaller energy range but with much higher resolution than previous workers. In an initial study[133] an excitation bandwidth of 1.7 Å was used, and seven band heads and the members of the 55-$cm^{-1}$ sequences were resolved and studied. The lifetimes of the band heads and the sequence bands associated with them show a steady decrease as one goes up in energy. Later an even narrower excitation bandwidth of only 0.5 $cm^{-1}$ was used.[134] The following vibronic levels were investigated: the $8(b_{1g})$ and $7(b_{1g})$ levels, the totally symmetric $9(a_g)$, $8(a_g)$, $4(a_g)$ levels, the combined vibrations $8(b_{1g})8(a_g)$ and $8(b_{1g})7(a_g)$, and the vibrationless $S_1$(origin); combinations of those with $3(b_{2g})$, $4(b_{1u})$, and an unknown vibration excited in 55-, 10-, and 6-$cm^{-1}$ sequences, respectively. The high resolution of the light source permitted the excitation at different energies within the same single band. In most cases a spectrum of lifetimes and nonexponentiality was found upon excitation of different energies inside one band. These effects are probably due to different rotational excitation. On the basis of the above result the authors warn that with a medium resolution bandwidth of, e.g., 10 $cm^{-1}$, a fluctuation in lifetime of more than 10% can be observed. Regarding the energy dependence of the lifetime, the enhancement of the decay rate, relative to the origin, was found to show a roughly linear dependence on excess energy in all observed sequence bands of the origin and most principal bands. The main exceptions were the 55-$cm^{-1}$ sequence members $(3b_{2g})$ of the $A^0(8b_{1g})$ and $E^0(8a_g)$ bands and the principal band $E^0(8b_{1g}8a_g)$. The nearly linear increase of the decay rate with excess energy for excitation at bandheads of different symmetry seems to indicate a small influence of vibronic symmetry on the lifetime. The anomaly observed when sequences of vibronic symmetry $3(b_{2g})$ were excited was explained on the basis that the $3(b_{2g})$ mode can couple $S_1$ to a final triplet state through vibronic spin–orbit coupling with $\pi\sigma^*/\sigma\pi^*$ intermediate states. At this point the reader should note that at the low excess energies employed by Schlag and co-workers that dominant nonradiative process is intersystem crossing, while the $S_1 \rightsquigarrow S_0$ internal conversion process proposed by Lim et al.[78a] has a negligible contribution. Since the enhancement upon excitation at the $3(b_{2g})$ band is not very large, it was concluded that possibly more than one promoting mode is active in the intersystem crossing process. Such a mode could be one of $b_{3g}$ symmetry, but no such mode has been identified in the absorption spectrum. In the case of sequence bands originating from $A^0(8(b_{1g}))$, the effect of excitation of $3(b_{2g})$ is pronounced while in the case of $B^0(7(b_{1g}))$ band the $3(b_{2g})$ vibration does not show any enhancement at all in the rate constant. Since the vibronic symmetry of $8(b_{1g})$ and $7(b_{1g})$ are the same, the differences are due to the symmetry of the vibration. Thus not only the vibronic induction of the transition but also the differing Franck–Condon factors must be considered in explaining the great variations in rate enhancement of the $3(b_{2g})$ vibrations when combined with the vibrations of different principal bands.

The effect of isotopic substitution (naphthalene-$h_8$ vs. -$d_8$) on the decay rate has also been studied[135] under high resolution (0.5 $cm^{-1}$). It was found that the origin shows a normal isotope effect of 1.23. Other vibronic bands composed of vibrations of species $3(b_{2g})$, $8(b_{1g})$, $9(a_g)$, and $8(a_g)$ show an inverted isotope effect ($k_H/k_D < 1$). A very interesting point is that the bands with vibronic symmetry $8(b_{1g})$ and $9(a_g)$ show the same inverse isotope effect, $k_H/k_D = 0.83$. Uy and Lim[125] explained the inverse isotope effect of the $8(b_{1g})$ level as due to vibronic spin–orbit coupling of $S_1$ with a higher $^3B_{3u}$ triplet. The above result of Boesl et al. seems to indicate that the inverse isotope effect is not a result of symmetry but an outcome of the particular amount of excess energy. The normal isotope effect at the origin is reduced as the energy is increased, finally becoming inverted. The maximum value for the inverse isotope effect ratio is at about 500 $cm^{-1}$ excess energy; above this energy the inverted effect is reduced and $k_H/k_D$ becomes one at about 900 $cm^{-1}$ above the origin.

An important observation is that if the plot $k_H/k_D$ vs. $E_{excess}$ is made at constant initial quantum state, all vibrations except the 10 $cm^{-1}$ $4(b_{1u})$ sequency, irrespective of symmetry, fall along the same smooth curve.[252] In this representation, the $b_{2g}$ vibrations behave completely analogous to the other vibrations (cf. ref 134). In the case of $k_{NR}$, both initial and final state vibronic levels are important and contribute to the Franck–Condon factors for intersystem crossing. Since the ratio $k_H/k_D$ is determined for the same vibronic level of the initial state of $C_{10}H_8$ and $C_{10}D_8$, then the $k_H/k_D$ spectrum should reflect changes in the final state. As the data of Boesl et al. show for all vibrations, except $4(b_{1u})$, the relation $k_H/k_D$ is a smooth function of excess energy. There are no rapid nonsystematic variations. The final states are expected to differ, in general, in symmetry. The above smooth behavior was therefore interpreted by Boesl et al.[135] as indicating that although, on the time scale of the experiment, no vibrational communication exists in the singlet state, rapid vibrational communication exists in the final triplet state. It was further suggested that a mechanism involving crossing to the second triplet $T_2$, with communicating vibronic states in $T_2$, can explain the inverse isotope effect.[136]

Recently Stockburger and co-workers in a series of articles have investigated in detail the spectral and dynamic properties of naphthalene in the dilute vapor phase. Stockburger et al.[137] have studied the fluorescence spectra originating from various single vibronic levels in the first excited singlet state of naphthalene-$h_8$ and -$d_8$, under collision-free conditions. The vibrational structure and intensity of the spectra was interpreted in terms of the vibronic coupling theory. In another article[138] the various possible intersystem crossing mechanisms were investigated. Five different coupling schemes involving direct spin–orbit coupling or vibronic spin–orbit coupling (see section II.A.3) in the singlet or triplet manifolds were examined. From symmetry selection rules and from results of spin-alignment experiments,[139] it was concluded that the leading mechanism (mechanism A) is one involving Herzberg–Teller coupling (HT) of the $S_1$ state with $\pi\sigma^*$ or $\sigma\pi^*$ states. According to calculations of Meyer et al.,[140] the second triplet ($T_2$) naphthalene is nearly degenerate with $S_1$ and the next higher ($T_3$) triplet also lies within the region of $S_1$. Stockburger et al. suggest therefore that a HT vibronic spin–orbit coupling involving resonance interactions with $T_2$ or $T_3$ may be important (mechanism B). Mechanism A is expected to be nearly independent of the special vibronic level initially excited in $S_1$, since for horizontal crossing to the quasicontinuum of $T_1$ there are always a number of final states which satisfy the symmetry conditions. The resonance mechanism B, however, depends critically on the initial as well as on the intermediate state, since the resonance as well as the symmetry condition must be satisfied. Therefore, one may expect large fluctuations for B in the various levels of $S_1$, while A should be approximately constant. Regarding the relative importance of mechanisms A and B, the authors conclude that in the case of resonance, B should be more important than A. The deuterium isotope effect is also expected to be different for the two mechanisms. Mechanism A is expected to show a normal isotope effect. On the other hand, the intersystem crossing rate constant according to B is inversely proportional to $\Gamma_2$ or $\Gamma_3$, the linewidth of the $T_2$ or $T_3$ resonance state, which is determined by the rate of the internal conversion to $T_1$. In turn, $\Gamma_{2,3}$ is proportional to a Franck–Condon factor which accounts for an energy gap of about 10 000 $cm^{-1}$ ($T_2$–$T_1$ energy gap) and therefore is expected to decrease on deuteration resulting in an inverse isotope effect for mechanism B.

Regarding the experimentally observed single vibronic level quantum yields, it was concluded that the variations in the quantum yield spectra reflect both variations in radiative $k_F^{\nu'}$ as well as in nonradiative $k_{ISC}^{\nu'}$. In the case of *N*-$h_8$ the yields for

$b_{1g}$ levels are on the average somewhat higher than for $a_g$ levels. The reason is that $k_F(b_{1g})$ on the average is somewhat greater than $K_F(a_g)$ due to vibronic coupling of the $^1B_{1u}$ and $^1B_{2u}$ states (see also Uy and Lim[1]). Plotting the data as $k_{ISC}^{\nu'}/k_F^{\nu'}$ vs. energy, a general trend is observed where $k_{ISC}^{\nu'}/k_F^{\nu'}$ increases with excess vibrational energy. Since $k_F^{\nu'}$ slightly increases with excess energy, this general increase is attributed to $k_{ISC}$.

A very important observation[138] is the large fluctuations in the quantum yield $\phi_F$ spectra. Various minima in $\phi_F$ are observed and are distributed over the whole energy range. In the $k_{ISC}^{\nu'}/k_F^{\nu'}$ representation, these minima correspond to maxima. The four vibrational levels of lowest energy have been investigated in more detail. These levels show pronounced isotope effects. For the two $a_g$ levels $0^0$ and $8^1$, the quantity $k_{ISC}/k_F$ decreases on deuteration (normal isotope effect) while an inverse deuterium effect is observed for the levels $\bar{8}^1$ and $9^1$. By combining lifetime and quantum yield data, absolute rate constants for these four levels were obtained. Stockburger and co-workers take the mean value of $k_{ISC}$ for the two normally behaving modes $0^0$ and $8^1$; then with respect to this mean value $k_{ISC}(9^1)$ increases by a factor of 3.16 in going from naphthalene-$h_8$ to naphthalene-$d_8$. It was proposed that process A dominates in the case of levels $0^0$ and $8^1$. On the other hand, if one accepts that the contribution of process A in the $9^1$ state is equal to the mean value $\bar{k}_{ISC}$ $(0^0,8^1)$, one obtains in units of $10^6$ $s^{-1}$ (N = naphthalene)

$$k_{ISC}(9^1) = k_{ISC}^{A}(9^1) + k_{ISC}^{B}(9^1)$$
$$= 2.13 + 0.67(\text{N-}h_8) \text{ or } 1.19 + 3.75(\text{N-}d_8).$$

This relation implies that process B is 5.6 times stronger for the deuterated compound. This fact was ascribed to an improvement of resonance conditions and to the inverse isotope effect due to $1/\Gamma$ dependence. Similar reasoning was applied to level $\bar{8}^1$ which behaves in a similar way to $9^1$.

In conclusion the authors suggest that the large changes in $k_{ISC}$ that occur in naphthalene within small energy ranges cannot be explained on the basis of HFG theory,[57] which is based on changes of Franck–Condon factors that account for a large energy gap. The explanation then of the data on naphthalene according to the authors requires the involvement of the resonance mechanism B.

The above results and conclusions refer to $S_1$ excitation. No information about single vibronic levels of $S_2$ could be obtained since, even in the collision-free limit, fluorescence always originates from $S_1$. Biacetyl sensitization experiments gave results analogous to those of Hsieh and Lim,[78c] and internal conversion was suggested to be important for excess energies over 8000 $cm^{-1}$.

Finally[141] the gas-phase phosphorescence spectra of naphthalene-$h_8$ and -$d_8$ were studied. Also, intersystem crossing yields of single vibronic levels in $S_1$ were determined from excitation spectra of biacetyl phosphorescence. These data support the idea that at low excess energies, intersystem crossing is the dominant process.

Very recently Schlag and co-workers[142] obtained single vibronic level fluorescence lifetimes of naphthalene excited by two-photon absorption. The first weak absorption band ($S_1 \leftarrow S_0$) in the two-photon case is placed on the rising background of the strong system ($S_2 \leftarrow S_0$) from which it borrows most of its intensity. Lifetimes measured at medium excess energies above $S_1$ may then be modified by this overlap. In the two-photon case this problem is absent, since there both the $S_1 \leftarrow S_0$ and $S_2 \leftarrow S_0$ are forbidden. Thus with two-photon excitation new vibronic levels can be excited and the measurements can be extended to higher energies. From the experimental results, the following general conclusions were reached: (a) The vibronic symmetry or vibronic parity does not seem to play a dominant role in the ISC Process. (b) No promoting mode for the ISC was found. (c) There is a monotonic dependence of fluorescence lifetime on energy for both one- and two-photon excitation. This is considered as an indication that Franck–Condon determines the radiationless processes in naphthalene and vibronic inductions and promoting modes are unimportant.

### a. Summary of Important Results on Naphthalene

Concluding our discussion of the experimental studies on naphthalene, we feel that several points are important enough to be brought up again in a summary. Regarding the dominant nonradiative channel in naphthalene at low excess energies, there seems to be agreement among different groups in identifying it with an $S_1 \rightsquigarrow T_1$ intersystem crossing process. There is a general smooth increase in $k_{NR}$ with excess energy in the low excess energy region. As particularly Schlag and co-workers have pointed out, the nonradiative relaxation rate from a particular vibronic level is determined not by the vibronic symmetry but primarily by the Franck–Condon factor as predicted by the HFG model. Evidence for an additional intersystem crossing channel has been presented by Stockburger and co-workers in the case where the excited vibronic level of $S_1$ is in resonance with the $T_2$ or $T_3$ state ($S_1 \rightsquigarrow T_2$ or $S_1 \rightsquigarrow T_3$ ISC). Although fluorescence from naphthalene always originates from vibronic levels of $S_1$, a change in the slope of $k_{NR}$ vs. $E_{excess}$ has been observed by Lim and co-workers at the threshold of the $S_2$ state. This behavior was interpreted as due to the different vibrational distributions produced by direct $S_1 \leftarrow S_0$ optical absorption or $S_2 \rightsquigarrow S_1$ internal conversion (Laor and Ludwig did not find any such break). At high excess excitation energies ($E_{excess} \gtrsim$ 10 000 $cm^{-1}$, $S_2$ state) a rapid increase of $k_{NR}$ with $E_{excess}$ was found by Lim and co-workers. In agreement with an earlier proposal by Porter and co-workers based on simplified theoretical considerations, Lim and co-workers assigned this rapid increase in $k_{NR}$ as due to the onset of fast $S_1 \rightsquigarrow S_0$ internal conversion. Another possibility could be that the $S_1$ state does not deactivate directly to $S_0$ but through some reversible photochemical path, e.g., valence isomerization (see also the discussion on benzene). Experimental study of this possibility is needed.

While in condensed phases substitution of hydrogen by deuterium always leads to a reduction of $k_{NR}$, in the low-pressure naphthalene vapor, inverse isotope effects ($k_{NR}^H/k_{NR}^D < 1$) have been found.

Another interesting aspect of the studies on naphthalene is the effect of the exciting light bandwidth on the lifetime and exponentiality of the decay. As Knight et al. found, broad-band excitation of many sequence bands resulted in nonexponential decays. This observation is of particular interest, especially in view of the importance attached to the nonexponentiality as a characteristic of intermediate coupling and "reversible" intersystem crossing (see sections on aza-aromatics and dicarbonyls). The experiments of Schlag and co-workers with even narrower exciting bandwidth suggest a possible rotational level (within the same vibronic band) dependence of $k_{NR}$. Explanations for these results and theoretical models investigating the effect of rotational excitation on the efficiency of the electronic relaxation process are needed.

### 5. Naphthylamine

Among the naphthalene derivatives, *naphthylamine* has received the most attention. For example the excess energy dependence of the decay processes of excited $\beta$-naphthyl-$h_7$-amine vapor has been studied by Hsieh et al.[143] and again, along with a parallel study of $\beta$-naphthyl-$d_7$-amine by Huang et al.[144]

It was found that the decay rate increases first slowly and then rapidly as the excess energy is increased. Since the fluorescence quantum yield shows a similar energy dependence, one

can conclude that the observed changes are due to changes of the nonradiative rate constant $k_{NR}$. The isotope effect is small at low excess energies and normal ($k_H/k_D > 1$) at higher energies; it increases and finally at high enough energies it becomes inverted ($k_H/k_D < 1$). The excitation wavelength at which a significant isotope effect appears practically coincides with the energy threshold above which the decay rate increases sharply with increasing excitation energy. This observed behavior is very similar to the behavior of naphthalene and its interpretation is completely analogous. At low excess energies the important nonradiative process is $S_1 \rightsquigarrow T_1$ while at high excess energies the $S_1 \rightsquigarrow S_0$ internal conversion dominates.

### 6. Anthracene

Laor et al.[145] were the first to study *anthracene* under isolated molecule conditions (0.2 Torr and 30-Å excitation bandwidth). The authors measured fluorescence lifetimes as a function of excess energy up to an excess energy of ~19 000 $cm^{-1}$. Instead of the monotonic decrease in lifetime with increasing excitation energy observed in other large aromatic hydrocarbons, the decay was found to be rather constant within several regions of excitation energy and to exhibit step-like changes at about 256 and 233 nm and a less pronounced one at about 351 nm. Laor et al. interpreted this behavior as indicating intersystem crossing to higher triplet states that come into resonance with increasing vibronic excitation. The location of these higher triplets is not known exactly and their energies have been inferred mainly on the basis of $\pi$-electron calculations.

Fischer and Lim[146] have observed that the fluorescence quantum yield of anthracene vapor (0.02 Torr and 1-nm bandpass) exhibits a step-like drop at about 255 nm, which corresponds to the onset of the $^1B_{3u}^+ \rightarrow {}^1A_{1g}$ absorption band. Their interpretation of the origin of the step-like drop in the quantum yield is different from that of Laor et al.[145] Fischer and Lim assume that the important deactivating process is intersystem crossing from $^1B_{2u}^+(S_1)$ to $^3B_{1g}^+(T_2)$ ($^3B_{1g}^+$ lies 500 $cm^{-1}$ below $^1B_{2u}^+$). Initial excitation of the $^1B_{3u}^+$ state is followed by $^1B_{3u}^+ \rightsquigarrow {}^1B_{1g} \rightsquigarrow {}^1B_{2u}^+$ internal conversion which produces a distribution of vibrational levels that enhances the $^1B_{2u}^+ \rightsquigarrow {}^3B_{1g}^+$ intersystem crossing. This vibrational distribution produced by the internal conversion process is more favorable for the $^1B_{2u}^+ \rightsquigarrow {}^3B_{1g}^+$ intersystem crossing than the vibrational distribution produced by direct excitation of vibronic levels of the $^1B_{2u}^+$ state. The intersystem crossing to higher triplets proposed by Laor et al.[145] is considered unlikely by Fischer and Lim on the basis that the vibrationally excited singlet provides a very large phase space (density of states) which is absent for the ground vibrational level of the higher triplet states. Furthermore, Fischer and Lim suggest that all the step variations observed by Laor et al.[145] may not be real.

Anthracene has also been studied by Beddard et al.[98] and by Huang et al.[147] Beddard et al. have obtained fluorescence lifetimes (0.04 Torr and ≤5-Å bandwidth) as a function of excess energy, up to an excess energy of 14 640 $cm^{-1}$. The lifetimes were found to show a remarkable constancy for excitation in $S_1$ and an abrupt change between 300 and 240 nm. Beddard et al. assumed that the nonradiative transition which is important in this case is $S_1 \rightsquigarrow T_1$, and the lack of any significant variation in lifetime is due to the fact that both the $S_1$ and $T_1$ states have $L_a$ symmetry. As a result of this fact the change in geometry between $S_1$ and $T_1$ was suggested to be very small and to reflect into small Franck–Condon factors for the intersystem crossing process. Huang et al.[147] have studied both anthracene-$h_{10}$ and anthracene-$d_{10}$ (0.1 Torr and 3.3-nm bandpass) over a wider excess energy range (~23 000 $cm^{-1}$). The results showed that the nonradiative decay rate remains nearly constant with initial increase in excitation energy, in agreement with Beddard et al.,[98] but increases in the region of high excess energy ($\tau$ = 5.00 ns at 365 nm, $\tau$ = 1.55 ns at 200 nm). The deuterium isotope effect on the radiationless decay rate was found to be small, and nearly constant, in the wavelength regions where the energy dependence of the decay rate is small, but to be relatively large for excitation wavelengths shorter than about 240 nm. The authors suggest that the near constancy of the decay with initial excess energy is due to an $S_1 \rightsquigarrow T_1$ intersystem crossing (small energy gap) while the smooth increase in the radiationless decay rate with increasing excitation energy below about 240 nm is due to the commencement of significant internal conversion to the ground state (large energy gap). The increase in the isotope effect in the same energy region is similarly interpreted.

### 7. Pyrene

*Pyrene* is one of the larger aromatic hydrocarbons that has received considerable attention. The first study of pyrene in the low-pressure vapor phase was that of Werkhoven et al.[148] In this study, pyrene at a pressure of about 0.1 Torr was excited by a frequency doubled ruby laser. The basic observation was that the fluorescence decay was not exponential. On the other hand, the decay became exponential upon addition of *n*-hexane vapor. These effects were observed for several temperatures in the range between 150 and 350 °C. The nonexponential decay of the fluorescence was interpreted by the authors as being due to emission from pyrene molecules with different degrees of vibrational excitation of the $S_1$ state. This conclusion was reached from considerations of the effect of hexane and from the fact that in the later stages of decay, when collisional deactivation has proceeded, the "formal" decay times become longer and seem to converge to the decay times for the fully relaxed vapor as obtained with hexane.

As possible explanations for the increasing fluorescence decay rate with excess vibrational energy the authors considered: (I) a decrease in the radiative lifetime and (II) an increase in the intersystem crossing rate with increasing vibrational energy. The $S_1 \rightarrow S_0$ radiative transition is partly of vibronic origin so a dependence of the radiative rate constant on vibrational excitation is expected. Also since a $T_2$ state was found to lie about 400 $cm^{-1}$ above $S_1$, the opening of a new intersystem crossing channel involving $T_2$ may come into existence upon vibrational excitation. From the relative effects of temperature on the fluorescence lifetime and quantum yield, it was concluded that although both effects are operative, the most important is the enhancement of the intersystem crossing process. In a subsequent paper by the same group,[149] pyrene was reexamined at even lower pressure ($10^{-3}$ Torr) and to a shorter time scale. The previous observations were in general verified. In the first stage of the decay, under conditions where the molecules can be considered as completely isolated, a short component with a lifetime of 70 ns was observed. Considering the excitation energy (28 800 $cm^{-1}$), the authors concluded that the molecule was prepared in an $S_1$ state with one quantum in a $b_{1g}$ (1106 $cm^{-1}$) and another one in a $a_g$ (572 $cm^{-1}$) mode, or in singly excited states of another $b_{1g}$ (1593 $cm^{-1}$) or $a_g$ (1636 $cm^{-1}$) mode. The $b_{1g}$ mode can mix through a Herzberg–Teller mechanism the $B_{3u}$ ($S_1$) state with the $B_{2u}$ ($S_2$) state; an $a_g$ mode could mix $B_{2u}$ with another configuration of the same symmetry. Taking into account the nonvibronically induced part of the transition moment, the authors concluded that when the system is prepared in a $\nu'(b_{1g}) = 1$ state an enhancement by a factor of 2.5 is introduced in the radiative decay, as compared to the case of $\nu'(b_{1g}) = 0$. Concerning the intersystem crossing enhancement, the possibility of vibronically induced spin–orbit coupling (through $b_{1g}$) of $^1B_{3u}$ with a $b_{2u}$ component of a $^3B_{3u}$ state has been considered. Neither the radiative enhancement nor the vibronically induced part of intersystem crossing could account for the 70-ns component. This short component was thought to be determined by the value of the vibrational redistribution rate

constant. In order to further clarify the origin of the short decay component, more measurements were made[150] at three different excitation energies on pyrene-$h_{10}$, pyrene-$d_{10}$, and 3-methylpyrene. The short component was absent upon the excitation of pyrene ($h_{10}$ and $d_{10}$) at the origin and was also absent in the case of 3-methylpyrene, excited at any of the above three frequencies. Apparently the fast component appears only upon excitation of an inducing mode. Upon consideration of all eight vibrational inducing fundamentals, it was estimated that the upper limit in the change of the radiative decay upon excitation of one quantum of an inducing mode is only 24%. To investigate the effect of vibronic excitation on the nonradiative decay, the authors employed the theoretical model of HFG.[57] It was estimated that if the optically excited mode is an inducing mode, the decay rate will change at most by a factor of 1.7, upon excitation of one quantum of it vs. excitation at the origin. If on the other hand the mode which is excited by one quantum is a promoting mode, a change by a factor of 2 was considered as an upper limit. Thus again the radiative and nonradiative enhancement cannot explain the large ratio of the short and long components of the decay (3.7–5.2). Since the radiative decay rate of pyrene depends on the quantum number of the inducing mode, it will change upon vibrational redistribution, making the redistribution process observable in the fluorescence decay. The short component then was attributed to the vibrational redistribution process.

In a more recent paper by the same group,[151] values for the radiative and nonradiative rates of pyrene as a function of excess energy were obtained by combining quantum yield and lifetime measurements. Under the assumption that the vibrational redistribution is fast compared to the total decay rate of the electronic state under consideration, the properties of the ensemble of molecules can be derived as an average of the properties of all states at that particular energy. The authors have computed the energy dependence of the radiative rate. Good agreement was found between the calculated dependence and the energy dependence of the long component of the decay. This agreement gives additional support to the identification of the long-lived component as arising from an ensemble of molecules in which the excess vibrational energy is randomly distributed over the available density of states.

Pyrene has also been studied by Beddard et al.[98] The decay times of pyrene at a pressure of 0.1 Torr were measured as a function of excess energy, up to an excess energy of about 11 000 $cm^{-1}$. Broad band excitation was used with bandwidth of 0.5 nm or less. At all energies except the highest one used (265 nm), the decays were nonexponential, with the short componert being of the same magnitude (90–100 ns) as that observed by the other investigator.[149-151] One important difference is that unlike Werkhoven et al.,[150] nonexponential decay was observed even upon excitation at the electronic origin.

In general, the pyrene decay curves were found to fall into two types: at 265 nm the decay is exponential for two decays; after this a slight tailing is seen, possibly due to pyrene–pyrene collisions. In the region 330–370 nm the decays are nonexponential initially, becoming exponential at longer times. From 280 to 330 nm, the total decays are a mixture of these two types. The authors did not provide any interpretation of their data, especially for the observed nonexponentiality upon excitation at the origin and the apparent discrepancy with the findings of the other studies.[150]

### 8. Other Aromatic Hydrocarbons

*Fluorene* has been studied by Huang et al.[152] over an excess energy range of ~15 000 $cm^{-1}$. Fluorescence lifetimes and quantum yields show almost identical energy dependence, both decreasing with excess erergy. For example, the lifetime $\tau$ is 13.0 ns at 2950 Å while $\tau$ = 3.2 ns at 2050 Å. The most interesting feature of the results is the step-like increase in the radiationless decay rate as the threshold for excitation of $S_2$ is crossed. This was attributed to a large change in the decay rate of $S_1 \rightsquigarrow T_1$ intersystem crossing, as the vibrational energy distribution in $S_1$ changes from the one determined by the Franck–Condon factor for $S_1 \leftarrow S_0$ optical absorption to the one governed by the Franck–Condon factors for $S_2 \rightsquigarrow S_1$ radiationless transition. The relatively sharp rise in the nonradiative decay rate at even higher energies was attributed to the commencement of an $S_1 \rightsquigarrow S_0$ internal conversion process. This proposal was supported by experiments on the excitation energy dependence of the quantum yield of sensitized phosphorescence of biacetyl. It was found that the quantum yield of $S_1 \rightsquigarrow T_1$ intersystem crossing in fluorene decreases with increasing excitation energy for molecules with large excess vibrational energies.

Radiationless transitions in *tetracene* have also been studied in the vapor phase as a function of excess energy. Fleming et al.[153] have found a very rapid decrease in the fluorescence lifetime as the largest compared to all other aromatic hydrocarbons previously studied by the same group.[98] The authors excluded the possibility that the change in the observed lifetime is due to a change in the radiative rate with excess energy. Also $S_1 \rightsquigarrow T_1$ intersystem crossing was not considered a likely candidate since both $S_1$ and $T_1$ states are $L_a$ states (see ref 98). The authors therefore concluded that the observed behavior is due to enhanced internal conversion from vibrationally excited levels. It should be mentioned at this point that Kearvell and Wilkinson[154] have found that tetracene, unlike other aromatic hydrocarbons, shows significant internal conversion to $S_0$ ($\phi_{IC} \approx 0.2$) even in solution.

Tetracene-$h_{12}$ and -$d_{12}$ along with *pentacene* has been the subject of another study by Okajima and Lim.[155] It was found that in tetracene the radiationless decay rate increases with initial increase in excitation energy, but it soon tapers off and becomes a slowly varying, monotonic, function of excess energy. The results were interpreted as indicating an increase in the internal conversion process $S_1 \rightsquigarrow S_0$ when moderate excess energy is given, by the absorption process, to the C–C stretching modes. At higher excess vibrational energies, vibrational redistribution becomes significant redistributing the excess energy from the C–C stretching modes to other vibrational modes and resulting in a slower increase in nonradiative decay with excess energy. The decay of rate of tetracene-$d_{12}$, while substantially smaller in magnitude than in $h_{12}$, increases faster with excitation in the C–C stretching modes.

Pentacene in solution has a very high yield of internal conversion ($\phi_{IC} \simeq 0.8$). Recently Soep[156] has been able to follow the internal conversion process in gaseous pentacene, by monitoring, through a pulsed laser, a transient absorption on the long-wavelength side of the ground-state absorption. This red shifted absorption band was attributed to excited vibrational levels of the ground state, populated by the internal conversion. The most prominent progression in the $S_1 \leftarrow S_0$ absorption involves excitation of the C–C stretching modes. Since these modes undergo a change in geometry between $S_0$ and $S_1$, one would expect them to act as good accepting modes, and a large increase in the rate of $S_1 \rightsquigarrow S_0$ internal conversion is expected with increasing excitation of these modes. The experimental results show exactly the opposite behavior. The decay rate as a function of excess energy initially decreases, then increases slowly again. This behavior was interpreted by Okajima and Lim[155] as indicating efficient vibrational redistribution in this considerably big molecule, even at low excess energy.

Other hydrocarbons that have been studied under "collision-free" conditions are *benz[a]anthracene* and *chrysene* by Beddard et al.[98] A general decrease of lifetime was observed as a function of excess excitation energy.

The isotope effect on the fluorescence lifetimes of "collision-free" *azulene* (azulene-$h_8$ vs. -$d_8$) has been studied by

Knight and Selinger.[157] It was found that the fluorescence lifetime decreases with excess energy while the isotope effect increases.

## B. Aza-Aromatic Molecules

### 1. Azabenzenes

As we have seen, nonradiative transitions in aromatic hydrocarbons show a statistical limit behavior. In most cases the behavior of corresponding aza-heterocyclic molecules is different, corresponding to an intermediate coupling case. This difference in behavior results from the presence of $n\pi^*$ states in heterocyclics, which in turn results in smaller $^1(n\pi^*)$–$^3(n\pi^*)$ separations, the possibility of small $^{1,3}(\pi\pi^*)$–$^{1,3}(n\pi^*)$ separations, and strong spin–orbit coupling between $^{1,3}(\pi\pi^*)$–$^{3,1}(n\pi^*)$ states.

The photophysical behavior of *pyrazine* (1,4-diazabenzene) in condensed phases and in the nearly saturated vapor corresponds to the statistical limit. At much lower pressures the behavior is completely different. In two studies by Tramer and co-workers,[158,159] the photophysical behavior of pyrazine was investigated upon excitation of approximately single vibronic levels of its $S_1$, $^1B_{1u}(n\pi^*)$ state. The pressure was varied between $10^{-2}$ Torr (low enough to avoid any collisions during the singlet lifetime, and to reduce the number of collisions to a few during the triplet lifetime) and ~100 Torr of pure pyrazine or pyrazine–$SF_6$ mixtures. Two important observations were made.

(a) The emission at sufficiently low (10–50 mTorr) pyrazine pressure consists exclusively of resonance fluorescence. The fluorescence yield decreases with increasing pressure (its drop is more rapid and stronger for the lower vibronic states) and remains unchanged at pressures varying between 20 and 200 Torr. The fluorescence spectrum remains rigorously unchanged with pressure.

(b) The phosphorescence appears to be induced by collisions and can be observed at pressures exceeding $5 \times 10^{-2}$ Torr. The phosphorescence spectrum does not show any dependence on the gas pressure or the exciting wavelength.

The fact that the emission is sensitive to collisions in the pressure range corresponding to $10^6$–$10^8$ collisions/s is incompatible with the decay time of pyrazine estimated from its radiative lifetime and fluorescence yield as $\tau = (2\text{–}5) \times 10^{-10}$ s. Moreover, when the fluorescence intensity ratio $(I_F)_p/(I_F)_{p\to 0}$ is plotted against the $SF_6$ pressure, a nonlinear Stern–Volmer plot is obtained. Linear Stern–Volmer plots are characteristic for exponentially decaying species.

The above findings were explained in ref 158 by proposing that the decay of pyrazine is nonexponential, composed of a short, pressure-independent decay and a long, pressure-dependent decay constant. Direct evidence of the nonexponentiality was presented in ref 159. The decay obtained by exciting with a nanosecond pulse was found to consist of a strong fluorescence pulse, the shape of which is practically identical with that of the exciting pulse and of a much weaker, longer decay. By using different exciting sources it was determined that the fast decay is faster than 2–3 ns. Because of its weakness, the lifetime of the long emission was determined indirectly. It was assumed that at high $SF_6$ pressure (10–20 Torr) the slow fluorescence is completely quenched, and the signal is composed of fast fluorescence and phosphorescence. The difference of the decay curves of the low-pressure pyrazine sample ($5 \times 10^{-2}$–1 Torr) from the high-pressure pyrazine–$SF_6$ mixtures (pyrazine partial pressure kept constant) plotted against time allows a rough evaluation of the long decay time. This decay time decreases, as was expected, with increasing pyrazine pressure. The lifetime extrapolated to zero pressure was evaluated as $\tau = 200 \pm 30$ ns. The phosphorescence decay, recorded during the first 100 $\mu$s is rigorously exponential and pressure independent in the pressure range of 0.2 to 10 Torr. The phosphorescence lifetime was determined to be $63 \pm 3$ $\mu$s.

The experimental data and especially the origin of the fast and slow fluorescences were interpreted in ref 158 in terms of the following model. The single vibronic level of the $S_1$ state $|S\rangle$ is strongly coupled to a dense manifold of triplet vibronic levels $\{T\}$ which are in turn: (a) coupled, in an isolated molecule, to the quasi-continuum of the ground-state levels $\{G\}$; and (b) coupled, by collisions, to a quasi-continuum of vibrational and rotational levels $\{T'\}$ of the same triplet ($\{T'\}$ are not directly coupled to $S_1$). The fast fluorescence decay constant $\lambda_f$ then corresponds, as in the statistical case, to the sum of the radiative and nonradiative widths of the initially excited Born–Oppenheimer singlet level: $\lambda_f = \Gamma_S + \Gamma_{ST}$. The decay constant of the slow component of the fluorescence of isolated molecules $\lambda_s$ is that of the quasi-stationary state resulting from the coupling of the $|S\rangle$ level with $N$ zero-order T levels. This decay constant is then described as $\lambda_s = \Gamma_S/N + \Gamma_T + \Gamma_{TG}$. The singlet emission probability is distributed between $N + 1$ levels, each of them being characterized by its own phosphorescent radiative width $\Gamma_T$ and nonradiative width $\Gamma_{TG}$. $\Gamma_{TG}$ depends strongly on the vibrational excess energy with respect to the vibrationless level of the $T_1$ state. The collisions couple the $\{T\}$ manifold with the $\{T'\}$ quasi-continuum and introduce a supplementary nonradiative width $\Gamma_{TT'}$ to the quasi-stationary state. The fluorescence yield is thus decreased and the molecule is transferred to the $\{T'\}$ levels uncoupled to the singlet manifold from which it can decay by phosphorescence emission $\Gamma_T$ or by a nonradiative transition $\Gamma_{T'G}$ to the ground state.

In ref 158 the results were interpreted in terms of the more general theoretical models proposed by Lahmani et al.[92a] and Delory and Tric.[19] A coherent excitation was assumed of $N + 1$ quasi-stationary states contained in an energy band $\Delta$ and resulting from a strong coupling of one radiative $|S\rangle$ level and a manifold of weakly radiative $|T\rangle$ levels (if $\rho_T$ is the density of T states and $V_{ST}$ is the coupling element, then $N = \pi^2 \rho_T{}^2 V_{ST}{}^2$). The T levels were considered to be randomly distributed. In the case of pyrazine, the following conditions were considered appropriate for the application of the theory: $\Delta \gg |\Gamma_S - \Gamma_T|$, $N \gg 1$. The decay in such a case is expected to be approximately biexponential:

$$I_F(t) = I_f \exp(-\lambda_f t) + I_S \exp(-\lambda_s t)$$

with

$$\lambda_f = \overline{\Gamma}_N + \Delta \simeq \Gamma_S/N + \Gamma_T + \Delta$$

$$\lambda_s = \overline{\Gamma}_N \simeq \Gamma_S/N + \Gamma_T$$

where $\Gamma$'s represent total widths and $I_s{}^0/I_f{}^0 = 1/(N + 1)$. Furthermore, in the case of pyrazine the condition $\Delta \gg \Gamma_N$ was considered applicable. The experimental data were then discussed in the light of the above theoretical models.

The relaxation processes in another diazabenzene, *pyrimidine* (1,3-diazabenzene), have been investigated by Baba and coworkers.[160] The authors studied the pressure and excitation energy dependence of the fluorescence quantum yield and lifetime of pyrimidine vapor in the pressure range $10^{-3}$–10 Torr. They found that the fluorescence decay has a fast component with a lifetime $\tau_f$ of the order of a nanosecond. The calculated radiative fluorescence lifetime is 0.2 $\mu$s. The fast lifetime was found to decrease with increasing excess energy $\Delta E$. For a given $\Delta E$, however, $\tau_f$ is essentially constant in the whole range of pressures studied. On the other hand, the fluorescence yield $\phi_F$ falls off rapidly on going from $p = 0$ to $p \simeq 50$ mTorr, suggesting that the fluorescence of the collision-free pyrimidine contains a slow component as well (not directly observed). Since the emission spectrum is itself independent of pressure, it was suggested that both components give the same spectrum. The slow component was estimated to have a collision-free lifetime

$(\tau_s)_{p\to 0}$ of 10 $\mu$s and $(\tau_s)_{p\to 0}$ was found to be fairly constant regardless of the magnitude of $\Delta E$. The corresponding quantum yield $(\phi_{F,slow})_{p\to 0}$ decreased significantly with increasing $\Delta E$, and this decrease was explained by assuming a corresponding lengthening of the radiative lifetime $\tau_{F,slow}$ of the slow component. The short and the long decay components were thought to be a result of a sequential decay analogous to the one proposed by Tramer and co-workers[159] for pyrazine.

Direct observation of the long component in the decay of pyrimidine was reported by Spears and El-Manguch.[161] The authors have performed decay measurements on pyrimidine excited to several higher vibrational levels above the 0,0 band (up to 2000 $cm^{-1}$). They found a dual emission lifetime for these states with decay times near 1 ns and 100–200 ns at 0.1 Torr.

Vemulapalli and Cassen[162] have studied the fluorescence of *s-tetrazine* (1,2,4,5-tetraazabenzene) in the collision-free region and also with different concentrations of quenchers. The 0,0 band and three sequence bands close to the 0,0 were excited, and 3-methylpentane and argon were used to quench the emission. The quantum yields of *s*-tetrazine were found to be low and to range from 0.01 to 0.05 over the wavelength range investigated. The results showed that the quantum yield has a small variation within a vibrational band envelope. This variation was tentatively explained as indicating a rotational quantum number dependence of the nonradiative process (see also the analogous observation of Schlag and co-workers[134] on naphthalene). The variation of the yield among different vibrational levels is unquestionable. The largest change is observed between the 0,0 and the $16b_1^1$ levels. Intersystem crossing was suggested to be the dominant nonradiative process. Bimolecular processes, vibrational deactivation and quenching of total fluorescence, were found to be very inefficient. The number of hard-sphere collisions needed for these processes ranged from 50 to several hundred, depending on the vibronic level.

Dynamic measurements on *s*-tetrazine vapor have been performed by McDonald and Brus[163] using dye laser excitation into single vibronic levels of the $^1B_{3u}$ (origin at 5514 Å) and $^3B_{3u}$ states. The 0,0 and three shorter wavelength bands of the $^1B_{3u}$ state were excited. In all cases an intense emission was observed with a time dependence identical with that of the laser pulse used (lifetime should be $\leq$100 ns). No second, longer decay component was detectable in the pressure range 1–680 mTorr. The radiative lifetime was estimated as ~900 ns. Considering the possible nonradiative paths deactivating the $^1B_{3u}$ state, the authors ruled out predissociation while fluorescence to a lower energy $^1n\pi^*$ was considered very unlikely. On the basis of density of states considerations, a dominant intersystem crossing was also considered unlikely. This conclusion seems to agree with the experimental fact that no phosphorescence can be seen upon $^1B_{3u}$ excitation even in condensed phases.[164] The only reasonable unimolecular nonradiative process then appeared to be a statistical limit internal conversion to the $^1A_g$ ground state.

The $^3B_{3u}$ state was excited directly and a weak phosphorescence was observed with a single exponential lifetime of ~72 $\mu$s. The phosphorescence quantum yield was estimated to be $\phi_p \leq 0.01$. It was suggested that the $^3B_{3u}$ lifetime may be controlled by a radiative transition to a possible lower lying $^3B_{1g}$ or $^3B_{2g}$ state. Finally, energy transfer experiments from triplet *p*-benzoquinone to $^3B_{3u}$ *s*-tetrazine supported the spin-forbidden character of the emission assigned as phosphorescence.

In a recent article, Knight and Parmenter[165] have combined measurements of fluorescence quenching, fluorescence quantum yields, and triplet formation yields, along with data from the literature, to construct a general picture of the decay of the $S_1$ state of six azabenzene vapors. The molecules studied were: *pyridine, pyrazine, pyrimidine, pyridazine, s-triazine* and *s-tetrazine*. Special emphasis has been given to the $S_1 \rightsquigarrow T$ intersystem crossing process in these molecules and the effect of collisions on this process. For all the molecules studied, the intersystem crossing from the vibrationless levels of the $S_1$ state has been studied (except for *s*-triazine which was excited at $\nu_6'$). Pyrazine was found to be the only azabenzene vapor which shows phosphorescence, and the method of triplet–triplet-sensitized phosphorescence of biacetyl was used to monitor triplet formation in the other cases.

In the case of pyridazine and *s*-tetrazine (through indirect evidence), no indications of triplet formation were found. It was proposed that a fast collision-free photochemical channel controls the $S_1$ decay. All other azabenzenes show triplet formation. The collisional quenching of the fluorescence of these azabenzenes (pyridine does not fluoresce) shows that the $S_1 \rightsquigarrow T$ process is collisionally induced. In the case of pyridine, the data suggest that triplet formation is at least in part collision-induced, but conclusive evidence for this is lacking. The triplet yields were found to reach a maximum limiting value at a pressure of added gas high enough that collisional quenching controls the $S_1$ decay. The limiting value of the triplet yield $\phi_T$ is about unity in pyrazine and pyrimidine. In pyridine and *s*-triazine, $\phi_T$ is only ~0.5. From this, it is concluded that an unidentified collisional channel competes effectively with collision-induced ISC in *s*-traizine and probably in pyridine too. The zero-pressure fluorescence quantum yields are less than $\sim 10^{-2}$ in all azabenzenes except for pyrimidine where it is $\geq$0.3.

### 2. Azanaphthalenes

The first $^1(\pi\pi^*)$ state of quinoxaline $^1A_1(^1L_b)$ lies only about 4100 $cm^{-1}$ above the lowest $^1(n\pi^*)$, $^1B_1$ state. Because of the small energy gap and favorable Franck–Condon factors, extensive mixing occurs between the $S_2$ and $S_1$ states. The observed diffuseness of the $S_2$ absorption has been ascribed by Hochstrasser and Marzzacco[166] to this kind of mixing. Another evidence of the strong $S_2$–$S_1$ coupling is the fact that upon $S_2$ excitation in the vapor, only $S_1 \rightarrow S_0$ emission is observed.[167] The $S_3$ state, $^1B_2(^1L_a)$ also overlaps with $S_2$.

The characteristics of the nonradiative decay of *quinoxaline* vapor (a few mTorr pressure) have been investigated first by McDonald and Brus.[168] Upon excitation (3 $cm^{-1}$ bandwidth) of the origin (369.3 nm) and other bands of the lowest $^1B_1(n_+\pi^*)$ state, a fluorescence "spike" was observed with the same dependence as their laser pulse ($\leq$50 ns). The fluorescence lifetime appears to be controlled by a statistical limit intersystem crossing resulting in $^3B_2 \rightarrow {}^1A_1$ phosphorescence. Excitation in the $^1(\pi\pi^*)$ region ($^1B_2$ and $^1A_1$ states, $\lambda_{exc} < 320$ nm) does not lead to resonance fluorescence. The decay in this case shows a short-lived "spike" ($\tau_F \leq 50$ ns) and a long-lived microsecond component, both emitting in the same spectral region red shifted with respect to the $^1(\pi\pi^*)$ resonance fluorescence (the investigation of the emission was done through band pass filters). The long, microsecond component is strongly excitation and pressure dependent.

The authors suggest that the zero-order vibronic levels of the $^1(\pi\pi^*)$ state are coupled strongly to vibronic levels of the $^1(n\pi^*)$ state, and in addition these hybrid singlet vibronic levels, $^1(\pi\pi^*) - {}^1(n\pi^*)$, are coupled via much weaker spin–orbit coupling to the triplet manifold. These triplet vibronic levels are in turn extensively hybridized. The fast decay was attributed to a rapid dephasing of an initial coherent superposition of the hybrid states, while the slow decay results from the independent decay of these hybrid states (sequential decay).

Soep and Tramer[101a] have extended the study of Brus and McDonald on quinoxaline[168] by measuring the kinetics of the triplet buildup and decay as well as the fluorescence quenching and phosphorescence induction effects in the gas pressure range of $10^{-3}$–10 Torr. Various excitation wavelengths were used corresponding to the $S_1 \leftarrow S_0$, $S_2 \leftarrow S_0$, and $S_3 \leftarrow S_0$ transitions.

At high pressure, the luminescence spectrum of quinoxaline was found to be composed of two well-separated systems in the 350–460-nm (fluorescence) and 460–540-nm (phosphorescence) wavelength range. The fluorescence is broad and is centered around 415 nm.[253] When the pressure was decreased, the structure of the spectrum remained unchanged while the relative intensity of phosphorescence decreased. Finally, below $\sim 10^{-2}$ Torr no phosphorescence was observed. At a fixed pressure the $I_P/I_F$ increased with increasing wavelength of excitation.

Fluorescence lifetime measurements showed a three-component decay composed of: (a) a prompt fluorescence with a very fast decay, $\tau_f < 0.3$ ns, suggestive of a statistical limit process; (b) a slow fluorescence with a decay time $\tau_s$ varying from 0.5 to $\sim 50$ $\mu$s. Combining direct lifetime measurements and Stern–Volmer quenching data, collision-free lifetimes, $(\tau_s)_{p\to 0}$, were determined for the long component and were found to decrease with decreasing wavelength ($(\tau_s)_{p\to 0} = 100$ $\mu$s at 340 nm and $(\tau_s)_{p\to 0} = 0.5$ $\mu$s at 265 nm). The ratio of the amplitudes of slow to fast component $I_s^0/I_f^0$ was also found, in accord with McDonald and Brus,[168] to decrease with decreasing wavelength; (c) the decay time $\tau_{T'}$ of the nonrelaxed triplet levels isoenergetic to the directly excited singlet levels was estimated from the kinetics of triplet–triplet absorption experiments and phosphorescence collision induction. The value obtained is of the order of $\sim 100$ $\mu$s.

To explain the above observations Soep and Tramer proposed a model analogous to the one used in the case of pyrazine.[158] According to this model, the particular vibronic level of the singlet state $|S\rangle$ is directly coupled to a set of triplet vibronic levels $\{T\}$ ($V_{ST} \neq 0$), while the set $\{T\}$ is coupled to another set of vibronic levels $\{U\}$ of the same triplet, by anharmonic coupling $\delta$ ($V_{TU} = \delta$ while $V_{SU} = 0$). In this model the prompt fluorescence arises from the decay of the nonstationary state $S$. The long fluorescence is the decay of the nonstationary $t$ states with a lifetime determined by the width $\delta$ of the $V_{ST}$ distribution. Finally, $\tau_{T'}$ is determined by the incoherent decay of individual molecular states, mainly "hot" phosphorescence or nonradiative decay because of negligible singlet character of these levels. The slow fluorescence lifetime $\tau_S$ is controlled by the anharmonic coupling $\delta$ which increases with increasing vibrational energy; therefore $\tau_S$ should decrease in the same way.

A parallel study of quinoxaline (1,4-diazanaphthalene) with other diazanaphthalenes, *quinazoline* (1,3-) and *cinnoline* (1,2-), has been performed by McDonald and Brus.[101b] Quinoxaline and quinazoline were found to behave completely analogously. Upon $S_1(n\pi^*)$ excitation, both molecules have a fast fluorescence decay ($\tau \leq 50$ ns) and a phosphorescence with a rise time of 1 $\mu$s (upper limit). Upon $S_2(\pi\pi^*)$ excitation, the fast ($\tau \leq 50$ ns) and the slow components (1–100 $\mu$s) are observed. The slow component is longer by a factor of $10^2$–$10^3$ than the calculated $S_2$ lifetime on the basis of the $S_2 \rightarrow S_0$ oscillator strength. The emission spectrum is red shifted with respect to the expected resonance emission and the $^1(\pi\pi^*)$ absorption spectrum is diffuse. Finally, in the collision-free region the ratio of the amplitudes of the fast to long component is about 5 to 20% with only mild dependence upon excitation wavelength.

Cinnoline, on the other hand, does not show any long-lived emission ($\tau \leq 50$ ns) after excitation into either the $^1n\pi^*$ or $^1\pi\pi^*$ states. The radiative lifetime is calculated to be $\sim 0.6$ $\mu$s, and therefore the observed lifetime is determined by a statistical limit nonradiative transition.

The difference between cinnoline on one hand and quinoxaline and quinazoline on the other was attributed to the different $S_2$–$S_1$ energy gaps. In cinnoline $\Delta E = 8830$ cm$^{-1}$ while in quinoxaline $\Delta E = 4880$ cm$^{-1}$ and in quinazoline $\Delta E$, 5010 cm$^{-1}$. The large $S_2$–$S_1$ gap in cinnoline would result in small $S_2$–$S_1$ mixing. On the other hand, cinnoline has a smaller $S_1$–$S_0$ gap than the other two isomers and as a result cinnoline is suggested to undergo significant internal conversion. The strong $S_2$–$S_1$ mixing in quinoxaline and quinazoline results in considerable broadening of the $S_2(\pi\pi^*)$ absorption spectra, $\sim 500$ cm$^{-1}$, to be compared with the 150-cm$^{-1}$ broadening observed in cinnoline.

In the same article the authors raise a very important question relevant to all cases where nonexponential decay has been observed (see also the section on dicarbonyls): Do the two fluorescent components occur *sequentially* in a given molecule, or *simultaneously* in different excited molecules? In another way, do all the excited molecules have the same wave functions, or are there some short-lived states and some long-lived states described by different wave functions which are excited separately? By changing the coherence properties of the light source, one could give an answer to this question.[11,19] For example, observation of nonexponential decay upon picosecond excitation (which has a large coherence width) would be an indication of sequential decay. In the absence of these kind of experiments, the author tried to answer this question on the basis of spectroscopic data. Regarding the way these short- and long-lived states could arise, the authors consider the following possibilities: (a) $S_1$ and $S_2$ states are mixed to form hybrid states. Only some of these hybrid states can now mix with long-lived triplets $T_L$ to produce longer lived hybrid S–$T_L$ states. (b) The S states mix with two kinds ($T_L$ and $T_S$) of long- and short-lived triplets. For example, these two triplets could be the fast-decaying $T_2(n\pi^*)$ states and the slow-decaying $T_1(\pi\pi^*)$ state. However, on the basis of spectroscopic observations by Hochstrasser and co-workers,[166,169] the authors suggest that the $T_2$ and $T_1$ states should be themselves heavily mixed. Also, in quinazoline, unlike in quinoxaline, the $S_2$ and $S_3$ $\pi\pi^*$ states are well separated. Excitation of the $S_2$ state in quinazoline results in a two-component decay suggesting that the two $^1(\pi\pi^*)$ states individually exhibit two-component behavior. Assuming therefore that the decay arises from two different states, the authors argue that it is difficult to understand why at a given excitation wavelength there are only two classes of states of widely differing lifetimes, without additional states of intermediate lifetimes; for example, why the S–$T_L$ coupling is either very strong or zero, or why the S levels form hybrid S–$T_L$ and S–$T_S$ states but not S–$T_L$–$T_S$ states? Although McDonald and Brus cannot definitely disprove this possibility of simultaneous decay, the complexity of the necessary requirements for the observation of it on the basis of independent decay model makes them favor the simpler possibility of a sequential decay.

## C. Dicarbonyls

### 1. Biacetyl

In an early study of biacetyl vapor, Parmenter and Poland[170] studied the fluorescence and phosphorescence emission as a function of pressure in the range of 40 to 0.1 Torr. A single excitation wavelength, 435.8 nm, was used and the following general conclusions were reached: (a) The fluorescence quantum yield of biacetyl is constant over the pressure range studied. (b) The phosphorescence yield is also corstant over this range provided that the experiments are done in a large diameter cell. (c) The triplet-emission yield decreases at pressures below about 0.1 Torr. This decrease is attributed to wall deactivation and not to a decrease in triplet formation.

From the behavior of the fluorescence as a function of pressure, it was concluded that the relative rates of radiative and nonradiative singlet decay remain constant in the range 40–0.1 Torr. The nonradiative process was assigned to an $S_1 \rightsquigarrow T$ intersystem crossing, although some internal conversion to the ground state could not be excluded. Since in the lower pressure limit (0.1 Torr) the biacetyl singlet is expected to be essentially collision free, the constancy of the emission yields with pressure seems to indicate that intersystem crossing is independent of collisions. On the basis of the above result and the fact that there

is a close match between the fluorescence quantum yield and lifetimes in solution[172] and in the gas phase,[171,173] it was concluded that the intersystem crossing process in biacetyl lies in the statistical limit. On the other hand, a calculation of the density of triplet states at the energy of 2500 $cm^{-1}$ above the origin of the triplet gave only about 100 states/$cm^{-1}$, a result that, according to the authors, should place biacetyl outside of the statistical limit.

In a study by McClelland and Yardley,[174] the dynamics of the fluorescence decay of biacetyl vapor (~1 Torr) was studied as a function of the excitation wavelength using 10–30-Å excitation bandwidth. The lifetime was found to vary smoothly from ~14 ns for excitation near 445 nm to ~6 ns for excitation at 372 nm. The fluorescence lifetime was reported to be essentially independent of pressure over the range 0.2–1 Torr and reasonably exponential (their data though display considerable scatter). The authors calculated a density of triplet states $\rho_T \leq 320$ states/$cm^{-1}$, for intersystem crossing from the vibrationless $S_1$ state, and agreed with Parmenter and Poland[170] that irreversible intersystem crossing should not be expected in biacetyl for long-wavelength excitation and low pressures. Quenching studies showed that both ground-state biacetyl and Ar vibrationally relax the excited molecules but do not quench the electronic excitation. Biacetyl removes ~700 $cm^{-1}$ of vibrational energy per collision while Ar removes ~90 $cm^{-1}$.

Special attention on the effect of excess energy on the phosphorescence of biacetyl have been given in a study by Moss and Yardley.[97] In this study Moss and Yardley reported measurements of intensity and decay rate of phosphorescence from biacetyl vapor (~1 Torr) excited into the $S_1(^1A_u)$ state as a function of additive pressure (0–50 Torr) and excitation wavelength (440.0–365.0 nm). The phosphorescence yield was found to decrease with increasing excitation wavelength and decreasing pressure. On the other hand, the phosphorescence decay rate showed no dependence on excitation wavelength or pressure. The constancy of the phosphorescence decay rate is easily understood since vibrational relaxation of the initially prepared, by the intersystem crossing process, triplet level is expected to be much faster than the phosphorescence decay under the experimental conditions. However, if some fraction of the vibrationally excited triplet molecules produced by the intersystem crossing were to decay by some nonradiative unimolecular process before vibrational relaxation could occur, then the phosphorescence yield would be lower than that of the thermalized triplet. This unimolecular nonradiative process was proposed to be the $T_1 \rightsquigarrow S_0$ intersystem crossing to the ground state. A kinetic analysis of the experimental data gave $k_{S\rightarrow T} = 1.0 \times 10^8\ s^{-1}$ and $k_{T_1\rightarrow S_0} = 4.5 \times 10^4\ s^{-1}$.

Drent et al.[175] studied the phosphorescence excitation spectrum of biacetyl as a function of pressure (1 Torr biacetyl + $N_2$ gas). They found three regions in the excitation spectrum with different pressure dependence. In the 500–465-nm energy region the excitation is a result of the direct absorption to the triplet. The phosphorescence signal (proportional to the phosphorescence yield) is independent of pressure. The photoexcitation spectrum in the 645–444 nm is structured and pressure dependent. The photoexcitation spectrum becomes broad and pressure independent below 444 nm.

It appears therefore that in the 645–444-nm region biacetyl behaves like a small molecule with the phosphorescence yield depending on pressure, while below 444 nm biacetyl behaves like a large (statistical limit) molecule. The reader should note that, in the previous studies of Parmenter and Poland,[170] biacetyl was excited at 435.8 nm (22 900 $cm^{-1}$). Drent et al. explained the above observations by involving a second $^3B_g$ triplet state in the intersystem crossing process for $\lambda_{exc}$ below 444 nm. Above 444 nm, the intersystem crossing proceeds to the $T_1$ state ($^3A_u$) which is located only about 1900 $cm^{-1}$ below the $^1A_u(S_1)$ state. Therefore this nonradiative process shows small molecule behavior. The existence of a $^3B_g$ state (above 22 500 $cm^{-1}$) gives a statistical limit behavior to the intersystem crossing process by increasing the effective density of states as well as by increasing the coupling between the singlet and triplet states. Without the existence of the $^3B_g$ state, only triplet levels of vibrational symmetry $b_g$ are coupled to the singlet state. The presence of the $^3B_g$ states introduces strong vibronic interactions via $b_u$ vibrations, between the $^3B_g$ and $^3A_u$ states, and therefore these states have to be counted in the effective density of states as well. Furthermore, the $^1A_u \leftrightarrow {}^3B_g$ interaction can proceed via two $a_u$ promoting modes, instead of only one $b_g$ promoting mode in the case of $^1A_u \leftrightarrow {}^3A_u$ interaction, thus leading to a higher density of effectively coupled states as well. Finally the fact that the $^3B_g$ state is much closer to the $^1A_u$ state than the $^3A_u$ state results in stronger mixing between the former two states.

As we mentioned, in this study the pressure was $p \geq 1$ Torr. In a subsequent study by the same group,[95] the photophysics of biacetyl was studied at a much lower pressure ($10^{-3}$ Torr). Under these conditions, excitation of biacetyl by 420.0-nm light (region III[175]) gave a short-lived (~10 ns) fluorescence, phosphorescence (~1.5 ms), and, in addition, a new emission of the same spectral composition as the fast fluorescence but with a nonexponential decay in the microsecond range. The ratio of the yields of the slow to fast fluorescence was found to be 3 at $10^{-3}$ Torr. The pressure dependence of the fast fluorescence was found to be weak and its lifetime to increase with pressure. The lifetime of the slow fluorescence on the other hand decreased with pressure and satisfied a Stern–Volmer plot. Finally the phosphorescence appeared to be collisionally induced, the phosphorescence signal increasing more than linearly with biacetyl pressure higher than $10^{-3}$ Torr. These results were interpreted as indicating that after excitation the molecule rapidly transfers ($k_{S\rightarrow T}$) to the triplet state giving the nanosecond decay. From the triplet state it can transfer back to the singlet ($k_{T\rightarrow S}$) giving rise to the microsecond emission. At the same time internal conversion occurs to the ground state ($k_{S\rightarrow S_0}$). Phosphorescence can occur only when the molecule is deactivated by collisions to a vibronic triplet state below the vibrationless excited singlet state. A kinetic analysis analogous to the one discussed in the theoretical section gave the following rate constants for the corresponding nonradiative processes: $k_{S\rightarrow S_0} = 2.4 \times 10^7\ s^{-1}$, $k_{S\rightarrow T} = 7.6 \times 10^7\ s^{-1}$, and $k_{T\rightarrow S} = 1.9 \times 10^5\ s^{-1}$. The kinetic treatment was then transformed to a quantum mechanical one according to Lahmani et al.,[92a] yielding a triplet density $\rho_T = 6.3 \times 10^5\ cm^{-1}$, coupling element $V_{ST} = 1.0 \times 10^{-5}\ cm^{-1}$, and the number of triplets interacting with the initial state $N = 400$.

### 2. Glyoxal and Methylglyoxal

The dynamics of the fluorescence decay of *glyoxal* from the $^1A_u(S_1)$ state at low pressure was investigated in a preliminary study by Yardley et al.[176] In this study glyoxal (3.7 mTorr) was excited by a 455.0-nm flash. At this pressure the observed lifetime of 2.17 μs was considered to be a collision-free lifetime. Extrapolation of Stern–Volmer plots to zero pressure gave essentially the same value. This collision-free lifetime was reported to be independent of wavelength over the range 451.0 to 458.5 nm.

Parmenter and co-workers[177,178] reported spectra, luminescence yields, and lifetimes of the emissions from the singlet $^1A_u(S_1)$ and triplet $^3A_u(T_1)$ states of glyoxal vapor at pressures between 3 mTorr and 10 Torr. The glyoxal was excited at about 1000 $cm^{-1}$ above the origin of $S_1$ by the 435.8-nm Hg line or with a flash at 434.5 nm. The 435.8-nm radiation pumps both the $4_0^1$ (excess energy 955 $cm^{-1}$) and $8_0^1 7_2^2$ (excess energy 1200 $cm^{-1}$) vibronic levels of the $S_1$ state. Only fluorescence was observed at the lowest pressures. This fluorescence excited at 435.8 nm contains appreciable structure from the zero-point

level even when the hard-sphere collision interval exceeds the radiative lifetime (~10 μs) calculated from the absorption spectrum, indicating efficient vibrational relaxation. The observed lifetime was shorter than 5 μs. Both $S_1$ and $T_1$ emissions are observed at pressures above about 0.1 Torr and both were found to be self-quenched. Other added gases like cyclohexane, Ar, and He were found to selectively quench only the $S_1$ emission. This quenching was assigned to collision-induced $S_1 \rightsquigarrow T_1$ intersystem crossing. The triplet yield was found to be near unity in 0.2 Torr of pure glyoxal. The phosphorescence yields indicate a fast nonradiative decay from high triplet vibrational levels. The special sensitivity of $T_1$ molecules to collisions with $S_0$ glyoxal (cross section $10^{-3}$ gas kinetic) was considered to be associated with the extensive photochemical activity which accompanies excitation at 435.8 nm. The major photochemical products are known to be CO and a polymer.[179] The $T_1$–$S_0$ collision product was not identified, but most likely it is the precursor to CO formation.

The study of the fluorescence lifetimes of glyoxal, at low pressures, as a function of excitation energy was carried out by van der Werf et al.[180] Three excitation regions, each giving rise to a different decay behavior, were distinguished. At low excitation energies (up to 420.0 nm) only a microsecond decay was observed. At higher energies (414.5–392.5 nm), the fluorescence decay was found to show, besides the long-lived component, a short-lived component of a few nanoseconds. Finally at high energies (above 392.5 nm) only the nanosecond emission could be observed. The spectra of both components (excitation 395.0 nm, $p$ = 90 mTorr, resolution 150 Å) were found to be identical.

The observed behavior was explained in terms of the increasing triplet-state density with excess excitation energy. At low excitation energies the triplet density is low, and the nonradiative behavior with respect to the triplet state is that expected for a small molecule limit. The decay rate is determined only by the zero-order singlet relaxation (radiative decay and probably internal conversion). At higher energies the singlet–triplet mixing is stronger, and the short decay is a result of constructive interference between the molecular states. The behavior now is that of intermediate coupling and the decay is determined by both the zero-order singlet relaxation and by the zero-order triplet decay. At high excitation energies the mixing of singlet and triplets is very strong, and the resulting molecular states are almost pure triplets. The triplet relaxation at high excess energies is very efficient, probably intersystem crossing to the ground state and/or photochemistry. As a result of this fast triplet relaxation, the behavior at high energies can be classified as belonging to the statistical limit.

The previous studies of the fluorescence lifetimes of glyoxal did not give enough information about the behavior of individual vibronic levels. Beyer et al.[181] measured collision-free lifetimes for 26 such vibronic levels of the $^1A_u$ state. These lifetimes were measured for most vibronic levels at pressures of the range 2–25 mTorr. The authors found that rotational relaxation may not be complete at the emitting level. With fixed wavelength of observation, this incomplete rotational relaxation can produce changes in observed lifetimes with variations in excitation wavelength over an absorption band. For example, with an observation bandpass centered on the $8_1^0$ emission band, the measured lifetime varies by a factor of 2 as excitation is varied across the 0,0 absorption band. Appropriate bandpass was used to avoid these effects due to rotational relaxation within the same band. The following general observations were made: The $8^1$ level, the only vibrational mode of glyoxal with $b_g$ symmetry ($8b_g$ is a C–H wag), has a significantly shorter lifetime than the other vibronic levels. $8b_g$ is important for vibronic coupling between the $^1A_u$ and $^1B_u$ states. It can also promote intersystem crossing from $^1A_u$ to $^3A_u$, but this process is not expected to be important at very low pressures. Most probably significant internal conversion to $^1A_g$ takes place from this level. The torsional mode $\nu_7$ (233 $cm^{-1}$) exhibits an approximately constant lifetime over a range of about 900 $cm^{-1}$ (4 quanta) of excess energy, a small molecule characteristic. The $5^1$, $4^1$, and $2^1$ levels, all of $a_g$ symmetry, show (in combination bands) a systematic decrease in the lifetime as vibrational energy increases. This behavior is reminiscent of large molecule behavior. Although no definite conclusion could be made, it was proposed that the observed variations in lifetimes are dominated by internal conversion to the ground state.

There have been a number of studies on the effect of collisions on the vibrational relaxation/redistribution of vibronically excited glyoxal. For example, Frad and Tramer[182] observed that upon excitation of various higher vibronic levels of glyoxal [$8^1$ (735 $cm^{-1}$), $2^1$ (1390 $cm^{-1}$), $8^1 4^1$ (1680 $cm^{-1}$)], the observed fluorescence is a superposition of resonance emission from the initially excited level and of thermally equilibrated fluorescence from the 0 level and $7^1$ (232 $cm^{-1}$) and $7^2$ (463 $cm^{-1}$) levels. For example, upon $8^1$ excitation of $2.5 \times 10^{-2}$ Torr of glyoxal, the relaxed fluorescence amounts to ~30% of the total. Since the average time between collisions (hard-sphere diameter $\sigma$ = 4 Å) is about 6 μs at this pressure while the zero-pressure lifetime of $8^1$ is about 0.8 μs, the probability of more than one collision per lifetime is negligible. One would have to assume a mechanism then which involves direct relaxation to the vibrationless level in a single collision. Such a mechanism involving the transfer of the total vibrational energy between two similar molecules with unit probability seems improbable. This objection will be removed if the vibrational relaxation does not take place by vibrational energy transfer ($V$–$V$), $M^*(\nu = n) + M'(\nu = 0) \rightarrow M^*(\nu = n - 1) + M'(\nu = 1)$, but by a resonance transfer of the purely electronic excitation ($E$–$E$): $M^*(\nu = n) + M'(\nu = 0) \rightarrow M(\nu = n) + M'^*(\nu = 0)$. This latter ($E$–$E$) mechanism has been already evidenced in the case of NO by Melton and Klemperer.[183] To investigate this possibility, Frad and Tramer studied the fluorescence of isotropic mixtures: glyoxal-$h_2$–glyoxal-$d_2$ upon selective single vibronic level excitation. The $E$–$E$ mechanism was found to be quite efficient.

An extensive study of the collisional quenching of low-lying levels of the $^1A_u(S_1)$ state of glyoxal by 24 collision partners has been reported by Beyer and Lineberger.[184] The quenching cross sections were found to vary from 1.3 to 22 Å, with polar quenchers having the larger cross sections. The quenching cross sections of the various gases were correlated using three different interaction models. The correlation for the nonpolar quenchers was good in all three models while a reasonable correlation for the polar quenchers was provided only by the model of Thayer and Yardley.[185] Since the model of Thayer and Yardley was formulated for a spin-forbidden process, the correlation should be viewed with caution. Oxygen was found to be an efficient quencher, a fact that can be ascribed to its triplet ground state and its ability to promote singlet–triplet ISC. The high efficiency of quenching of $^1A_u$ glyoxal by $^1A_g$ ground-state glyoxal is indicative of an additional long-range interaction. Regarding the nature of the intermolecular interaction due to polar quenchers, it should be due to either the strong electric field associated with the permanent dipole at short range or hydrogen bonding. The relative production rates of the $^3A_u$ state and loss rates of the $^1A_u$ state in collisions with various gases were found to agree very well. This was considered as indicating that different quenching molecules act by mixing the same states although there is a difference in the efficiency of mixing. The two states being mixed must be the $^1A_u$ and $^3A_u$. Other channels could have been photochemistry and $S_1 \rightsquigarrow S_0$ internal conversion. There is no evidence for significant photochemistry for low excitation energy in the $^1A_u$. In addition, it seems that photochemistry from higher vibrational levels follows intersystem crossing to the $^3A_u$ state.[175] Considering the internal conversion process to the ground state, it is logical to assume that it will be

independent of collisions since the density of states of $^1A_g$ at the energy of $^1A_u$ is $\sim 10^7$–$10^8$ per $cm^{-1}$, giving a statistical limit behavior.

Studies of the collisional quenching of the triplet state of glyoxal, $^3A_u$, have been carried out by Yardley.[186] The quenchers used were glyoxal, $O_2$, NO, and di-*tert*-butyl nitroxide [$(+)_2$NO]. The self-quenching cross section was found to be considerable ($\sim 8 \times 10^{-2}$ Å$^2$) and to decrease ($\sim 2 \times 10^{-2}$) upon deuteration. NO and $(+)_2$NO were found to be extremely efficient quenchers, cross sections $\sim 1/6$ gas kinetic. $O_2$ is a factor of 400 less efficient than NO and $(+)_2$NO. Photochemistry was considered important in the quenching mechanism of the triplet state.

Recently, Photos and Atkinson[187] used the technique of time-resolved single vibronic level (TRSVL) spectroscopy for the study of collisionally induced vibrational relaxation. Glyoxal, at a pressure of 0.2 Torr, was excited to the $5^1$ level of the $^1A_u(S_1)$ state, and the resulting fluorescence was resolved both with respect to wavelength and time.

A different type of experiment on the photophysics of glyoxal has been performed by Matzuzaki and Nagakura.[188] These investigators found that an external magnetic field influences the fluorescence yield of glyoxal. An $Ar^+$ laser was used to excite the $^1A_u(0^0)$ state of glyoxal, and the resulting fluorescence was found to decrease by ~20% in the presence of a magnetic field of about 10 kG. On the other hand the absorption intensity of the $^1A_u(0^0) \leftarrow {}^1A_g(8^1)$ transition was not affected by the magnetic field. This fact indicates that the nonradiative decay of $^1A_u(0^0)$ is enhanced by the magnetic field. Stern–Volmer plots of self-quenching in the presence of the magnetic field showed that the collision-free lifetime is shortened by the application of the field, while the collisional quenching rate constant remains unchanged. These facts indicate that the magnetic field quenching is due to the enhancement of an intramolecular nonradiative process. Time-resolved spectra of the emission from glyoxal (0.8 Torr) in the presence of a magnetic field showed the presence of a new emission not previously seen in the fluorescence or phosphorescence spectra of glyoxal. The collision-free lifetime of this new emission was found to be 67 μs. The authors interpreted this emission as being due to emission from vibrationally excited $^3A_u$ glyoxal ($^3A_u(n)$). The observed magnetic quenching was then explained as due to an enhancement by the field of the $^1A_u(0) \rightsquigarrow {}^3A_u(n)$ intersystem crossing process. No explanation on the detailed mechanisms of this enhancement was provided.

Coveleskie and Yardley[87,189] have studied the fluorescence decay of *methylglyoxal* (MGL) vapor, excited to the $^1A''(S_1)$ state, as a function of additive pressure and excitation wavelength. At high pressures (~2 Torr MGL or ~100 mTorr MGL + more than 5 Torr Ar) two exponential decays are observed corresponding to phosphorescence (millisecond time scale, spectral region 500–620 nm) and fluorescence (nanosecond time scale, spectral region 440–520 nm). The decay rate of fluorescence (100 mTorr MGL + 5 Torr Ar) increases smoothly and linearly over the 2500-$cm^{-1}$ span in vibrational energy studied. This high-pressure behavior is analogous to that observed for biacetyl by McClelland and Yardley.[174] At low pressures and long wavelength excitation (origin at 449.2 nm) the decay becomes nonexponential. The decays have been analyzed as a sum of two exponentials $\lambda_1$ and $\lambda_2$. For pressures 50–120 Torr, the decay constant $\lambda_1$ and the ratio of initial intensities ($I_1/I_2$) remain relatively constant, with $\lambda_1$ increasing very slowly and $I_1^0/I_2^0$ slowly decreasing with increasing pressure. On the other hand, $\lambda_2$ increases by a factor of 2 as the methylglyoxal pressure is increased from 50 to 120 Torr. Both components of the nonexponential fluorescence were found to have similar spectral nature.

The low pressure behavior was interpreted on the basis of a reversible intersystem crossing mechanism as discussed in the theoretical section. A nonexponential decay could also arise if the laser excited two different electronic states that decayed independently, but the authors argued against such a possibility. Furthermore, Coveleskie and Yardley[87] transformed the kinetic data to quantum mechanical quantities through the theoretical model of Lahmani et al.[92a] This transformation gave a density of triplet accepting levels for excitation at the origin of $S_1$ of $\sim 10^4$ states/$cm^{-1}$. For the small singlet–triplet energy gap of ~2500 $cm^{-1}$ the calculated density of stages is ~50 states/$cm^{-1}$. This discrepancy of three orders of magnitude was ascribed to involvement of vibronic levels of the ground state. Since a similar discrepancy involving the density of states has been found[95] in the case of biacetyl, Covaleski and Yardley proposed a similar $S_0$ participation in the case of biacetyl.

Additional data on methylglyoxal have been presented recently by van der Werf.[86] Covaleskie and Yardley[22] studied methylglyoxal up to an excess energy of 1115 $cm^{-1}$ while van der Werf extended the study to 5000 $cm^{-1}$ excess energy. In comparable energy regions their results agree quite well.

In his study, van der Werf[86] studies and compares the photophysical behavior of all three dicarbonyls: glyoxal, methylglyoxal, and biacetyl. The model he uses considers a zero-order $|s\rangle$, effectively coupled to $N$ zero-order triplet states of a manifold $|T\rangle$. The coupling matrix elements are $V_{ST}$ and the singlet and triplet level densities are $\rho_S$ and $\rho_T$, respectively. When $N \gg 1$ or even $N \geq 1$ the fluorescence decay can be roughly written as the sum of two exponentials. van der Werf defines two separate regions in the singlet spectrum. At low energies the singlet widths ($\lambda_{fast}$) are much smaller than the mean level separation ($\rho_S^{-1}$), and the singlet levels in this case are considered as isolated. The numbers of effectively coupled triplets is then $N = 2\pi^2 V_{ST}^2 \rho_T^2$. At higher energies, however, the singlet widths may overlap ($\lambda_{fast} > \rho_S^{-1}$). Then $N$ becomes the ratio of densities $N = \rho_T/\rho_S$.

The differentiation between the two regions was used to explain differences of the pressure dependence of the slow fluorescence. If the singlet levels are isolated, the cross section for slow fluorescence quenching is expected to be large, because a collision capable of removing a very small amount of energy (exceeding the width $\lambda_{fast} \simeq 5 \times 10^{-4}$ $cm^{-1}$) is sufficient to transfer the molecule to a state without resonantly coupled singlet character. Long-range collisions then play an important role in the quenching process. van der Werf calls these regions between the zero-order singlet containing these nonfluorescent states "black holes". In the region where the singlet widths overlap, one needs to remove a larger amount of energy to effectively decouple the states. In such a case only head-on collisions may be effective and smaller collisional quenching cross sections will be obtained. In the case of biacetyl, in the region of the black holes, the fluorescence quenching efficiencies were found to amount up to 5.5 times the 6-Å diameter hard-sphere cross sectior. An energy loss exceeding $5 \times 10^{-4}$ $cm^{-1}$ is sufficient for decoupling the states. In the overlap region the cross section of the effective collisions was determined to be about 50% of the hard-sphere cross section.[284] van der Werf has also shown that while the experimental values for the ratios $\rho_T/\rho_S$ agree well with calculated ratios, the values of $\rho_T$ and $\rho_S$ are both larger by a factor of ~10 than the calculated values. This fact was explained as due to the presence of rovibrational levels coupled together by the Coriolis interaction.[255] On the basis of this idea about the importance of rotational levels, the effect of collisions could be due to vibrational relaxation, rotational relaxation, or, because of the Coriolis mixing, to a combination of both.

Comparing other properties of the three molecules, van der Werf notes that in all three cases the total decay rate is dominated by the radiationless decay. The total decay rate constant of the singlet state, $k^S$, and the corresponding triplet rate constant, $k^T$, increase rapidly with excess energy in the case of biacetyl and methylglyoxal. In the case of glyoxal, the evidence is not conclusive.

Regarding the nonradiative process responsible for the energy variation of $k^S$ and $k^T$, van der Werf points out that a photophysical internal conversion, intersystem crossing process, or photochemical process could be responsible. The RRKM theory[190] of chemical reactions also predicts that the photochemical rate would increase rapidly with energy; in accord with some studies of the hexafluorobiacetyl[191] at higher energies both $k^S$ and $k^T$ could represent at least partially photochemical rates. The fact that $k^T$ (methylglyoxal) > $k^T$ (biacetyl) seems also to agree with the prediction of the RRKM theory that a photochemical rate will decrease with increasing size of the molecule.

### 3. Benzoquinone

A different type of dicarbonyl molecule whose single vibronic level photophysical dynamics have been studied is *p-benzoquinone-$h_4$* and *-$d_4$* (BQ). Brus and McDonald[192] studied BQ upon excitation of several vibronic levels of the $^1B_g(S_1)$ and $^3A_u(T_2)$ states. Direct excitation of $^3A_u$ states gave rise to $^3A_u \rightarrow {}^1A_g$ phosphorescence with a lifetime of 28.4 ± 0.7 μs (37.6 ± 0.7 μs for BQ-$d_4$). This lifetime was found to be independent of BQ pressure down to 7 mTorr and also independent of Ar pressure. This phosphorescence lifetime is ~45 times shorter than expected on the basis of the radiative decay. Two possibilities were considered for the deactivation mechanism of the $^3A_u$ state (a) $^3A_u(T_2) \rightsquigarrow {}^1A_g$ intersystem crossing, or (b) $^3A_u(T_2) \rightarrow {}^3B_{1g}(T_1)$ infrared fluorescence. Although the IR fluorescence was not experimentally studied, this radiative process was considered the most probable deactivating process. Excitation of four vibronic bands of the $^1B_{1g} \leftarrow {}^1A_g$ system led to double exponential decay at nonzero pressures for both BQ-$h_4$ and BQ-$d_4$. The experimental observations indicate that the laser initially populates molecular states exhibiting single exponential decay with collision-free lifetimes 7 to 15 μs. At nonzero pressures collisions depopulate these initial states with at least partial conversion into the vibrationally equilibrated $^3A_u$ state. The ratio of the $^1B_{1g}$ radiative rate to the $^3A_u$ radiative rate is at least a factor of 30 lower than expected from oscillator strength calculations. This fact, along with the observed diffuseness of the $^1B_{1g} \rightarrow {}^1A_g$ absorption bands, was considered as evidence of intermediate strong coupling of the vibronic levels of $^1B_{1g}$ with vibronic levels of lower excited states. Collisional relaxation of the intermediate strong coupling states is nearly gas kinetic. The $^3A_u$ state is easily deactivated by $O_2$ and especially NO (cross section 12.6 Å$^2$).

## D. Monocarbonyls: Photophysical and Photochemical Behavior

### 1. Formaldehyde and Other Aldehydes

*Formaldehyde* is the simplest of the carbonyl molecules. An understanding of the photophysical and photochemical decay pathways in this molecule provides a good test for the existing theoretical descriptions of these phenomena. In addition, from a practical point of view, the formaldehyde photochemistry is important in the chemistry of polluted atmospheres,[193] and it also forms the basis of isotope separation techniques for carbon and hydrogen.[194-196]

Yeung and Moore[197] studied the mechanisms of predissociation, quenching and energy transfer for single vibronic levels of the first excited singlet state of formaldehyde ($^1A_2$). The fluorescence lifetimes have been studied as a function of pressure, and by extrapolation zero-pressure lifetimes have been obtained. The zero-pressure lifetimes showed the following general features.

(a) The lifetime decreases rapidly and smoothly with increasing vibrational excitation. In the case of $D_2CO$, 4000 cm$^{-1}$ of vibrational energy causes the lifetime to decrease by two orders of magnitude.

(b) The lifetimes do not vary greatly with the particular normal vibration excited, though they are by no means monotonic in total vibrational energy. As an example, excitation of out-of-plane bending quanta, $4^1 \rightarrow 4^3$, almost always decreases the lifetime more rapidly than the general trend.

(c) The lifetimes are independent of rotational quantum number. The $4^1$ and $2^24^1$ bands of $D_2CO$, for which measurements were made at both high and low rotational quantum numbers, show no effect of rotation on the lifetime observed.

(d) The lifetimes exhibit a large isotope effect. $D_2CO$ lifetimes are roughly a factor of 20 longer than $H_2CO$ lifetimes. Those for HDCO are much closer to $H_2CO$ than to $D_2CO$. The radiative lifetime of the $^1A_2$ state was estimated from the absorption spectrum to be ~5 μs, and it is not expected to vary greatly with increasing vibrational excitation. Therefore, the much shorter lifetimes observed must result from an enhancement of nonradiative processes.

The photochemistry of formaldehyde excited at its $S_1(^1A_2)$ state has been extensively studied by Calvert and co-workers,[198,199] and two primary photochemical channels were recognized:

(1) $H_2CO + h\nu \rightarrow H_2 + CO$
(2) $H_2CO + h\nu \rightarrow H + HCO$

The nonradiative process at low pressures is then, most likely, spontaneous predissociation to either molecular (1) or radical products (2). At higher pressures, collision-induced dissociation and energy transfer may take place.

Concerning the mechanism of the predissociation process, the following facts should be considered[197]: (a) The $S_1$ state correlates with the H + HCO* products, so direct dissociation from $S_1$ cannot occur for energies below the H + HCO* limit, near 40 000 cm$^{-1}$ (* denotes electronic excitation). (b) The $T_1$ state dissociates to ground state H + HCO but there is a barrier, which is estimated to be about 30 600 cm$^{-1}$, for this dissociation. (c) The $S_0$ surface correlates directly to the H + HCO ground state. $S_0$ also dissociates to the ground state of $H_2$ + CO, although there is a large energy barrier for this process. Therefore, at the total energy of the selectively excited vibronic levels, the only possibility was considered to be dissociation on the $S_0$ surface.

To assess the importance of the two mechanisms, radical (H + HCO) vs. molecular ($H_2$ + CO), Yeung and Moore[197] studied the photoproducts from photolysis of mixtures of $H_2CO$ and $D_2CO$. The ratio of HD to $D_2$ is a measure of the relative importance of the radical and molecular dissociation processes. Photolysis at 347.2 nm gave the following product distribution: $H_2$:HD:$D_2$:CO = 0.5:0.2:3.3:3.9. The result at 347.2 nm shows that molecular dissociation dominates for the $4^0$ and $4^1$ levels of $D_2CO$. At 319.3 nm, $2^24^3$ level, $D_2$:HD = 4.1. This shows that the radical mechanism becomes increasingly important with increasing energy. This result can be rationalized in the mechanism involving $S_0$ dissociation. If the threshold for radical formation is higher than the barrier for molecular dissociation, then the statistical unimolecular decomposition theory would predict that the rate of radical formation will increase more rapidly than the rate of molecule formation as the excitation energy increases.

At higher pressures there is the possibility of collision-induced nonradiative processes. It was found that the collisional quenching parallels very closely the collisionless nonradiative decay. It seems therefore very reasonable to assume that the effect of the collisions is to supply a perturbation which couples the $S_1$ vibronic level to a set of approximately isoenergetic quasi-continuous dissociative $S_0$ levels. In self-quenching, formaldehyde is quite effective, with a cross section up to three

hard-sphere radii, while rare gases are less effective. Analysis of the photoproducts gave again $H_2$, CO, H, and HCO.

In another study, Miller and Lee[200] also measured fluorescence decay times and fluorescence quantum yields from various single vibronic levels of the $^1A_2(S_1)$ state of formaldehyde. The total decay rates were decomposed to radiative and radiationless rates. The measured lifetimes appeared to be two to four times shorter than the ones measured by Yeung and Moore.[197] The nonradiative lifetimes, $\tau_{NR}$, for the progression of the C–O stretch mode $\nu_2'$, containing the excitation of the out-of-plane bending mode $\nu_4'$ ($4^1$ and $4^3$), were found to be shorter than for the similar progression containing the excitation of the asymmetric C–H stretch mode $\nu_5'$. The authors considered this fact a strong indication that $\nu_4'$ is a promoting mode for the nonradiative transition. Regarding the radiative lifetimes, it was found that $\tau_F(5^1) = 0.75 \pm 0.15$ μs, a value which is about three times shorter than $\tau_F(4^1) = 1.9 \pm 0.4$ μs. This was considered as an indication that the vibronically induced radiative transition $^1A_2 \rightarrow {}^1A_1$ (or $^1A'' \rightarrow {}^1A'$) is promoted more strongly by the vibration of the $b_2$ species ($\nu_5'$) than by the vibration of $b_1$ species ($\nu_4'$), unlike in the case of absorption.

In an interesting experiment, Miller and Lee[201] used triplet benzene ($^3B_{1u}$) to sensitize through energy transfer the triplet state of formaldehyde. These investigators found that approximately 33% of the triplet formaldehyde ($^3A_2$) produced in this way decomposes to give $H_2$ and CO; no evidence for radical products was found. The above finding was interpreted as indicating the importance of a $T_1 \rightsquigarrow S_0$ intersystem crossing. The resulting hot ground state, $S_0(\nu)$ then decomposes to give $H_2$ + CO. If the above is true, then in the presence of an $S_1 \rightsquigarrow T_1$ intersystem crossing, the $T_1$ state could be also an intermediate to the molecular dissociation of formaldehyde. This is contrary to the mechanism of Yeung and Moore[197] in which the triplet state of formaldehyde was not involved at all.

More information about the dynamics of the $^3A_2$ state of formaldehyde came from the study of Luntz and Maxson.[202] These investigators studied the behavior of the $^3A_2$ formaldehyde upon direct $T_1 \leftarrow S_0$ excitation with a tunable laser. Phosphorescence was not observed from $H_2CO$ upon $^1A_2(S_1) \leftarrow {}^1A_1(S_0)$ excitation, and this fact was considered as evidence against the occurrence of $^1A_2 \rightsquigarrow {}^3A_2$ intersystem crossing. $H_2CO$ and $D_2CO$ at pressures of the order of a Torr and at a temperature of −78 °C (to avoid $^1A_2$ hot bands) were directly excited by a tunable laser. A moderately strong emission was observed from $D_2CO$ but not from $H_2CO$ under the same conditions. The excitation spectra of the observed emission from $D_2CO$ mirror the $^3A_2$ $D_2CO$ absorption spectrum, supporting the idea that the observed emission is $^3A_2 \rightarrow {}^1A_1$ phosphorescence. Quenching studies gave cross sections of $\sigma_{D_2CO} \leq 0.01$ Å$^2$, $\sigma_{Ar} \leq 0.01$ Å$^2$, and $\sigma_{NO} = 22 \pm 5$ Å$^2$. NO is known as an efficient triplet state quencher and the high quenching cross section for the $D_2CO$ emission also supports the triplet character of it.

The observed $^3A_2$ $D_2CO$ lifetime at high pressure is 16.9 ± 0.5 μs (which represents the lifetime of a vibrationally relaxed $^3A_2$). The absence of emission from $H_2CO$ implies a much shorter lifetime for the $^3A_2$ in $H_2CO$. An estimated upper limit is 0.4 μs, for levels above the $1^+$ level. The radiative lifetime of $^3A_2$ $H_2CO$, on the other hand, was estimated as ~2 ms. The much shorter measured lifetimes point to an efficient nonradiative process. The $^3A_2$ state correlates with H + HCO but the excitation energies used in the study of Luntz and Maxson are below the H + HCO dissociation limit (estimated to be at ~30 500 cm$^{-1}$). If $T_1$ dissociation seems improbable, the other possibility is then $^3A_2 \rightsquigarrow {}^1A_1$ intersystem crossing followed by dissociation to $H_2$ + CO on the $S_0$ surface.[201] The molecular predissociation rate from $^3A_2$ is almost as fast as in the $^1A_2(S_1)$ state. Since the electronic matrix element for $^3A_2 \leftrightarrow {}^1A_1$ coupling is expected to be smaller than the coupling of $^1A_2 \leftrightarrow {}^1A_1$, one must conclude then that the Franck–Condon factors are more favorable for $^3A_2 \leftrightarrow {}^1A_1$ coupling. From this proposed mechanism of decay one may expect a sharp increase in decay with increasing vibrational energy in $^3A_2$, and the phosphorescence yield may be very small near the $^1A_2$ origin. Therefore Luntz and Maxson suggest that the inference that $^1A_2(S_1) \rightsquigarrow {}^3A_2(T_1)$ intersystem crossing is not taking place because of the absence of phosphorescence upon $^1A_2(S_1)$ excitation should be viewed with caution.

In a recent publication, Houston and Moore[203] reexamined the mechanism of formaldehyde photochemistry. The authors monitored the appearance rate, relative yield, and vibrational distribution of the CO photoproduct detected either by its infrared fluorescence or by its absorption of a CW CO laser. In previous work, Moore and co-workers[197] have suggested, as we discussed earlier, that the mechanism of formaldehyde photochemistry is $S_1 \rightsquigarrow S_0 \rightarrow H_2 + CO$. The findings of Miller and Lee[201] on the benzene-sensitized decomposition of formaldehyde suggested the possibility of the $S_1 \rightsquigarrow T_1 \rightsquigarrow S_0 \rightarrow H_2 +$ CO mechanism. The short phosphorescence lifetimes measured by Luntz and Maxson[202] could also be considered in support of this $S_1 \rightsquigarrow T_1 \rightsquigarrow S_0 \rightarrow H_2 + CO$ mechanism. The measuring of the appearance rate of the photoproduct would help distinguish between the two possibilities. Houston and Moore found that the CO from either $H_2CO$ or $D_2CO$ is produced (337.1 nm excitation) with a collisionless rate of less than 0.26 μs$^{-1}$ (appearance time ~4 μs). The appearance rate varies linearly with pressure, and from the corresponding Stern–Volmer plots they found the collision-induced rates $k_{H_2CO} = 1.65 \pm 1.12$ μs$^{-1}$ Torr$^{-1}$ and $k_{D_2CO} = 0.96 \pm 0.07$ μs$^{-1}$ Torr$^{-1}$. The appearance rate of CO even at higher energies (305.5 nm) is slow. On the other hand the zero-pressure lifetimes for 337.1-nm excitation are much shorter; namely, $\tau_{H_2CO} \simeq 46$ ns and $\tau_{D_2CO} \simeq 870$ ns.[204] From consideration of the above findings, one thing that we can immediately conclude with certainty is that formaldehyde does not dissociate directly from the $S_1$ state. The delay indicates that there is at least one intermediate state between $S_1$ and photoproducts. The nature of the intermediate on the other hand is not clear. As Houston and Moore state, the $T_1(^3A_2)$ state is an attractive possibility but there are also some opposing facts. Brand and Stevens[205] have examined the formaldehyde spectrum for $S_1$–$T_1$ perturbations and found little evidence for such perturbations. In addition the small density of triplet levels isoenergetic with the $S_1$ origin (~0.02/cm$^{-1}$) makes it very unlikely that under collision-free conditions $T_1$ can provide a dissipative channel for $S_1$. The self-quenching studies of the $^3A_2$ state of $D_2CO$ by Luntz and Maxson[202] give a quenching rate slower than the collision-induced production of CO, but the studies were not conducted at the same conditions. Another possibility is that the highly excited vibrational levels of the $S_0$ state itself (see also Yeung and Moore[197,206] are very weakly coupled to the continuum so that they exist for many microseconds before dissociation. While for the higher pressure region this interpretation was found sufficient to explain most of the observed phenomena, difficulties arise at the collision-free regime. For a long-lived $S_0$ to form a dissipative manifold for $S_1$, its level density must be greater than $2\pi_c\tau$, where $\tau$ is the shorter of the $S_1$ or $S_0$ lifetimes. Based on the $\tau(S_1)$ lifetime its density is much greater than the calculated density of $S_0$ at the origin of $S_1$ for $H_2CO$ which was found to be about 10 states/cm$^{-1}$. Neither, therefore, of the two possibilities seems entirely satisfactory. Houston and Moore suggest the possibility of a combination of both plus other possibilities such as collision complexes.

Regarding the energy distribution in the photoproducts, it was found[203] that although the amount of energy as CO vibration increases with increasing excitation energy, the CO vibrational energy accounts for less than 5% of the energy available to the products at the measured dissociation wavelengths. There is a

possibility[203] that much of this energy is deposited as vibrational energy of $H_2$.

Recently Miller and Lee[207] have reported new measurements on the fluorescence yields and lifetimes for $H_2CO$, $D_2CO$, and HDCO excited at the $4^1$ vibronic level (the $\nu_4'$ is a $b_1$ out-of-plane wagging mode). For $H_2CO$ they found $\phi_F \simeq 0.035$ and $\tau = 0.082$ $\mu$s; for HDCO $\phi_F \simeq 0.05$ and $\tau = 0.141$ $\mu$s; for $D_2CO$ $\phi_F \simeq 1.0$ and $\tau = 4.5$ $\mu$s. The corresponding lifetimes reported by Yeung and Moore[197] are 0.282, 0.29, and 4.63 $\mu$s, respectively. As we see, there is disagreement between the two groups except in the case of $D_2CO$. The origin of the disagreement is not clear. Accepting the data of Miller and Lee, we note a large isotope effect on the nonradiative rate constants: $k_{NR}(D_2CO)$ is about $10^3$ smaller than $k_{NR}(H_2CO)$. Such large deuterium isotope effects on predissociation have not been observed previously. A relatively smaller isotope effect was also observed on the radiative rate constant ($k_F(H_2CO)/k_F(D_2CO) = 2.0$).

From the studies on other simple *linear aldehydes* we mention the study of Hansen and Lee.[208] In this study radiative and nonradiative rates of aldehydes of the type RCHO with R having two to six carbons have been measured in the gas phase. The observed radiative rates were found to be about three orders of magnitude smaller than the nonradiative rates. Calculated radiative lifetimes using the Strickler–Berg equation[209] agree with the observed ones except in the case of acetaldehyde. The nonradiative decay mechanisms were considered to be an $S_1 \rightsquigarrow T_1$ intersystem crossing process and type II photochemical processes. Concerning the energy dependence of $k_{NR}$, Hansen and Lee[208] note that for excitation energies below 35 000 $cm^{-1}$, acetaldehyde and propanal show only a small energy dependence. On the other hand, the rest of the aldehydes that possess $\gamma$ hydrogen and can undergo the type II photochemical process show large energy dependence. The sharp decline of the fluorescence yield of acetaldehyde above about 35 000 $cm^{-1}$ could be due to the onset of an $S_1 \rightsquigarrow S_0$ internal conversion process followed by photochemistry to give $CH_4$ and CO.[210]

Among unsaturated aldehydes, *propynal* ($HC{\equiv}CCHO$) has been studied in detail, especially in relation to the problem of collisional quenching. Thayer and Yardley,[211] upon excitation with 382.1-nm laser pulses corresponding to the origin of the $^1A''(S_1)$ state of propynal, observed a microsecond emission corresponding to $^1A'' \rightarrow {}^1A'$ fluorescence. The collision-free fluorescence lifetime was determined as 0.978 $\mu$s. The quenching of the fluorescence has been studied using 19 different collision partners with dipole moments ranging from 0 to 3.95 D. From Stern–Volmer plots the quenching cross sections were obtained and found to range from 8 to 176 Å$^2$. Nonpolar quenchers have cross sections smaller than gas kinetic cross sections while the polar ones have higher cross sections increasing with dipole moment up to 176 Å$^2$ for the most polar $CH_3CN$. The authors also formulated a theoretical model to explain the quenching efficiency of the various gases. In another study,[212] Thayer and Yardley combined the fluorescence intensity measurements with lifetime measurements to obtain all eight rate constants that appear in their relaxation mechanism. Under collision-free conditions both intersystem crossing and internal conversion (from the origin) were found to be important, with intersystem crossing dominating. The apparent irreversible intersystem crossing from the origin of $^1A''$ to $^3A''$ was considered puzzling since the calculated density of triplets was found to be only 0.5 states/$cm^{-1}$. The cross sections for collision-induced intersystem crossing and collision-induced internal conversion were found to be 60 and 30 Å$^2$, respectively. Again, as in the collision-free case, intersystem crossing appears to be the dominant process. Thayer et al.[213] studied the effect of selective vibronic excitation on both the collision-free and higher pressure relaxation dynamics. The unimolecular decay rate of the singlet was found to increase with increasing energy. The variation of collision-induced ISC and IC rate constants with excess energy was found to parallel the variation of collision-free rate constants.

Special attention to the photochemical channel of nonradiative relaxation of excited propynal has been given in a study by Kumar and Huber.[214] These investigators obtained fluorescence and phosphorescence excitation spectra of propynal up to 6000 $cm^{-1}$ above the origin of $S_1$. In addition they determined the relative yield of the photoproduct CO ($\phi_{diss}$) over the above energy range. Using 0.6 Torr of propynal, they found that excitation into different vibronic levels of $S_1$ does not alter significantly the phosphorescence quantum yield ($\phi_p$) as long as the excess energy does not exceed 2900 $cm^{-1}$ ($2_0^1$). However, at 2952 $cm^{-1}$ above the origin of $S_1$, a sharp decrease of $\phi_p$ is observed. Since this behavior of $\phi_p$ coincides with a steep increase of $\phi_{diss}$, it appears that a new nonradiative path of photochemical nature opens up at this energy. In the presence of 100 Torr of He the excitation spectrum follows the absorption spectrum to higher energies than in the absence of He. The onset of the photodecomposition seems to be pushed up by 1300 $cm^{-1}$. In addition, the intensity of the phosphorescence excited with $E_{vib} \leqslant 2900$ $cm^{-1}$ is enhanced by 1.8 times over that without He. The supression of the photodecomposition following excitation of the $2^1$ level by He is an indication that one or more pressure-dependent deactivation paths successfully compete with photochemistry between 2900 and 6000 $cm^{-1}$. On the basis of the measurements of the CO production, phosphorescence enhancement, and previous studies on the $S_1$ predissociation limit by Brand et al.[215] the authors suggest that photodecomposition takes place from the $S_1$ surface while collision-induced ISC is the competing process.

### 2. Ketones

A study of the radiative and nonradiative processes in symmetrically substituted, *methylated acetones* has been performed by Hansen and Lee.[216] The observed radiative lifetimes were compared with calculated radiative lifetimes using the Strickler–Berg equation.[209] The calculated values were found to be greater than the observed by a factor of 8–9. This discrepancy was attributed to the change of the puckered geometry of the $^1(n,\pi^*)$ state of the ketone near the chromophore. The nonradiative decay is much faster than the radiative decay, which accounts for less than 1% of the overall deactivating processes of the $S_1$ state of the ketones. The dominating nonradiative process in these compounds is considered to be an $S_1 \rightsquigarrow T_1$ intersystem crossing. For example, for acetone at low excess energies, $\phi_{ISC} \simeq 1.0$.[217] The fluorescence lifetime, dominated by the ISC process, is lengthened by the $\alpha,\alpha'$ substitution of methyl groups. According to Hansen and Lee this is a result of the restriction, due to the steric hindrance introduced by the methyl groups, of the out-of-plane C–O vibrations which act as promoting modes for the $S_1 \rightsquigarrow T_1$ ISC.

Fluorescence lifetime and quantum yield measurements on *acetone* and acetone-$d_6$ in the thermally equilibrated gas phase have been performed by Halpern and Ware.[218]

Unlike the simple linear ketones such as acetone that do not have well-resolved spectra, cyclic rigid ketones show a structured spectrum and allow single vibronic level excitation studies. *Cyclobutanone* has been studied in detail.[219,220] Fluorescence quantum yields have been measured and photoproduct analysis has been performed upon excitation of cyclobutanone with $\lambda_{exc}$ = 305.0–335.0 nm and ~0.5 Å resolution. It was found that the value of $\phi_F$ is ~0.002 for $\lambda_{exc}$ higher than ~319.0 nm (pressure 5 Torr), but it suffers a sharp drop at shorter wavelengths, e.g., $\phi_F < 4 \times 10^{-6}$ for $\lambda_{exc} < 310.0$ nm. The nonradiative channels at low excess energies are considered to be a dominant ISC and a less important IC. The photoexcited cyclobutanone is known to decompose to give two kinds of products by the two main fragmentation modes shown in eq 48. The ratio of photoproducts $C_3/C_2$ was rationalized earlier[221] as representing the ratio

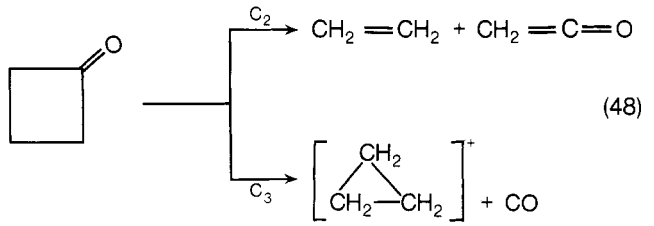


(48)

$k_{ISC}/k_{IC}$ at low excess energies. The sharp drop in $\phi_F$ for $\lambda_{exc} \leq 319.4$ nm was attributed to the onset of a fast predissociation process. The photoproduct ratio also shows a sharp change in the same region, and the new nonradiative channel appears to favor $C_2$ photoproducts.

The low-pressure photophysics and photochemistry of *halogenated ketones* have been investigated by several researchers. Halpern and Ware[222] studied the fluorescence lifetimes of *hexafluoroacetone* (HFA) vapor, excited at four different wavelengths and in the pressure range 0.1–700 Torr. Under isolated conditions the fluorescence decay of HFA was found to be exponential and the lifetime to decrease gradually with increasing excitation energy. With ~4500 $cm^{-1}$ excess energy the decay rate is enhanced by a factor of 2. The energy dependence of the nonradiative rate constant was found to be much weaker than that predicted by RRKM theory for the unimolecular decomposition rate. The authors suggest that for energies less than ~6000 $cm^{-1}$ intersystem crossing is the dominant nonradiative process. At intermediate pressures the fluorescence decay was found to be nonexponential due to vibrational relaxation. From an analysis of the decay curves it was concluded that the hard collision mechanism for vibrational relaxation was inconsistent with the data. The data supported a cascade model with one intermediate level. The second-order vibrational relaxation rate constant was found to be ca. one-third the hard-sphere value. Recently Knecht[223] has suggested that not only intersystem crossing but internal conversion is also important in deactivating the $S_1$ state of HFA. The importance of the latter process increases with increasing excitation energy.

A variety of other halogenated ketones has been studied by Hackett and Phillips.[224] In a series of papers the authors studied the spectroscopic properties and the electronic and vibrational relaxation dynamics of *1-fluoroacetone, 1,1,1-trifluoroacetone, 1-chloropentafluoroacetone, 1,3-dichlorotetrafluoroacetone,* and *1,1,3-trichlorotrifluoroacetone.* It was found that increase in photon energy causes an exponential increase in $k_{NR}$ which was attributed either to decomposition from the singlet manifold or to an enhancement of nonradiative decay to a short-lived, presumably dissociative, triplet state.

Studies on *perfluorocyclobutanone* (PFCB) at low pressures have been performed by Lewis and Lee.[225,226] It was found that the fluorescence lifetime of an "isolated" molecule of PFCB in its $S_1$ state (origin at ~410.0 nm) with little vibrational energy is ~110 ns. Both the fluorescence quantum yield and lifetime at low pressure (<0.2 Torr) remain approximately constant from $\lambda_{exc}$ = 420.0 to 380.0 nm. Below $\lambda_{exc}$ = 380.0 nm, these quantities gradually decrease and they are diminished by a factor of 100 at $\lambda_{exc}$ = 348 nm, indicating that a new nonradiative channel has become important.[225] PFCB in analogy with cyclobutanone undergoes photochemistry as follows

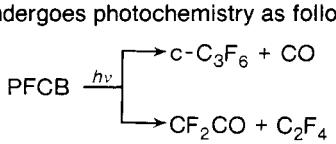


The $C_3/C_2$ product ratio drops by a factor of 20 by changing the excitation wavelength from 405 to 334 nm. Direct sensitization of the $T_1$ state of PFCB by triplet benzene showed[226] that the $T_1$ state decomposes mainly to C-$C_3F_6$ and CO. On the basis of these facts and other evidence, it was suggested that at low excess energies $S_1 \rightsquigarrow T_1$ intersystem crossing dominates while at higher energies $S_1 \rightsquigarrow S_0$ internal conversion becomes more important. Earlier Phillips[227] had studied the photolysis of PFCB, but at higher pressures, and had concluded that the PFCB photodecomposition involves only the $S_1$ state.

### 3. Aromatic Carbonyls

One of the important systems in the development of the ideas on intermediate coupling behavior has been the aromatic carbonyl *benzophenone.* Benzophenone is probably the first system for which the model involving simultaneous strong and weak coupling of the initially prepared state to two sets of final states (see also the section on aza-aromatics) has been proposed. Busch, Rentzepis, and Jortner[228] studied the time and energy-resolved luminescence of benzophenone (≤1 Torr) excited at about 2800 $cm^{-1}$ above the origin of the $S_1$ state. The decay was found to be nonexponential with a short lifetime component $\tau \simeq 10$ μs and a long component $\tau \simeq 200$ μs. The spectrum of the fast and slow decaying emissions were found to be the same. Their relative intensities appeared to depend both on wavelength and on pressure. The observed increase of $I_s/I_f$ with increasing pressure (in the range $p \geq 10^{-2}$ Torr) suggests that the triplet levels are at least partially populated by a collisional mechanism. At very low pressure $p = 10^{-4}$ Torr, $I_s/I_f \simeq 0.2$–0.3, which indicates that the long emission is exhibited even in the absence of collisions.

The following model was proposed to explain the experimental results. The optically accessible zero-order singlet state, S, does not couple with all the states in the triplet manifold (total density ~$10^5$ states/$cm^{-1}$) with the same efficiency, because of wrong symmetry or unfavorable Franck–Condon factors. There is therefore a small number $n$ of triplet levels, T, which will be strongly coupled to S, while a larger number of triplet levels is weakly coupled to S. This physical situation was then described by considering each of the $n + 1$ levels which resulted from strong coupling being weakly coupled to a large number of {T'} states in the triplet manifold. This weak coupling will result in a long radiative component in the isolated molecule being characterized by the radiative width $\Gamma_{T'}^{-1} \approx \Gamma_T^{-1}$. On the other hand, the total energy density of triplet states quasidegenerate with S provides a fast decay time, independent of the coupling strength, of $\simeq 10$ μs for the decay of the singlet state into this dense manifold. On the basis of the above model it is expected that collisions will broaden the strongly coupled S + T states resulting in vibrational relaxation. This collisionally induced relaxation of the T states will decrease the decay time and reduce its quantum yield. On the other hand, the yield of the long-lived component arising from the vibrationally relaxed states in the triplet manifold (which are populated by the deactivation of the strongly coupled states) is expected to increase with increasing pressure.

Hochstrasser and Wessel[229] have also studied the fluorescence decay of benzophenone vapor at low pressures. In agreement with Busch et al.,[228] the fluorescence decay was found to be nonexponential with a fast and a low component. A somewhat different model from that proposed by Busch et al.[228] was suggested for the explanation of the experimental results.

The aromatic carbonyl *benzaldehyde* has also been studied in the dilute vapor phase. The photochemical behavior of benzaldehyde at low pressures was found to vary with excitation energy and with the nature of the electronic state being excited.[230] The same was found to be true for the phosphorescence yield.[231,232] Baba and co-workers,[232] for example, found that the phosphorescence quantum yield at a pressure of 2 mTorr is essentially constant in the region of $S_1 \rightsquigarrow S_0$ absorption. However, in the energy region between the $S_1 \rightsquigarrow S_0$ and $S_2 \rightsquigarrow S_0$ absorptions an abrupt reduction in the phosphorescence yield takes place. At pressures higher than 500 mTorr, on the other hand, the quantum yield is nearly constant throughout the two

**TABLE IV. Review Papers on Radiationless Transitions**

| Date | Author(s) | Title | Ref no. |
|---|---|---|---|
| 1966 | S. K. Lower and M. A. El-Sayed | The Triplet State and Molecular Electronic Processes in Organic Molecules | 240 |
| 1968 | B. R. Henry and M. Kasha | Radiationless Molecular Electronic Transitions | 241 |
| 1969 | J. Jortner, S. A. Rice, and R. M. Hochstrasser | Radiationless Transitions in Photochemistry | 242 |
| 1971 | E. W. Schlag, S. Schneider, and S. F. Fischer | Lifetimes in Excited States | 136 |
| 1972 | K. F. Freed | The Theory of Radiationless Transitions in Polyatomic Molecules | 16b |
| 1972 | C. S. Parmenter | Resonance Fluorescence and Nonradiative Relaxation in Polyatomic Gases | 243 |
| 1973 | B. R. Henry and W. Siebrand | Radiationless Transitions | 28 |
| 1974 | J. Jortner and S. Mukamel | Preparation and Decay of Excited Molecular States | 12 |
| 1974 | G. W. Robinson | Molecular Electronic Radiationless Transitions from Excited States | 13a |
| 1974 | G. H. Atkinson, C. Parmenter, and M. W. Schuyler | Single Vibronic Level Fluorescence | 244 |
| 1974 | J. T. Yardley | Dynamic Properties of Electronically Excited Molecules | 245 |
| 1975 | S. A. Rice | Some Comments on the Dynamics of Primary Photochemical Processes | 246 |
| 1975 | M. A. El-Sayed | Double Resonance and the Properties of the Lowest Excited Triplet State of Organic Molecules | 247 |
| 1976 | J. Jortner and S. Mukamel | Molecular Radiationless Processes | 248 |
| 1976 | S. Leach | Electronic Spectroscopy and Relaxation Processes in Small Molecules | 249 |
| 1976 | K. F. Freed | Energy Dependence of Electronic Relaxation Processes in Polyatomic Molecules | 10 |

absorption regions. This behavior has been explained[230,232] in terms of an $S_2 \rightsquigarrow T_j$ intersystem crossing followed by decomposition of benzaldehyde from the $T_j$ state to give benzene and carbon monoxide.

## IV. Discussion

### A. Summary

In the condensed phase, vibrational relaxation/redistribution is usually fast compared to the other radiative and radiationless relaxation rates. As a result, the luminescence dynamics of the excited molecule are, in most cases, independent of the excitation wavelength. In the low-pressure gas phase, on the other hand, we have seen that the nonradiative decay rate, $k_{NR}$, usually increases with increasing excess energy above the electronic origin. The radiative decay rate, $k_F$, may also change to some extent. But in general $k_F$ does not dominate the decay rate of large organic molecules, even in the gas phase. In many cases it is observed that the particular distribution of vibrational energy, rather than just the total energy, is important in determining the relaxation rate. There is in addition some recent evidence that different rotational excitations within a single vibronic band can affect significantly the rate of radiationless decay. Also, the nature of the radiationless process may itself change as the excitation wavelength becomes shorter. For example, at low excess energies the dominant relaxation process may be an $S_1 \rightsquigarrow T_1$ intersystem crossing. At higher energies the dominant process could be an $S_1 \rightsquigarrow S_0$ internal conversion, an $S_1 \rightsquigarrow T_{j>1}$ intersystem crossing, or possibly photochemistry (i.e., a radiationless transition involving isomerization or fragmentation). Even in cases where resonance emission is not observed from higher $S_n$ ($n \geq 2$) states, the dynamics of the electronic relaxation from $S_1$ are effected by the initial excitation to these higher states.

The decay curves of excited molecules in condensed media are almost always exponential. On the other hand, in the low-pressure gas-phase nonexponential decay is characteristic of the intermediate coupling case. The nonexponential decay has also been associated with a concept of "reversible radiationless transitions," as discussed in sections II and III. The observation that upon deuteration of aromatic hydrocarbons the nonradiative decay rate is reduced was crucial in the development of the understanding of the mechanism of radiationless transitions. In certain gas-phase cases a new, inverse isotope effect ($k_{NR}^H/k_{NR}^D < 1$) is observed.

### B. Photochemistry and Radiationless Processes

Photochemical relaxation is also different under isolated molecule conditions. Virtually all of the discussion in our review has referred to nonradiative electronic relaxation processes which involve transitions between bound states with essentially identical nuclear geomtries. As has been stressed by several earlier workers, however, there is no fundamental reason why radiationless transition theory cannot be extended to include molecular rearrangements. Rice and co-workers have done so explicitly for the large amplitude vibrational motion involving the inversion mode in aniline[120] and for the cis–trans isomerizations involving the torsional modes in substituted styrenes,[233] stilbenes,[234,235] and polyenes.[236] Hydrogen-atom transfers and abstractions have been rationalized by Heller[237] and by Pocius and Yardley[238] in terms of CH stretches being the most efficient acceptors of vibrational energy in the radiationless conversion of electronic excitation. More general photodissociation processes have also been treated from this point of view. The electronic relaxation process leaves the molecule with a lot of vibrational energy localized in a few nuclear motions. If this vibrational energy distribution corresponds to above-threshold excitation of a reaction coordinate, and if vibrational energy exchange is not too fast, then the molecule can isomerize or dissociate directly. Otherwise, one must wait for the appropriate unimolecular reaction to take place on the lower potential energy surface. The extension of radiationless transition theory to include these photochemical applications is quite nontrivial, especially in the case of dissociation where the dynamics of coupled-nuclear-motion fragmentation must be accounted for. This has been stressed most recently by Gelbart[239] in his review of polyatomic photodissociation mechanisms, and earlier by Rice[246] and by Henry and Siebrand.[28] By far the most thorough discussion of the modern approach to photochemical dynamics and its relationship to the theory of intramolecular electronic relaxation and vibrational energy distribution is given by Rice.[246]

### C. Future Studies

More experimental studies are needed on the extent of vibrational energy redistribution in the excited electronic states of large molecules, especially on the variation of its efficiency with excess energy. The concept of local modes should be further investigated particularly in reference to studies of electronic relaxation and vibrational energy redistribution. Studies with very narrow bandwidth sources could investigate the effects of rotational excitation on both the photophysical and photochemical relaxation; theoretical studies in the same area are also needed. More studies of radiationless transitions under excitation

over an extended energy range (excitation of higher states) are desirable. Experiments are needed employing excitation of variable bandwidth and pulse duration to test the predictions of the various theories on preparation of initial states and their subsequent decays. More picosecond spectroscopy studies of very fast photophysical relaxation (from higher electronic states) would be very important. For photofragmentations, say, the branching ratios, appearance times, and internal excitations of products can be measured as function of exciting light energy. Nozzle beam studies of radiationless transitions of vibrationally and rotationally cold molecules could remove the present problems associated with thermal vibro-rotational excitation in the ground state. More attention should be paid to possible "reversible" photochemical processes, such as the valence isomerizations of benzene. An elucidation of the channel III process in benzene is needed. The newly found effects of external magnetic fields on radiationless decay rates should be studied in detail both experimentally and theoretically. More photochemical radiationless transition studies of unstable species (e.g., radicals) are needed, especially because of their astrophysical interest.

Finally, as mentioned in sections II and III, theoretical studies are needed to clarify problems such as: the magnitude of the electronic matrix elements and their dependence on excess energy; the concept of promoting modes; the description of anharmonicity and frequency changes; the discrepancy between theoretical and experimentally fit values of final state densities and coupling strengths in "intermediate" case molecules; and determination of the "mechanism" of a given radiationless transition.

Table IV gives references to other review papers in the general area of radiationless transitions.

*Acknowledgments.* P. A. and M. A. E. thank the United States Energy Research and Development Administration and the Office of Naval Research for financial support. W. M. G. acknowledges the partial support of this research by the National Science Foundation and NATO Scientific Affairs Office. He is also grateful to the Alfred P. Sloan Foundation and Camille and Henry Dreyfus Foundation for their fellowship support.

## V. References and Notes

(1) B. K. Selinger and W. R. Ware, *J. Chem. Phys.*, **53,** 3160 (1970); **52,** 5482 (1970).
(2) K. G. Spears and S. A. Rice, *J. Chem. Phys.*, **55,** 5561 (1971).
(3) C. S. Parmenter and M. W. Schuyler, *Chem. Phys. Lett.*, **6,** 339 (1970).
(4) See, for example, V. Fano, *Phys. Rev.*, **124,** 1866 (1961).
(5) J. N. Murrell and J. M. Taylor, *Mol. Phys.*, **16,** 609 (1969).
(6) G. W. Robinson and R. P. Frosch, *J. Chem. Phys.*, **37,** 1962 (1962); **38,** 1187 (1963); G. W. Robinson, *ibid.*, **47,** 1967 (1967).
(7) G. R. Hunt, E. F. McCoy, and I. G. Ross, *Aust. J. Chem.*, **15,** 591 (1962); J. P. Byrne, E. F. McCoy, and I. G. Ross, *ibid.*, **18,** 1589 (1965).
(8) W. Siebrand, *J. Chem. Phys.*, **44,** 4055 (1966); **46,** 440 (1967); **47,** 2411 (1967); W. Siebrand and D. F. Williams, *ibid.*, **46,** 403 (1967); **49,** 1860 (1968).
(9) M. Bixon and J. Jortner, *J. Chem. Phys.*, **48,** 715 (1968).
(10) K. F. Freed, *Top. Appl. Phys.*, **15,** 1 (1976).
(11) W. Rhodes, *Chem. Phys.*, **4,** 259 (1974); *Chem. Phys. Lett.*, **11,** 179 (1971); *J. Chem. Phys.*, **40,** 20th Reunion Soc. Chem. Phys. (1970); *J. Chem. Phys.*, **50,** 2885 (1969).
(12) J. Jortner and S. Mukamel, in "The World of Quantum Chemistry", R. Daudel and B. Pullman, Ed., Reidel, Boston, 1974, p 145.
(13) (a) G. W. Robinson in "Excited States", Vol. 1, E. Lim, Ed., Academic Press, New York, N.Y., 1974, p 1; (b) G. W. Robinson and C. A. Langhoff, *Chem. Phys.*, **5,** 1 (1974).
(14) V. G. Plotnikov and G. G. Konoplev, *Chem. Phys. Lett.*, **23,** 541 (1973).
(15) See, for example, L. I. Schiff, "Quantum Mechanics", 3rd ed, McGraw-Hill, New York, N.Y., 1968.
(16) The concept of $t_{max}$ has been developed most fully by K. F. Freed, in (a) *J. Chem. Phys.*, **52,** 1345 (1970); (b) *Top. Cur. Chem.*, **31,** 105 (1972).
(17) W. M. Gelbart, D. F. Heller, and M. L. Elert, *Chem. Phys.*, **7,** 116 (1975).
(18) E. J. Heller and S. A. Rice, *J. Chem. Phys.*, **61,** 936 (1974).
(19) J. M. Delory and C. Tric, *Chem. Phys.*, **3,** 54 (1974).
(20) For the relevant literature on quantum beats see, for example, the discussion in M. Bixon, J. Jortner, and Y. Dothan, *Mol. Phys.*, **17,** 109 (1969).
(21) W. Siebrand, *Chem. Phys. Lett.*, **14,** 23 (1972).
(22) R. Lefebvre and J. Savolainen, *J. Chem. Phys.*, **60,** 2509 (1974).
(23) F. Mies and M. Krauss, *J. Chem. Phys.*, **45,** 4455 (1966).
(24) S. A. Rice, I. McLaughlin, and J. Jortner, *J. Chem. Phys.*, **49,** 2756 (1968); K. G. Kay and S. A. Rice, *ibid.*, **57,** 3041 (1972); K. G. Kay, *ibid.*, **60,** 2370 (1974).
(25) R. Lefebvre and J. A. Beswick, *Mol. Phys.*, **23,** 1223 (1972).
(26) A. Nitzan, J. Jortner, and P. M. Rentzepis, *Mol. Phys.*, **22,** 585 (1971); A. Nitzan, J. Jortner, and B. J. Berne, *ibid.*, **26,** 281 (1973).
(27) E. J. Heller and S. A. Rice, *J. Chem. Phys.*, **61,** 936 (1974).
(28) B. R. Henry and W. Siebrand, in "Organic Molecular Photophysics", Vol. 1, J. B. Birks, Ed., Wiley, New York, N.Y., 1973, Chapter 4, pp 153–237, and references to earlier work contained therein.
(29) M. A. Ratner and B. R. Sundheim (*Chem. Phys. Lett.*, **10,** 56 (1971)) have discussed how intersystem crossing can provide a mechanism for electronic-to-rotational conversion of energy, but this effect has been argued to be negligible by V. Lawetz, G. Orlandi, and W. Siebrand (*J. Chem. Phys.*, **56,** 4045 (1972)).
(30) M. Born and J. R. Oppenheimer, *Ann. Phys.*, **84,** 459 (1927); M. Born and K. Huang, "Dynamical Theory of Crystal Lattices", Oxford, 1954, Chapter 14.
(31) O. Atabek, A. Hardisson, and R. Lefebvre, *Chem. Phys. Lett.*, **20,** 40 (1973).
(32) K. K. Docken and J. Hinze, *J. Chem. Phys.*, **57,** 4928 (1972).
(33) D. M. Burland and G. W. Robinson, *Proc. Natl. Acad. Sci. U.S.A.*, **66,** 257 (1970).
(34) B. Sharf and R. Silbey, *Chem. Phys. Lett.*, **4,** 561 (1970).
(35) G. Orlandi and W. Siebrand, *Chem. Phys. Lett.*, **8,** 473 (1971).
(36) K. F. Freed and W. M. Gelbart, *Chem. Phys.*, **10,** 187 (1971).
(37) R. Lefebvre, *Chem. Phys. Lett.*, **8,** 306 (1971).
(38) (a) W. Siebrand, *Chem. Phys. Lett.*, **6,** 192 (1970); (b) B. R. Henry and W. Siebrand, *J. Chem. Phys.*, **54,** 1072 (1971); (c) V. Lawetz, G. Orlandi, and W. Siebrand, *ibid.*, **56,** 4058 (1972); (d) references given in B. R. Henry and W. Siebrand in "Organic Molecular Photophysics", Vol. 2, J. Birks, Ed., Wiley, New York, N.Y., 1975.
(39) A. C. Albrecht, *J. Chem. Phys.*, **33,** 157, 169 (1960).
(39a) M. A. El-Sayed, *J. Chem. Phys.*, **38,** 2834 (1963).
(40) F. Metz, S. Friedrich, and G. Hohlneicher, *Chem. Phys. Lett.*, **16,** 353 (1972).
(41) A. Nitzan and J. Jortner, *J. Chem. Phys.*, **56,** 3360 (1972).
(42) K. F. Freed and S. H. Lin, *Chem. Phys.*, **11,** 409 (1975).
(43) For a brief but interesting historical account of the "Golden Rule", see pp 4 and 5 of ref 13a.
(44) M. Abramowitz and I. A. Stegun, "Handbook of Mathematical Functions", (NBS Applied Math. Series), No. 55, U.S. Government Printing Office, Washington, D.C., 1970.
(45) (a) W. Siebrand, *J. Chem. Phys.*, **44,** 4055 (1966); (b) W. Siebrand and D. F. Williams, *ibid.*, **46,** 403 (1967); (c) W. Siebrand, *ibid.*, **46,** 440 (1967); (d) *ibid.*, **47,** 2411 (1967); (e) W. Siebrand and D. F. Williams, *ibid.*, **49,** 1860 (1968).
(46) B. Sharf and R. Silbey, *Chem. Phys. Lett.*, **5,** 314 (1970).
(47) F. Metz, *Chem. Phys. Lett.*, **22,** 186 (1973).
(48) S. H. Lin and R. Bersohn, *J. Chem. Phys.*, **48,** 2732 (1968); *ibid.*, **44,** 3759 (1966).
(49) R. Englman and J. Jortner, *Mol. Phys.*, **18,** 145 (1970).
(50) R. Kubo and Y. Toyozawa, *Progr. Theor. Phys.*, **13,** 160 (1955).
(51) See review and list of references in J. J. Markham, *Rev. Mod. Phys.*, **31,** 956 (1959).
(52) See, for example, ref 8, 14, 16, and 17.
(53) W. Siebrand, *J. Chem. Phys.*, **55,** 5843 (1971).
(54) S. Fischer, *J. Chem. Phys.*, **55,** 5844 (1971).
(55) K. F. Freed and J. Jortner, *J. Chem. Phys.*, **52,** 6272 (1970).
(56) S. Fischer, *J. Chem. Phys.*, **53,** 3195 (1970). Using a correlation function interpretation of the Golden Rule sum which is essentially equivalent to the many-phonon formalism, Fischer obtained, among other results, an expression for $k_s(0)$ which is identical with eq 5 in the text.
(57) D. F. Heller, K. F. Freed, and W. M. Gelbart, *J. Chem. Phys.*, **56,** 2309 (1972); *Chem. Phys. Lett.*, **23,** 56 (1973).
(58) M. G. Prais, D. F. Heller, and K. F. Freed, *Chem. Phys.*, **6,** 1 (1974).
(59) F. Metz, *Chem. Phys.*, **9,** 121 (1975).
(60) J. R. Christie and D. P. Craig, *Mol. Phys.*, **23,** 345, 353 (1972).
(61) I. Kühn, D. F. Heller, and W. M. Gelbart, preprint.
(62) K. G. Spears and S. A. Rice, *J. Chem. Phys.*, **55,** 5561 (1971).
(63) B. R. Henry and W. Siebrand, *J. Chem. Phys.*, **49,** 5369 (1968); R. J. Hayward, B. R. Henry, and W. Siebrand, *J. Mol. Spectrosc.*, **46,** 207 (1973); R. J. Hayward and B. R. Henry, *ibid.*, **50,** 58 (1974); **57,** 221 (1975); *Chem. Phys.*, **12,** 387 (1976).
(64) R. Wallace, *Chem. Phys.*, **11,** 189 (1975).
(65) R. L. Swofford, M. E. Long, and A. C. Albrecht, *J. Chem. Phys.*, **65,** 179 (1976).
(66) D. M. Burland and G. W. Robinson, *J. Chem. Phys.*, **51,** 4548 (1969).
(67) S. Fischer, *Chem. Phys. Lett.*, **11,** 577 (1971).
(68) A. L. Stanford and S. Fischer, *Chem. Phys.*, **1,** 99 (1973).
(69) N. Shimakura, Y. Fujimura, and T. Nakajima, *Theor. Chim. Acta*, **37,** 77 (1974).
(70) C. Guttman and S. A. Rice, *J. Chem. Phys.*, **61,** 651 (1974).
(71) J. H. Callomon, J. E. Parkin, and R. Lopez-Delgado, *Chem. Phys. Lett.*, **13,** 125 (1972).
(72) C. S. Parmenter and M. W. Schuyler in "Transitions Nonradiative Moleculaire", Reunion Soc. Chem. Phys., 20th, 1969, p 92 (*J. Chim. Phys. Suppl.*, 1969–70).
(73) See data cited in C. S. Parmenter, *Adv. Chem. Phys.*, **22,** 365 (1972).
(74) D. Craig, *J. Chem. Soc.*, 2147 (1950).
(75) V. Lawetz, W. Siebrand, and G. Orlandi, *Chem. Phys. Lett.*, **16,** 448 (1972).
(76) G. D. Gillispie and E. C. Lim, *Chem. Phys. Lett.*, **34,** 513 (1975).
(77) G. S. Beddard, G. R. Fleming, O. L. J. Gijzeman, and G. Porter, *Chem. Phys. Lett.*, **18,** 481 (1973).

(78) S. F. Fischer, A. L. Stanford, and E. C. Lim, *J. Chem. Phys.*, **61,** 582 (1974).
(79) E. W. Schlag and H. von Weyssenhoff, *J. Chem. Phys.*, **53,** 3108 (1970).
(80) M. G. Rockley and D. Phillips, *Chem. Phys. Lett.*, **21,** 181 (1973).
(81) (a) J. C. Hsieh, C. S. Huang, and E. C. Lim, *J. Chem. Phys.*, **60,** 4345 (1974); (b) *Chem. Phys. Lett.*, **28,** 130 (1974); (c) J. C. Hsieh and E. C. Lim, *J. Chem. Phys.*, **61,** 736 (1974).
(82) (a) S. F. Fischer and E. C. Lim, *Chem. Phys. Lett.*, **26,** 312 (1974); (b) S. F. Fischer, A. L. Stanford, and E. C. Lim, *J. Chem. Phys.*, **61,** 582 (1974).
(83) L. E. Brus and J. R. McDonald, *J. Chem. Phys.*, **61,** 97 (1974), and references cited therein.
(84) See, for example, P. B. Sackett and J. T. Yardley, *J. Chem. Phys.*, **57,** 152 (1972).
(85) A. E. Douglas, *J. Chem. Phys.*, **45,** 1007 (1966).
(86) R. van der Werf (Doctoral Dissertation, Gröningen, 1976). Discussion of and references to earlier work on the emission properties of the 1,2-dicarbonyls are given here.
(87) R. A. Coveleskie and J. T. Yardley, *Chem. Phys.*, **9,** 275 (1975).
(88) W. M. Gelbart and K. F. Freed, *Chem. Phys. Lett.*, **18,** 470 (1973).
(89) M. Bixon and J. Jortner, *J. Chem. Phys.*, **50,** 3284 (1969).
(90) See references contained in ref 4 and 5.
(91) A. Nitzan, J. Jortner, and P. M. Rentzepis, *Proc. R. Soc. London, Ser. A*, **327,** 367 (1972).
(92) (a) A. Lahmani, A. Tramer, and C. Tric, *J. Chem. Phys.*, **60,** 4431 (1974); (b) C. Tric and J. M. Delory, *Chem. Phys.*, **3,** 59 (1974); (c) C. Tric, *Chem. Phys. Lett.*, **21,** 83 (1973).
(93) C. W. Ashpole, S. J. Formosinho, and G. Porter, *Proc. R. Soc. London, Ser. A*, **323,** 11 (1971).
(94) H. Baba, A. Nakamjima, M. Aoi, and K. Chihara, *J. Chem. Phys.*, **55,** 2433 (1971).
(95) R. P. van der Werf, D. Zevenhuijzen, and J. Kommandeur, *Chem. Phys. Lett.*, **27,** 325 (1974).
(96) B. Soep, C. Michel, A. Tramer, and L. Lindqvist, *Chem. Phys.*, **2,** 293 (1973).
(97) A. Z. Moss and J. T. Yardley, *J. Chem. Phys.*, **61,** 2883 (1974).
(98) G. S. Beddard, G. R. Fleming, O. L. J. Gijzeman, and G. Porter, *Proc. R. Soc. London, Ser. A*, **340,** 519 (1974).
(99) K. F. Freed and D. F. Heller, *J. Chem. Phys.*, **61,** 3942 (1974), and private communication.
(100) C. A. Langhoff and G. W. Robinson, *Mol. Phys.*, **26,** 249 (1973).
(101) See, for example: (a) B. Soep and A. Tramer, *Chem. Phys.*, **7,** 52 (1975); (b) J. R. McDonald and L. E. Brus, *J. Chem. Phys.*, **61,** 3895 (1974).
(102) C. S. Parmenter and M. W. Schuyler, *Chem. Phys. Lett.*, **6,** 339 (1970).
(103) B. K. Selinger and W. R. Ware, *J. Chem. Phys.*, **53,** 3160 (1970).
(104) A. C. Albrecht, *J. Chem. Phys.*, **33,** 156 (1960).
(105) S. J. Strickler and R. A. Berg, *J. Chem. Phys.*, **37,** 814 (1962).
(106) W. R. Ware, B. K. Selinger, C. S. Parmenter, and M. W. Schuyler, *Chem. Phys. Lett.*, **6,** 342 (1970).
(107) W. M. Gelbart, K. G. Spears, K. F. Freed, J. Jortner, and S. A. Rice, *Chem. Phys. Lett.*, **6,** 345 (1970).
(108) D. Phillips, *J. Photochem.*, **1,** 97 (1972).
(109) C. S. Parmenter and M. D. Schuh, *Chem. Phys. Lett.*, **13,** 120 (1972).
(110) A. S. Abramson, K. G. Spears, and S. A. Rice, *J. Chem. Phys.*, **56,** 2291 (1971).
(111) K. Nakamura, *J. Chem. Phys.*, **53,** 998 (1970).
(112) C. Guttman and S. A. Rice, *J. Chem. Phys.*, **61,** 661 (1974).
(113) C. Guttman and S. A. Rice, *J. Chem. Phys.*, **61,** 651 (1974).
(114) G. L. Loper and E. K. C. Lee, *Chem. Phys. Lett.*, **13,** 140 (1972).
(115) P. H. Chereson, D. R. Worsnop, and F. S. Wettack, *J. Photochem.*, **5,** 159 (1976).
(116) K. C. Janda, J. M. Koert, and F. S. Wettack, *J. Photochem.*, **1,** 345 (1973).
(117) H. von Weyssenhoff and F. Kraus, *J. Chem. Phys.*, **54,** 2387 (1971).
(118) M. Wuak and M. Stockburger, *J. Mol. Spectrosc.*, **43,** 87 (1972).
(119) W. R. Ware and A. M. Garcia, *J. Chem. Phys.*, **61,** 187 (1974).
(120) R. Scheps, D. Florida, and S. A. Rice, *J. Chem. Phys.*, **61,** 1730 (1974).
(121) R. C. Brown, M. G. Rockley, and D. Phillips, *Chem. Phys.*, **7,** 41 (1975).
(122) M. G. Rockley and D. Phillips, *J. Photochem.*, **3,** 365 (1974).
(123) M. G. Rockley and D. Phillips, *Chem. Phys. Lett.*, **27,** 393 (1974).
(124) G. R. Fleming, O. L. J. Gijzeman, and S. H. Lin, *Chem. Phys. Lett.*, **21,** 527 (1973).
(125) J. O. Uy and E. C. Lim, *Chem. Phys. Lett.*, **7,** 306 (1970).
(126) V. Laor and P. K. Ludwig, *J. Chem. Phys.*, **54,** 1054 (1971).
(127) A. J. Watts and H. J. Strickler, *J. Chem. Phys.*, **44,** 2433 (1966).
(128) E. C. Lim and J. O. Uy, *J. Chem. Phys.*, **56,** 3374 (1972).
(129) E. C. Lim and C. S. Huang, *J. Chem. Phys.*, **58,** 1247 (1973).
(130) A. E. W. Knight, B. K. Selinger, and I. G. Ross, *Aust. J. Chem.*, **26,** 1159 (1973).
(131) J. M. Blondau and M. Stockburger, *Chem. Phys. Lett.*, **8,** 436 (1971).
(132) G. S. Beddard, S. J. Formosinho, and G. Porter, *Chem. Phys. Lett.*, **22,** 235 (1973).
(133) E. W. Schlag, S. Schneider, and D. W. Chandler, *Chem. Phys. Lett.*, **11,** 474 (1971).
(134) V. Boesl, H. J. Neusser, and E. W. Schlag, *Chem. Phys. Lett.*, **31,** 1 (1975).
(135) V. Boesl, H. J. Neusser, and E. W. Schlag, *Chem. Phys. Lett.*, **31,** 7 (1975).
(136) E. W. Schlag, S. Schneider, and S. F. Fischer, *Annu. Rev. Phys. Chem.*, **22,** 465 (1971).
(137) M. Stockburger, H. Gattermann, and W. Klusmann, *J. Chem. Phys.*, **63,** 4519 (1975).
(138) M. Stockburger, H. Gattermann, and W. Klusmann, *J. Chem. Phys.*, **63,** 4530 (1975).
(139) H. Sixl and M. Schwoerer, *Chem. Phys. Lett.*, **6,** 21 (1970).
(140) Y. H. Meyer, R. Astier, and J. M. Leclercq, *J. Chem. Phys.*, **56,** 801 (1972).
(141) H. Gattermann and M. Stockburger, *J. Chem. Phys.*, **63,** 4541 (1975).
(142) V. Boesl, H. J. Neusser, and E. W. Schlag, *Chem. Phys. Lett.*, **42,** 16 (1976).
(143) J. C. Hsieh, C. S. Huang, and E. C. Lim, *J. Chem. Phys.*, **60,** 4345 (1974).
(144) C. S. Huang, J. C. Hsieh, and E. C. Lim, *Chem. Phys. Lett.*, **37,** 349 (1976).
(145) V. Laor, J. C. Hsieh, and P. K. Ludwig, *Chem. Phys. Lett.*, **22,** 150 (1973).
(146) S. F. Fischer and E. C. Lim, *Chem. Phys. Lett.*, **26,** 312 (1974).
(147) C. S. Huang, J. C. Hsieh, and E. C. Lim, *Chem. Phys. Lett.*, **28,** 130 (1974).
(148) C. J. Werkhoven, P. A. Geldof, M. F. M. Post, J. Langelaar, R. P. H. Rettschnick, and J. D. W. van Voorst, *Chem. Phys. Lett.*, **9,** 6 (1971).
(149) C. J. Werkhoven, T. Deinum, J. Langelaar, R. P. H. Rettschnick, and J. D. W. van Voorst, *Chem. Phys. Lett.*, **11,** 478 (1971).
(150) C. J. Werkhoven, T. Deinum, J. Langelaar, R. P. H. Rettschnick, and J. D. W. van Voorst, *Chem. Phys. Lett.*, **30,** 504 (1975).
(151) C. J. Werkhoven, T. Deinum, J. Langelaar, R. P. H. Rettschnick, and J. D. W. van Voorst, *Chem. Phys. Lett.*, **32,** 328 (1975).
(152) C. S. Huang, J. C. Hsieh, and E. C. Lim, *Chem. Phys. Lett.*, **37,** 349 (1976).
(153) G. R. Fleming, C. Lewis, and G. Porter, *Chem. Phys. Lett.*, **31,** 33 (1975).
(154) A. Kearvell and F. Wilkinson, *Chem. Phys. Lett.*, **11,** 472 (1971).
(155) S. Okajima and E. C. Lim, *Chem. Phys. Lett.*, **37,** 403 (1976).
(156) B. Soep, *Chem. Phys. Lett.*, **33,** 108 (1975).
(157) A. E. W. Knight and B. K. Selinger, *Chem. Phys. Lett.*, **12,** 419 (1971).
(158) F. Lahmani, A. Frad, and A. Tramer, *Chem. Phys. Lett.*, **14,** 337 (1972).
(159) A. Frad, F. Lahmani, A. Tramer, and C. Tric, *J. Chem. Phys.*, **60,** 4419 (1974).
(160) K. Uchida, I. Yamazaki, and H. Baba, *Chem. Phys. Lett.*, **38,** 133 (1976).
(161) K. G. Spears and M. El-Manguch, paper presented at the VIIIth International Conference on Photochemistry, Edmonton, Canada, 1975.
(162) G. K. Vemulapalli and T. Cassen, *J. Chem. Phys.*, **56,** 5120 (1972).
(163) J. R. McDonald and L. E. Brus, *J. Chem. Phys.*, **59,** 4966 (1973).
(164) M. Chowdhury and L. Goodman, *J. Chem. Phys.*, **36,** 548 (1962); **38,** 2979 (1963).
(165) A. W. Knight and C. S. Parmenter, *Chem. Phys.*, **15,** 85 (1976).
(166) R. M. Hochstrasser and C. J. Marzzacco, *J. Chem. Phys.*, **51,** 5015 (1969).
(167) H. J. Dewey and S. G. Hadley, *Chem. Phys. Lett.*, **17,** 574 (1972).
(168) J. R. McDonald and L. E. Brus, *Chem. Phys. Lett.*, **23,** 87 (1973).
(169) R. H. Clark, R. M. Hochstrasser, and C. J. Marzzacco, *J. Chem. Phys.*, **51,** 5015 (1969).
(170) C. S. Parmenter and H. M. Poland, *J. Chem. Phys.*, **51,** 1551 (1969).
(171) L. G. Anderson and C. S. Parmenter, *J. Chem. Phys.*, **52,** 466 (1970).
(172) H. L. J. Backström and K. Sandros, *Acta Chem. Scand.*, **14,** 48 (1960).
(173) H. Okabe and W. A. Noyes, Jr., *J. Am. Chem. Soc.*, **79,** 801 (1957).
(174) G. M. McClelland and J. Yardley, *J. Chem. Phys.*, **58,** 4368 (1973).
(175) E. Drent, R. P. van der Werf, and J. Kommandeur, *J. Chem. Phys.*, **59,** 2061 (1973).
(176) J. T. Yardley, G. W. Holleman, and J. I. Steinfeld, *Chem. Phys. Lett.*, **10,** 266 (1971).
(177) L. G. Anderson, C. S. Parmenter, and H. M. Polland, *Chem. Phys.*, **1,** 401 (1973).
(178) L. G. Anderson, C. S. Parmenter, H. M. Polland, and J. D. Rau, *Chem. Phys. Lett.*, **8,** 232 (1971).
(179) C. S. Parmenter, *J. Chem. Phys.*, **41,** 658 (1964).
(180) R. van der Werf, E. Schutten, and J. Kommandeur, *Chem. Phys.*, **11,** 281 (1975).
(181) R. A. Beyer, P. F. Zittel, and W. C. Lineberger, *J. Chem. Phys.*, **62,** 4016 (1975).
(182) A. Frad and A. Tramer, *Chem. Phys. Lett.*, **23,** 297 (1973).
(183) L. A. Melton and W. Klemperer, *J. Chem. Phys.*, **55,** 1468 (1971).
(184) R. A. Beyer and W. C. Lineberger, *J. Chem. Phys.*, **62,** 4024 (1975).
(185) C. A. Thayer and J. T. Yardley, *J. Chem. Phys.*, **57,** 3992 (1972).
(186) J. T. Yardley, *J. Chem. Phys.*, **56,** 6192 (1972).
(187) E. Photos and G. H. Atkinson, *Chem. Phys. Lett.*, **36,** 34 (1975).
(188) A. Matzuzaki and S. Nagakura, *Chem. Phys. Lett.*, **37,** 204 (1976).
(189) R. A. Coveleskie and J. T. Yardley, *J. Am. Chem. Soc.*, **97,** 1667 (1975).
(190) See, for example, D. J. Robinson, and K. A. Holbrook, "Unimolecular Reactions", Wiley, Interscience, New York, N.Y., 1972; W. Forst, "Theory of Unimolecular Reactions", Academic Press, New York, N.Y., 1973.
(191) G. B. Porter and W. J. Reid, *J. Photochem.*, **3,** 27 (1974).
(192) L. E. Brus and J. R. McDonald, *J. Chem. Phys.*, **58,** 4223 (1973).
(193) D. M. Rank, C. H. Townes, and W. J. Welch, *Science*, **174,** 1083 (1971).
(194) E. S. Yeung and C. B. Moore, *Appl. Phys. Lett.*, **21,** 109 (1972).
(195) V. S. Letokhov, *Chem. Phys. Lett.*, **15,** 221 (1972).
(196) J. Marling, *Chem. Phys. Lett.*, **34,** 84 (1975).
(197) E. S. Yeung and C. B. Moore, *J. Chem. Phys.*, **38,** 3988 (1973).
(198) B. A. Degraff and J. G. Calvert, *J. Am. Chem. Soc.*, **89,** 2247 (1967).
(199) R. D. McQuigg and J. G. Calvert, *J. Am. Chem. Soc.*, **91,** 1590 (1969).
(200) R. G. Miller and E. K. C. Lee, *Chem. Phys. Lett.*, **33,** 104 (1975).
(201) R. G. Miller and E. K. C. Lee, *Chem. Phys. Lett.*, **27,** 475 (1974).
(202) A. C. Luntz and V. T. Maxson, *Chem. Phys. Lett.*, **26,** 553 (1974).
(203) P. L. Houston and C. B. Moore, *J. Chem. Phys.*, **65,** 757 (1976).

(204) A. P. Baronavski and C. B. Moore, to be published.
(205) J. C. D. Brand and C. G. Stevens, *J. Chem. Phys.*, **58,** 3331 (1973).
(206) E. S. Yeung and C. B. Moore, *J. Chem. Phys.*, **60,** 2139 (1974).
(207) R. G. Miller and E. K. C. Lee, *Chem. Phys. Lett.*, **41,** 52 (1976).
(208) D. A. Hansen and E. K. C. Lee, *J. Chem. Phys.*, **63,** 3272 (1975).
(209) S. J. Strickler and R. A. Berg, *J. Chem. Phys.*, **37,** 814 (1961).
(210) A. S. Archer, R. B. Cundall, and T. F. Palmer, *Proc. R. Soc. London, Ser. A,* **334,** 411 (1973).
(211) C. A. Thayer and J. T. Yardley, *J. Chem. Phys.*, **57,** 3992 (1972).
(212) C. A. Thayer and J. T. Yardley, *J. Chem. Phys.*, **61,** 2487 (1974).
(213) C. A. Thayer, A. V. Pocius, and J. T. Yardley, *J. Chem. Phys.*, **62,** 3712 (1975).
(214) D. Kumar and J. R. Huber, *Chem. Phys. Lett.*, **38,** 537 (1976).
(215) J. C. D. Brand, J. H. Callomon, and J. K. G. Watson, *Can. J. Phys.*, **39,** 1508 (1961).
(216) D. A. Hansen and E. K. C. Lee, *J. Chem. Phys.*, **62,** 183 (1975).
(217) G. M. Breuer and E. K. C. Lee, *J. Phys. Chem.*, **75,** 989 (1971).
(218) A. M. Halpern and W. R. Ware, *J. Chem. Phys.*, **54,** 1271 (1971).
(219) J. C. Hemminger and E. K. C. Lee, *J. Chem. Phys.*, **54,** 1405 (1971).
(220) J. C. Hemminger and E. K. C. Lee, *J. Chem. Phys.*, **56,** 5284 (1972).
(221) N. E. Lee and E. K. C. Lee, *J. Chem. Phys.*, **50,** 2094 (1969).
(222) A. M. Halpern and W. R. Ware, *J. Chem. Phys.*, **53,** 1969 (1970).
(223) D. A. Knecht, *Chem. Phys. Lett.*, **33,** 325 (1975).
(224) P. A. Hackett and D. Phillips, *J. Phys. Chem.*, **78,** 665 (1974); **78,** 671 (1974); **78,** 679 (1974).
(225) R. S. Lewis and E. K. C. Lee, *J. Chem. Phys.*, **61,** 3434 (1974).
(226) R. S. Lewis and E. K. C. Lee, *J. Phys. Chem.*, **79,** 167 (1975).
(227) D. Phillips, *J. Phys. Chem.*, **70,** 1235 (1966).
(228) G. E. Busch, P. M. Rentzepis, and J. Jortner, *J. Chem. Phys.*, **56,** 361 (1972).
(229) R. M. Hochstrasser and J. E. Wessel, *Chem. Phys. Lett.*, **19,** 156 (1973).
(230) M. Berger, I. L. Goldblatt, and C. Steel, *J. Am. Chem. Soc.*, **95,** 1717 (1973).
(231) J. Metcalfe, R. G. Brown, and D. Phillips, *J. Chem. Soc., Faraday Trans. 2,* 71, 409 (1975).
(232) T. Itoh, T. Takemura, and H. Baba, *Chem. Phys. Lett.*, **40,** 481 (1976).
(233) M. H. Hui and S. A. Rice, *J. Chem. Phys.*, **61,** 833 (1974).
(234) W. M. Gelbart and S. A. Rice, *J. Chem. Phys.*, **50,** 4775 (1969).
(235) W. M. Gelbart, K. F. Freed, and S. A. Rice, *J. Chem. Phys.*, **52,** 2460 (1970).
(236) J. N. Kushick and S. A. Rice, *J. Chem. Phys.*, **64,** 1612 (1976).
(237) A. Heller, *Mol. Photochem.*, **1,** 257 (1969).
(238) A. V. Pocius and J. T. Yardley, *J. Chem. Phys.*, **61,** 2779 (1974).
(239) W. M. Gelbart, *Annu. Rev. Phys. Chem.*, **28,** (1977).
(240) S. K. Lower and M. A. El-Sayed, *Chem. Rev.*, **66,** 199 (1966).
(241) B. R. Henry and M. Kasha, *Annu. Rev. Phys. Chem.*, **19,** 161 (1968).
(242) J. Jortner, S. A. Rice, and R. M. Hochstrasser, *Adv. Photochem.*, **7,** 149 (1969).
(243) C. S. Parmenter, "MTP International Review of Science", Vol. 3, "Spectroscopy", A. D. Buckingham and A. D. Ramsay, Ed., Butterworths, London, 1972, p. 297.
(244) G. H. Atkinson, C. Parmenter, and M. W. Schuyler, "Creation and Detection of the Excited State", Vol. 3, W. R. Ware, Ed., Marcel Dekker, New York, N.Y., 1974.
(245) J. T. Yardley, in "Chemical and Biochemical Applications of Lasers", Vol. 1, C. B. Moore, Ed., Academic Press, New York, N.Y., 1974, p 231.
(246) S. A. Rice in "Excited States", Vol. 2, E. C. Lim, Ed., Academic Press, New York, N.Y., 1975, p 1111.
(247) M. A. El-Sayed, *Annu. Rev. Phys. Chem.*, **26,** 235 (1975).
(248) J. Jortner and S. Mukamel in "Molecular Energy Transfer", R. Levine and J. Jortner, Ed., Wiley, New York, N.Y., 1976, p 178.
(249) S. Leach in ref 248, p 163.
(250) Note that eq $f_1(t)$ is an oscillating function of $t$ and that its Fourier transform (eq 31), *which is proportional to* $k_s(0)$, is therefore mathematically undefined. This should not be surprising since we started with eq 28 which equates the radiationless decay rate to a discrete sum over $\delta$ functions. This point was glossed over in most of the papers[52] on $k_s(0)$ since they immediately approximated the integral in eq 31 by the contribution from its saddle point. That is, the $[-\infty \gtrless t \gtrless +\infty]$ real line was (implicitly) deformed into a contour in the complex plane which runs through the saddle point of the integrand $I(t)$ and which runs off to infinity in a way that allows $I(t)$ to go to zero. This step is the analogue of our having "tamed" the $\delta$ functions earlier by $\Sigma_{n_1} \rightarrow \int dn_1$, and comprises a similar statement of the "large" molecule limit.
(251) For benzene, for example, it is found[57] that a frequency change in $\nu_1$ of 10% leads to predicted relative reates for the $\nu_1$ progression which increase exponentially; the actual value of $\Delta\omega_1$ is almost certainly several times smaller, consistent with the linear increase observed. In other cases, large $\Delta\omega$'s might indeed be obtained. For example, the exponential increase measured for such molecules as $\beta$-naphthylamine[79] and parafluorotoluene[80] very probably arises from large geometry and/or frequency changes in the amine and methyl groups, respectively.
(252) The $4(b_{1u})$ vibration that appears anomalous is the only odd parity vibration studied. It is a bending mode where the two rings of naphthalene are bending around the two central C atoms.
(253) This fluorescence appears to be different from the fluorescence spectrum displayed by Dewey and Hadley.[167] Their spectrum shows some vibrational structure with 1300-$cm^{-1}$ intervals, and it is blue shifted with respect to the spectrum of Soep and Tramer. Tramer and Soep report though that both the fluorescence and phosphorescence have the same excitation spectra that reproduce the main features of the quinoxaline absorption spectrum.
(254) As one goes from biacetyl to glyoxal, the density of vibronic states is reduced because of the smaller number of vibrating atoms. This means that the size of the black hole region should increase on going from biacetyl to glyoxal and this is observed experimentally [86].
(255) Note that Coveleskie and Yardley[87] ascribed the same discrepancy to involvement of vibronic levels of the $S_0$ state and not to rotational levels. The deviation between experimental and calculated $\rho_T/\rho_S$ ratios is maximal in methylglyoxal, a fact that was attributed[86] to the lower symmetry of this molecule which results in less severe symmetry restrictions for the Coriolis coupling.